Formation, stability and in vitro activity of colloidal systems for gene delivery

Azahara Rata Aguilar

Doctoral Programme in Physics and Space Sciences
Biocolloid and Fluid Physics Group
Applied Physics Department
University of Granada

Formation, stability and in vitro activity of colloidal systems for gene delivery

por

Azahara Rata Aguilar

Licenciada en Bioquímica

Supervisores del trabajo:

Antonio Martín Rodríguez
Catedrático de Física Aplicada

Juan Luis Ortega Vinuesa
Profesor titular de Física Aplicada

Ana Belén Jódar Reyes
Profesora titular de Física Aplicada

Este trabajo de investigación se presenta
para alcanzar el grado de
Doctor por la Universidad de Granada
Granada, 2014

La doctoranda Azahara Rata Aguilar y los directores de la tesis Antonio Martín Rodríguez, Juan Luis Ortega Vinuesa y Ana Belén Jódar Reyes, garantizamos, al firmar esta tesis doctoral, que el trabajo ha sido realizado por la doctoranda bajo la dirección de los directores de la tesis y hasta donde nuestro conocimiento alcanza, en la realización del trabajo, se han respetado los derechos de otros autores a ser citados, cuando se han utilizado sus resultados o publicaciones.

En Granada a

Directores de la Tesis   Doctoranda

Fdo. Antonio Martín Rodríguez

Fdo. Juan Luis Ortega Vinuesa

Fdo. Ana Belén Jódar Reyes

A mi familia y amigos por su apoyo incondicional

"Now, here, you see, it takes all the running you can do, to keep in the same place. If you want to get somewhere else, you must run at least twice as fast as that!"

— Lewis Carroll, Through the Looking-Glass.

Agradecimientos

Escribir estas líneas supone el inicio del final de esta aventura llamada tesis, un momento para echar la vista atrás y hacer balance de los últimos años. Y lo que me viene a la mente son personas. Personas que han estado desde el principio o que han aparecido después. Personas a las que creí que no volvería a ver y personas a las que tuve que mirar dos veces. Personas con las que he reído (mucho), llorado (lo justo), bailado (¿el trololó es un baile o una forma de vida?), viajado (demasiado, según las malas lenguas), nadado (ejem) y hasta disparado (bolas de pintura...) Y a todas ellas quiero agradecer esos momentos que hacen que la vida merezca la pena.

Gracias ante todo a mis tres supervisores, Antonio, Juan Luis y Ana Belén, porque sin ellos no estaría escribiendo esto dentro del plazo... De hecho no lo estaría escribiendo, porque no creo que hubiese llegado al final del camino si ellos no me hubieran tendido la mano cuando tropezaba o frenado cuando corría en la dirección equivocada. Pero por encima de todo les agradezco que me hayan permitido caminar libre. Y la paciencia. Y la gestión de las crisis. Y las risas. Y todo lo que he aprendido de y con ellos. Gracias.

Aprovecho también para agradecer la beca FPU de Ministerio, que ha hecho posible esta investigación, y los proyectos MAT2010-20370 y MAT2013-43922-R del MICINN por la financiación.

Tengo tantas personas en mente cuando pienso en el Grupo de Física de Fluidos y Biocoloides, que me perdonarán si no las nombro todas. Gracias a Julia, porque sin su ayuda el pulpo me habría estrangulado (o yo a él). A Peula, porque aunque los caminos se separaron siempre tiene lista una sonrisa, o unas palabras de ánimo. A Maria José, que me ha hecho sentir que siempre estaba disponible si lo necesitaba, aunque esté metida en mil cosas. A Conrado, Miguel Heredia y Belén por su buena disposición y ayuda (especialmente para la organización del JICI), y por solucionarme siempre lo

que podrían haber sido catástrofes administrativas. A José Antonio, nuestro técnico, porque sin su ayuda mis pequeñas locuras académicas no hubieran sido posibles. A Fernando Vereda, que mantiene a salvo los guantes y el alcohol, a Delfi, por las conversaciones y los ánimos, a Roque, por esa pasión por la ciencia, a Alberto, por valorar mi trabajo cuando más lo necesitaba, a Arturo, por su objetividad y sinceridad, a Miguel Ángel, por la fantástica web de reservas, a María, Jorge y Jerónimo por su ayuda con la docencia, a Cabrerizo, por sus chistes y por no enfadarse porque no le entiendo una palabra. A Pepe, Juan de Vicente, Curro, Paco, Inmaculada, Mª Carmen y en general toda esa gente que con una sonrisa por el pasillo, o un ¿cómo te va? amable me han alegrado el trabajo de estos años en el grupo. También a Ángel Delgado, por su omnipresencia tranquilizadora y su amabilidad.

Y cómo no, quiero dar las gracias a mis compañeros de la excelentísima Sala de Becarios, que seguramente leerán estas palabras en alto, a ser posible en mi presencia para avergonzarme, como ya es tradición. Va por ustedes. En primer lugar me vais a permitir que agradezca a mi compi de penurias, congresos y de osos, digo cervezas, Paola. Gracias por tu filosofía de vida, por esas conversaciones absurdas de discoteca y por todos esos pequeños tesoros que regalas con tanto cariño. A Carmen, por su amistad y sinceridad, por las inolvidables tardes en el Amsterdam y sobre todo por su carácter impulsador (que no impulsivo, aunque también un poco), que tanto echo de menos. A Juan Pablo, perro ladrador, por su sentido del humor y por cuidar de mí, y por enseñarme tanto aunque quizá ni lo sepa. A César, mi gallirrego favorito que se fue demasiado pronto y con el que viví tantas cosas. A Pablo, por encargarse de la secretaría de la Sala de Becarios, por sus terapias de chupitos y las tardes en el Sonora. Y hablando de Sonora, Luisma, my weapon, por hacer de cemento y sobre todo por las risas. Ah, los del gimnasio me han pedido que te de las gracias también de su parte. A José Antonio. A Felipe, que mantiene a raya a las cucarachas, se transforma con un hacha y siempre está de buen humor. Y a su mini versión, Jesús Felipe, por los abrazos, el piedra/papel/tijera, las guerras de cosquillas y su entusiasmo. Jose, que era broma, gracias por la frescura, la inocencia y el optimismo, por tus contagiosas ganas de vivir y las historias demasiado explícitas. A Diego, que todo lo que tiene de desastre lo tiene de buena persona. Gracias por escucharme, animarme, entenderme sin palabras y cuidarme. A Germán, que nunca te negará ayuda, o un abrazo

que no pides pero necesitas. A Amelia a lo mejor no le doy las gracias, por dejar el listón demasiado alto. Bueno, venga, pero sólo porque eres una bellísima persona y me has enseñado que la constancia en el trabajo no está reñida con el ocio. A Miguel Wulff, por dedicarme su tiempo cuando llegué al grupo y por su optimismo. A Leo, por su preocupación sincera y su disposición, y por su habilidad para las manualidades que tanto envidio. A Miguel F., Fernando y Teresa por esos necesarios momentos de despotricar contra la gota. A Álvaro, con su humor ácido y su poder de hipnosis. A Inma, con su sonrisa de anuncio siempre preparada. A Irene Adroliber, por su presencia constante en la sala, que hace más llevaderos esos momentos fatídicos de subir tarde del laboratorio cuando las cosas no han ido bien. Y aunque no son de la sala, también a Geraldine, por su entusiasmo y por hacerme ver los caracoles de otra forma, a Ricardo, Kasia y Laura, que sólo cruzarme con ellos por el pasillo me hace sonreír, a Paloma por su frescura y a Maria del Mar, mi gran descubrimiento de Escocia, porque esas sonrisas de desconocidas por el pasillo han terminado en una amistad de película, de las de montar a caballo al viento y recorrer el mundo vendiendo pulseritas. Gracias por las locuras, los abrazos, por los siempre animados buenos días y por creer en mí.

I want to thank all the people that I met during my short stay in Munich. Thanks to Prof. Wagner and Prof. Bräuchle for the opportunity to work at their amazing labs, and for all the things that I learned there. To Nadia and Frauke, for all the support and fruitful discussions. To Ellen, always happy and optimistic, Vroni, Adriano, Uli and Petra for making my stay there so pleasant.

Quiero agradecer también a mis Paulas por su apoyo incondicional. A Paula Martos, perdida y encontrada, por entenderme mejor que yo misma, por escucharme y animarme y por los buenos consejos. Y a Paula Morales, porque no importa cuánto tiempo pase o cuantos kilómetros nos separen, que siempre parece que nos vimos ayer. A Carmen Gil, que siempre me consigue artículos para los que no tengo acceso, y a la que también creía perdida. A Dani, Eugenio, Gustavo, Cova y María, porque no importa cómo de mal haya ido el día, que siempre que hay un mensaje en el grupo me hace reír. Y a Nuria, porque si no fuera por ella hay días que no saldría de casa.

Y desde luego quiero dar las gracias a las personas que lo aguantan todo, con las que no hay que fingir y que siempre están ahí: mi familia. A mi madre, que siempre manda saludos para las partículas, hasta para las que no se portan bien y agregan. Gracias por el apoyo, por escuchar mis quejas durante horas y por todo lo que has hecho por mí. Gracias también a Willy, por cuidar de ella, por los ánimos y el cariño. A mis dos hermanas, Natalia y Susi, que sospecho que no saben muy bien a qué me dedico pero a las que siento siempre cerca, aunque sea a través de un teléfono móvil. También a Ignacio y Luisa, que para mí ya son familia, y que siempre hacen lo posible para que me relaje y olvide las preocupaciones. Y a mis cobayas, que durante algún tiempo eran los que esperaban en casa impacientes a que volviera del laboratorio. A mi Spike, con sus pasitos de oso, y sus topetazos de rinoceronte, que empezó esta locura conmigo y no pudo terminarla. Y a Parker, que respondía con ronroneos a los clicks del ratón mientras yo escribía la tesis.

Y como no, se lo debo todo a Iván, la persona más importante de mi vida. Por entenderme, mimarme, apoyarme y animarme. Porque no hacen falta explicaciones, ni palabras. Porque el encierro durante la escritura de esta tesis no me lo imagino con ninguna otra persona. Y mi vida tampoco.

Azahara Rata Aguilar

Granada, 3 de Noviembre de 2014

CONTENTS

Summary

The condensed structure of DNA in living cells has motivated extensive experimental and theoretical studies. Over the last twenty years, the number of publications devoted to DNA condensation has grown exponentially, especially due to its importance for the development of safer alternatives to viral gene delivery. Cationic polymers spontaneously form interpolyelectrolyte complexes (IPEC) with DNA mainly due to the strong electrostatic interaction between them. Polymeric structures "*à la carte*" can be obtained with the help of modern polymer chemistry, allowing the rational design of condensing agents with different functional domains. It is striking, though, the scarce attention paid to the colloidal properties and behavior of polyplexes in spite of the key role of size, stability, electrical and interfacial properties, or morphology, in the success of the system.

This dissertation is aimed to bridge the gap between the rational design of cationic polymers for gene delivery and the corresponding transfection efficiency *in vitro*, through extensive physicochemical characterization of the colloidal systems. More specifically, we evaluated the role of short and long hydrophobic moieties in the DNA condensation process and the subsequent properties of the system, analyzing features such as the size, electrical properties, temporal stability, morphology, interaction with a model membrane and ultimately, the transfection efficiency *in vitro*. Formulation variables, such as the pH and the ionic strength were also investigated.

This multidisciplinary project required the use of a wide variety of experimental techniques, ranging from biological procedures, such as bacterial transformation, mammalian cell culture or toxicity assays, to physicochemical tools, including dynamic and static light scattering, electron microscopy, or nanoparticle tracking analysis (NTA). What particularly stands out is the use of the pendant drop technique to evaluate the interaction of the polyplexes/polymers with a model membrane, which consists in a phospholipid monolayer at the air/water interface.

The in depth biophysical study performed in this thesis provides a better understanding of the DNA condensation process and some of the factors that modulate it. The role of the hydrophobic interactions in DNA compaction

was further explored in this dissertation, and this force was found to modulate not only the size and morphology of the polyplexes, but also the stability, the interaction with a model membrane, the transfection efficiency and even if the polyplex is formed or not. The experimental techniques used to characterize the complexes have been proved efficient to establish differences based on the condensation mechanism, and indirectly, on the structure of the polymer.

Resumen

El ADN presenta una estructura compacta en las células que ha motivado numerosos estudios teóricos y experimentales. A lo largo de los últimos veinte años, el número de publicaciones dedicadas a la condensación del ADN ha crecido exponencialmente, especialmente debido a su importancia para el desarrollo de alternativas más seguras que las virales para el transporte de genes. Los polímeros catiónicos forman de manera espontánea complejos interpolielectrolito (CIPE) con el ADN, debido principalmente a la fuerte interacción electrostática entre ellos. Gracias a la química de polímeros actual, pueden obtenerse estructuras poliméricas a la carta que permiten el diseño racional de agentes condensantes con diferentes dominios funcionales. Sin embargo, resulta chocante la escasa atención que reciben el comportamiento y las propiedades coloidales de los también llamados poliplejos, a pesar del papel fundamental que juegan el tamaño, la estabilidad, las propiedades eléctricas e interfaciales, o la morfología, en el éxito del sistema.

Esta tesis se propone reducir la brecha entre el diseño racional de polímeros catiónicos para el transporte de genes, y su correspondiente transfección in vitro, a través de una amplia caracterización fisicoquímica de los sistemas coloidales. Más específicamente, hemos evaluado el papel de cadenas hidrofóbicas de diferentes longitudes en el proceso de condensación del ADN y las posteriores propiedades del sistema, analizando aspectos como el tamaño, las propiedades eléctricas, la estabilidad temporal, la morfología, la interacción con una membrana modelo, y finalmente la eficacia de transfección in vitro. También se ha investigado la influencia de parámetros como el pH y la fuerza iónica en la condensación.

El desarrollo de un proyecto multidisciplinar como éste, exige la utilización de una amplia variedad de técnicas que abarcan desde procedimientos biológicos, como la transformación de bacterias, los cultivos de células de mamífero o ensayos de toxicidad, hasta herramientas fisicoquímicas como la dispersión de luz dinámica y estática, la microscopía electrónica o el análisis de la trayectoria de partículas (NTA, del inglés nanoparticle tracking analysis). Destaca particularmente el uso de la gota pendiente para

evaluar la interacción de los poliplejos/polímeros con una membrana modelo constituida por una monocapa de fosfolípidos en la interfaz aire/agua.

El profundo estudio biofísico que se ha realizado en esta tesis proporciona un mejor entendimiento del proceso de condensación del ADN y de algunos de los parámetros que lo modulan. En este trabajo hemos investigado el papel de las interacciones hidrofóbicas en la compactación del ADN, y los resultados indican que esta fuerza no sólo modula el tamaño y la morfología de los poliplejos, sino también la estabilidad, la interacción con una membrana modelo, la eficacia de transfección e incluso si el poliplejo se forma o no. Se ha demostrado que las técnicas experimentales utilizadas para la caracterización de los complejos son eficaces para establecer diferencias entre ellos basadas en el mecanismo de condensación, e indirectamente, en la estructura del polímero utilizado.

1

INTRODUCTION

The first chapter introduces the DNA condensation process and highlights the motivation of the research conducted in the thesis and the main objectives.

Contents

1.1   Research context and objectives

This thesis was carried out at the Fluids and Biocolloids Physics group, which belongs to the Applied Physics Department of the University of Granada. The research conducted in this dissertation was developed within the framework of the MAT2010-20370 and MAT2013-43922-R (MICINN, Spain) projects.

During the last ten years, the supervisors of this thesis, Dr. Jódar-Reyes, Dr. Ortega-Vinuesa and Prof. Dr. Martín-Rodríguez, along with Dr. Peula-García, have been working on a multidisciplinary project related to the physicochemical characterization of colloidal systems for gene/drug/biomolecules delivery. The ultimate goal of their research would be to optimize the preparation and storage conditions of such systems of interest in nanobiotechnology.

The success of any delivery system intended for use under physiological conditions will greatly depend on its colloidal properties and bulk behavior, i.e. size, stability, electrical properties and morphology among others. However, most of the papers devoted to gene delivery are focused mainly on the transfection efficiency, and there appears to be a lack of attention to the physicochemical characterization and/or the colloidal properties of gene delivery systems. Figure 1.1 shows the number of articles devoted to the topics indicated, as an example, published per year according to the ISI Web of Knowledge.
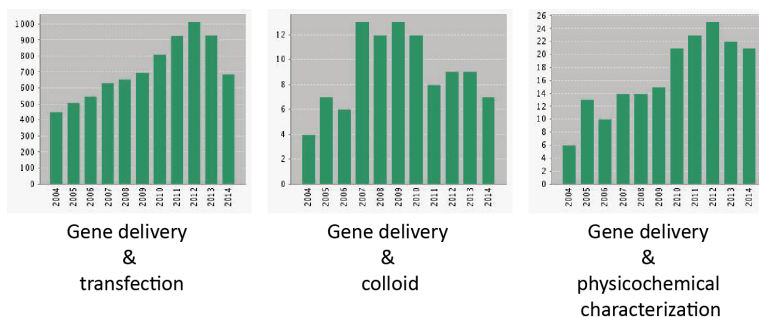
Figure 1.1: Results of searching in Web of knowledge the topics indicated. The bars indicate the number of published articles per year.

In this context, the aim of this thesis is the colloidal characterization of gene delivery systems based on the condensation of DNA with cationic polymers, laying the groundwork for the establishment of a relationship between the structure of the condensing agent and its effectiveness in transfection.

The specific goals of this dissertation were developed in collaboration with the different research groups that synthesize the cationic polymers:

 - **Poly(β-aminoester)s** (Chapter 3 and chapter 4): Dr. Borrós, Grup d'Enginyeria de Materials (GEMAT), University Ramon Llull.
 - **PAMAM dendrimers** (Chapter 5): Dr. Santoyo-González, Organic Chemistry Department, University of Granada.
 - **Linear poly(amidoamine)s** (Chapter 6): Dr. Wagner, Pharmaceutical Biotechnology, Ludwig Maximilian University.

Detailed information about the materials used in this research project can be found in Chapter 2. The objectives of this thesis are therefore defined as follows:

1) To determine the influence of hydrophobic moieties on the condensation process and on the colloidal properties and bulk behavior of the polyplexes.

   a. Short hydrophobic moieties (Chapter 3): An extensive characterization will be done in order to elucidate the role of this modification in the size, stability and transfection efficiency of the polyplexes.

   b. Long hydrophobic moieties (Chapters 5 and 6): In addition to the characterization of the colloidal properties of the particles, the interaction with a cell membrane model will be investigated by determining the adsorption kinetics and the interfacial dilatational modulus of a phospholipid monolayer at the air/water interface. The obtained results will be correlated to the transfection efficiency of the complexes.

2) To evaluate the influence of formulation variables on the properties and *in vitro* activity of polyplexes.

a. pH (Chapter 4): A different value of pH from the physiological one will be used to condense DNA in order to evaluate the consequences in size, stability and *in vitro* activity of the polyplexes.

b. Ionic strength (Chapter 6): The effect of the initial concentration of sodium chloride (NaCl) on the size, morphology and transfection efficiency will be evaluated.

A brief description of the fundamental concepts and background related to DNA condensation and gene delivery are provided in this first chapter to facilitate a deeper understanding of the problem addressed in this research.

1.2 Fundamental concepts and background

Nearly every living cell and virus contains nucleic acids, either DNA or RNA, to encode their genetic information. Each base pair has a length of 0.34 nanometers and diploid human cells have an average length of $6 \cdot 10^9$ base pairs (bp). This means that the nucleus of a single cell with just a few microns contains roughly 2 meters of DNA (if stretched out)[1]. This would be comparable to packing an extremely thin thread of the length of the Titanic into a marble!

DNA is naturally coiled into dense compact forms in a process known as DNA packaging[2]. DNA is essential for cell functioning and every process is based on the genetic information that it stores. This means that this tightly condensed nucleic acid must become accessible to the enzymes involved in replication, transcription and repair processes. In fact, the interplay between different states of compaction is related to gene regulation[3,4]. For that purpose, different systems of packaging are found in nature, from simple mechanisms in phages to more sophisticated structures such as the chromatin in eukaryotes.

Chromatin is the name given to the complex formed by DNA and certain proteins called histones. DNA is wrapped around octamers of these positive proteins in a beads-on-a-string configuration. Chromatin is further coiled into a shorter and thicker fiber with an approximate diameter of 30 nm. Finally, DNA becomes even highly compacted during the metaphase of the

cell cycle. Chromosomes are formed to allow the partition of the genomic material into the daughter cells. Once the cell has divided, its chromosomes uncoil again.

Particular attention has been paid to the male germ cells[5]. In order to optimize the swimming ability of the gametes, the DNA needs to be super-compacted finding a greater than tenfold increase in compaction compared with somatic chromatin. Further studies on this topic found out that most of the histones are replaced by small protamines in sperm cells. This has inspired posterior in vitro DNA condensation studies[6,7].

DNA condensation or compaction is therefore understood as the decrease of the volume occupied by DNA to an orderly collapsed state[8]. In the next sections we will address some of the main issues in DNA condensation and its application for gene delivery.

1.2.1 | DNA in solution

Deoxyribonucleic acid (DNA) is a polyelectrolyte in which the basic units are nucleotides bound by phosphodiester linkages. Nucleotides are molecules composed by the sugar deoxyribose, a phosphate group and a nitrogenous base that might be purine (adenine, guanine) or pyrimidine (cytosine, thymine). Figure 1.2 shows the structure of the four nucleotides that form DNA.

The sequence that these monomers follow is not trivial, since it stores all the fundamental information required to perpetuate life. This information may be deciphered by using a set of rules known as genetic code[9]. The nucleotides are grouped three by three in the so-called codons, and they are translated into aminoacids, which in turn form proteins. Since there are four nucleotides and the codons are organized in triplets, there will be $4^3 = 64$ possibilities, as shown in Figure 1.3.

Returning to the structure of DNA, the phosphate groups are ionized at physiological pH due to its low pKa, providing one negative charge per nucleotide. One strand of DNA can be seen as a highly negatively charged polymer with hydrophobic side groups. Intuitively, two equal chains with
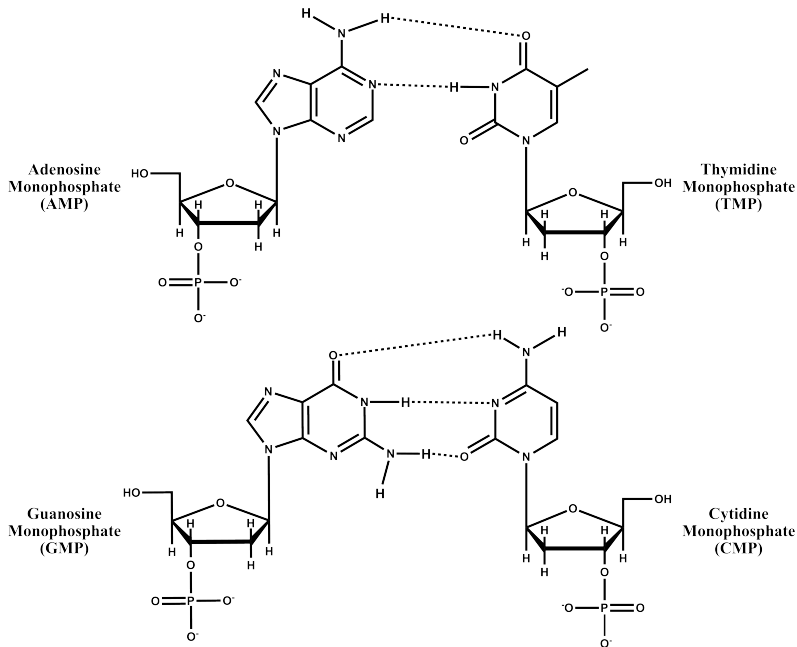
Figure 1.2: Structures of deoxynucleotides and complementary pairing.

such a negative charge will be expected to repel each other in solution. However, DNA is usually found double-stranded. This can be explained if we consider the amphiphilic nature of DNA and the interactions among the nitrogenous bases of the nucleotides[10].

(a) Base stacking: The bases are planar or nearly planar and consequently they can be stacked parallel one on top of the other. Intermolecular van der Waals are short-ranged interactions, falling off with the sixth power of the distance $(1/r^6)$. The base stacking maximizes this attractive interaction through the closest possible distance.

(b) Base pairing: The bases can form hydrogen bonds through their multiple donors and acceptors. The geometrical restriction given by the base stacking leads to the phenomenon known as complementary pairing. According to the model proposed by Watson and Crick[11], adenine would form two hydrogen bonds with thymine, while guanine would form three hydrogen bonds with cytosine (see Fig. 1.2). The hydrogen bonds found in the base pairs are mutually stabilized, which means that each hydrogen bond induces a dipole that reinforces another hydrogen bond.

Figure 1.3: The genetic code.

(c) Hydrophobic interactions: Due to the hydrophobic character of the nitrogenous bases, the molecules of water are structured around them. The stacking of the bases helps minimizing the contact with water, which is released resulting in entropy gain that favors pairing.

Accordingly, DNA in solution will be generally forming the very well known double helix structure, with the negatively charged phosphates on the outside and the bases located inside.

1.2.2 | DNA condensation in vitro

The condensed structure of DNA in living cells[12] has motivated extensive experimental and theoretical studies with the participation of several disciplines, such as biology, biochemistry, physics or physical chemistry. Many chemical agents are known to cause DNA condensation, either by reducing the electrostatic repulsion between DNA segments, or by excluding volume

to the unfolded DNA chain. Some of them are briefly commented here.

1.2.2.1 Polycations

Cationic polymers spontaneously form interpolyelectrolyte complexes (IPEC) with DNA due to the strong attractive electrostatic interaction between them[13]. DNA-polymer complexes are also known as polyplexes and their popularity has increased over the last twenty years. The huge advances in polymer chemistry have allowed the synthesis and modification of wide libraries of on-demand polymers for diverse purposes[14].

Typical examples of polycations used to condense DNA are polyethyleneimine[15], polypeptides[16] such as polyarginine or polylysine, polyaminoamides[17], chitosan[18], and many others[19, 20].
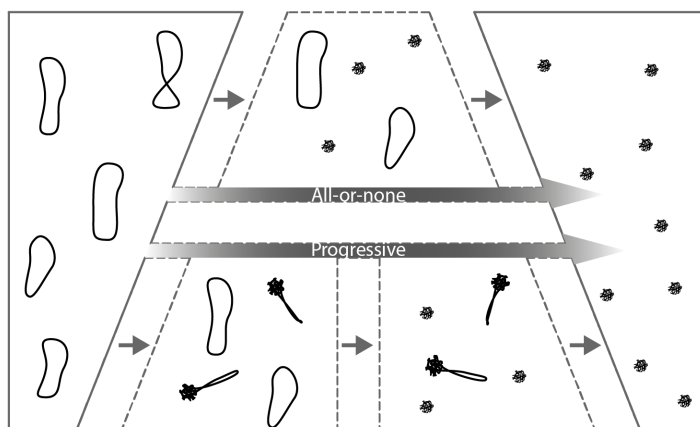
Figure 1.4: Condensation pathways upon addition of cationic polymer to DNA.

The DNA coil-globule transition induced by polycations can proceed through all-or-none compaction (interchain segregation) or through progressive compaction (intrachain segregation)[21] as schematized in Figure 1.4. Polymers with low valency (multivalent cations) induce all-or-none compaction and they need to be added in excess to achieve full compaction. On the other hand, when long polycations are used, the collapse might proceed via intermediate structures or directly from the coil to the globule, depending on the concentration of salt[22] and on the chemical nature of the polymer[23].

In both cases segregation appears at intermediate concentrations of the cationic polymer.

1.2.2.2   Other condensing agents

a) Multivalent cations

Many studies since the seventies have demonstrated that multivalent cations can induce DNA condensation in vitro[24]. Toroidal structures similar to those from bacteriophages where found when using the naturally occurring trivalent polyamine spermidine[25]. Spermine, with 4 positive charges per molecule, was also used succesfully[26]. Conversely, neither the diamine putrescine nor divalent cations such as Mg^{2+} were able to compact DNA. Based on these evidences, the inorganic trivalent metal ion complex $Co(NH_3)_6^{3+}$ was tested and similar structures were found[27]. While the cation valence has a fundamental role in the condensation process, it was found that the spacing of the charges also influences the efficiency of the compaction agent. A geometrical fit between both positive and negative charges gives the best results[28]. In addition, the methylene groups between the amino groups in polyamines might interact with DNA via hydrophobic contacts[29].

b) Crowded environment of neutral polymer

According to the previous section, monovalent cations such as Na^+ cannot condense DNA. But there is an exception, the so-called ψ-condensation[30] (psi, polymer and salt induced). When high concentrations of monovalent cations are added to a DNA solution along with neutral polymers, compaction takes place[31]. The neutral polymer excludes volume to DNA due to unfavorable contact between them. The space available for DNA in its extended conformation decreases at a critical concentration of the neutral polymer and collapse occurs. Polyethylene glycol (PEG) is one example of polymer that induces psi-condensation and it has been widely studied[32, 33].

c) Surfactants

Cationic surfactants can compact DNA into individual nanoparticles[34, 35]. Apart from the electrostatic interactions between the positively charged polar heads and DNA, a strong dependence on the hydrophobic tail length has been found. Apparently, hydrophobic interactions favor compaction and

the process is similar to the formation of micelles. The binding of cationic surfactants to DNA seems to be cooperative and it occurs at concentrations below the CMC[36].

Anionic surfactants do not induce a conformational change in DNA as expected. Nonionic surfactants, on the other hand, produce DNA collapse by means of an increase of the osmotic pressure[37], a process similar to the psi condensation previously mentioned.

d) Liposomes

Lipoplex is a term used to designate complexes formed by DNA and liposomes. Those complexes have been used since the eighties to efficiently deliver exogenous DNA into eukaryotic cells with therapeutic purposes[38]. The negatively charged DNA was initially believed to wrap around the positively charged liposomes, maintaining their size and shape[39]. It was not until the use of the freeze-fracture electron microscopy that it was seen that DNA acted as a fusogenic agent and induced morphological changes such as multilamellar complexes, spaghetti and meatball structures, hexagonal phases and others[40–42]. Motivated by the high cytotoxicity of cationic liposomes, some investigations have been focused on anionic liposomes[43–45]. This type of lipoplexes is usually formed by mediation of multivalent cations, typically Ca^{2+}.

1.2.3   Forces in DNA condensation

DNA condensation can only occur if the attractive interactions are stronger than the repulsive ones. In this section we will analyze some of the forces involved in the complicated process of DNA compaction.

1.2.3.1   *Bending*

The stiffness of DNA is quantified with a parameter known as persistence length, which is the distance over which the direction of a polymer segment persists due to limited flexibility of the polymer. The persistence length of DNA depends on the ionic strength of the medium, since at low salt concentration the repulsion between the negatively charged phosphates is

high. It has been calculated that at the physiological salt concentration the persistence length of DNA is about 30-50 nm (90-150 bp)[46]. In spite of such a high stiffness, due to the typical lengths of DNA this polyelectrolyte can be considered as a wormlike chain, except for short DNA, which behaves as a rigid rod.

The energetic cost of bending DNA might be overcome by using condensing agents[24] or even through sequence-directed bending[47,48].

1.2.3.2   *Mixing entropy*

When DNA is compacted, the solvent is excluded, due to favorable interactions between DNA and the condensing agent. There is an entropic loss caused by the demixing of DNA and solvent[24]. The configurational entropy of the unfolded DNA homogeneously mixed with the condensing agent and the molecules of the solvent is higher than that of the collapsed state. Accordingly, mixing entropy opposes DNA condensation.

1.2.3.3   *Hydration entropy*

The hydration entropy gain[49] emerges from the reconfiguration of the water molecules that are bound to DNA when it is unfolded. When the condensing agents interact with DNA, rearrangement or release of water molecules occurs, increasing the overall entropy of the system[24]. Consequently, DNA condensation is favored.

1.2.3.4   *Electrostatic interactions*

As stated previously, DNA has one phosphate group per nucleotide. This means that on average, DNA has a negative charge each 0.17 nm, which makes electrostatic interactions the most significant forces involved in DNA condensation. In solution, DNA is usually accompanied by monovalent counterions such as Na^+. Those positively charged ions will be attracted to the macroion (DNA) but thermal energy will tend to send them away. Whether the counterions are kept close to DNA or free in solution will depend on the electrostatic-entropic balance.

Manning described a polyelectrolyte in solution as an infinite charged rod and concluded that if the surface has a sufficiently high charge density, the

Coulomb potential energy would overcome the entropy penalty and the counterions will remain condensed on the cylinder[50]. Instead of localized salt-like interactions, the counterions are kept mobile forming an ionic cloud that minimizes the entropic cost. Consequently, the effective charge of the polyelectrolyte is reduced proportionally to the valence of the counterion. 89-90 % of the charge of DNA must be neutralized to induce condensation as estimated by Wilson and Bloomfield[51]. Monovalent and divalent cations cannot condense DNA, because they are not capable of reducing that much the charge of DNA.

Most of the condensing agents considered in previous sections are positively charged to interact with the negative charges of DNA. Since counterions are initially condensed onto the DNA, the cationic polymer must compete with those ions. As a result, counterions are released, which means an entropic gain that favors the polycation-DNA interaction. In fact, calculations of the free energy were done and it was found that the entropic term is twice as large as the enthalpic term that considers all the electrostatic contributions[52]. Surprisingly, the condensation process induced by a cationic compound is not electrostatically driven, but entropically. As a consequence of the counterions release, the formed complex might be overcharged, which could not be possible otherwise due to repulsion.

1.2.3.5   *Like-charge attraction*

It was clear from Manning's theory and many other classical mean-field studies that counterions and cationic compounds reduced the overall charge of DNA. But the advances in polyelectrolyte theories demonstrated the emergence of a short-range attraction force between the negatively charged chains of DNA when multivalent cations were added. This phenomenon of like-charge attraction (which cannot be explained with mean-field theories because they always yield repulsion) is based on correlations between the multivalent cations condensed onto the polyelectrolyte[53].

Correlations occur as a consequence of the strong interactions of the multivalent cations with DNA and with each other. The cationic compounds are not randomly positioned, but they form a strongly correlated liquid on the surface of DNA to gain some energy[54].

The electrostatic repulsion between the multivalent cations produces an alternating pattern of positive and negative segments on the surface of DNA. Those segments will adjust to each other to minimize the energy, giving rise to short-range attractive forces[55].
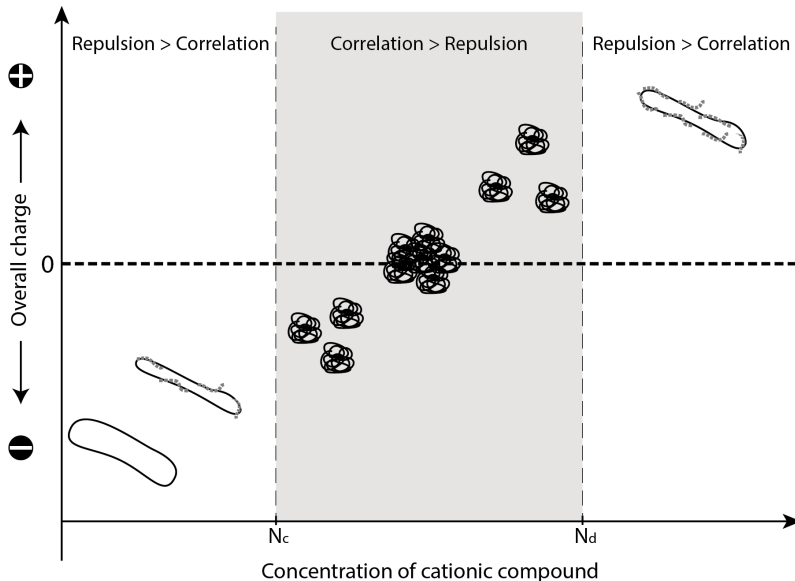
Figure 1.5: Phase diagram illustration of the reentrant condensation of plasmid DNA based on the competition between electrostatic repulsion and correlation attraction.

From the competition between electrostatic repulsion and the correlation attractive forces, three regimes can be distinguished during DNA compaction, usually know as reentrant condensation[56], and the corresponding phase diagram is shown in Figure 1.5. At low concentration of the cationic compound, complexes with DNA are formed, but the Coulombic repulsion is predominant and DNA remains unfolded. Above a critical concentration of multivalent cation, N_c, the correlation attraction appears and DNA is condensed into negatively charged complexes. At the neutralization point there is no electrostatic repulsion, and neutral complexes are formed. In absence of other mechanisms of stabilization, such as steric or hydration forces, those complexes will aggregate. Further addition of multivalent cations leads to charge inversion, and positively charged complexes are found, which might be kinetically stable due to strong interparticle electrostatic forces. However, it was observed that above the concentration N_d, repulsion

overcomes the correlation attractive forces again and DNA is re-dissolved adopting an elongated conformation positively charged. The re-dissolution is rarely observed with long polycations.

The phase diagram is defined by the two concentrations required for condensation and redissolution, but the boundaries depend on several parameters. The decondensation depends on the DNA length, the chemical nature and length of the polycation used, and the monovalent salt concentration. The distance between N_c and N_d can vary as a function of DNA concentration and monovalent salt. To sum up, keeping constant the concentration and length of DNA, the phase diagram will depend on the chemical nature of the condensing agent and on the concentration of monovalent salt.

1.2.3.6   *Hydrophobic interaction*

Hydrophobic interactions may also contribute to DNA condensation. In fact, the hydrophobic forces are fundamental for many biological processes, such as the protein folding or the formation of the lipid bilayer of the membranes. Unfortunately, this effect is not yet well understood and it is usually overlooked, though it is being increasingly recognized. Qualitatively it can be understood as a force that causes clustering of hydrophobic moieties[57]. Thus, lipophilic modification of the condensing agents can benefit the DNA compaction as a result of the gain in hydrophobic energy that results of close packing of the hydrophobic segments. Some authors observed a cooperative binding of amphiphilic condensing agents, such as surfactants, liposomes or covalently modified polycations as a consequence of the hydrophobic interaction[58–60]. The influence of this interaction, that can be stronger than hydrogen bonds or Van der Waals forces, remains to be thoroughly investigated and it will be one of the aims of this dissertation.

1.2.4   Gene delivery

The interest in DNA condensation has increased over the last twenty years and the number of publications on this topic has grown explosively. One of the reasons is the theoretical studies on the properties of polyelectrolytes and the interaction forces involved in compaction that DNA has allowed.

But it is probably due to the emergence of the so-called gene therapy that DNA compaction is in the limelight.

1.2.4.1   Definition of gene therapy

Gene therapy is a promising therapeutic strategy that ensures the introduction of intact genetic material into a human cell in order to cure or prevent a disease with genetic basis[61]. Theoretically, it consists in the application of one of these three therapeutic approaches:

- Insertion of a functional gene that replaces a distorted gene.
- Inactivation of a mutated gene.
- Introduction of genes that express proteins that might help to fight the disease (i.e. pro-apoptotic enzymes, prodrugs...)

However, in practice gene therapy must struggle with so many obstacles that it has led to disillusionment and a sense of failure. We cannot forget that since the first human gene therapy trial performed in 1989 by Rosenberg[62] and his team, more than 2000 clinical gene therapy trials were performed up to 2014. Maybe the current approaches will never succeed. But deeper understanding of DNA encapsulation and the properties of the resulting particles will be a key to success. Quoting Theodore Friedmann, "gene therapy will happen, but in good time"[63].

1.2.4.2   Gene vectors

Gene vectors are defined as the "systems designed to aid the transference of an exogenous gene to the cell, facilitating its entry and intracellular bioavailability and enabling its expression at the appropriate level for an adequate time period[64]".

Viruses are natural vectors which efficiently deliver their genomes into the host cells where their genetic material is successfully expressed. By using genetic engineering it is relatively easy to modify viral particles to replace the pathogenic sequences by the therapeutic ones. The result of this modification has been called a viral vector, and consequently, all the chemical-based DNA carriers are known as non-viral vectors.

The *in vivo* efficiency of viral vectors has not yet been overcome by the non-viral ones, but the immunogenicity and high costs of production of viral vehicles limit their use and motivate the investigation of better "artificial viruses[65]". Nevertheless, non-viral vectors are routinely used for the synthesis *in vitro* of viral vectors[66] and some formulations have been proven efficient for the induction of pluripotent cells[67, 68].

Non-viral vectors are usually formed by condensing DNA with the chemical compounds mentioned in Section 1.1.2. Consequently, their transfection ability will be related to the nature and structure of the condensing agent, but also to the environmental parameters that modulate the condensation process.

1.2.4.3 *Biological barriers to gene delivery*

The lower efficiency of nonviral gene vectors when compared to viral systems is mainly due to their inability to overcome the numerous barriers encountered along the *in vivo* transfection process, which are schematized in Figure 1.6. We will further examine each step in order to understand the requirements that the ideal gene vector should meet.

a) Protection of the plasmid DNA

If the decided administration route is intravenous, it has to be taken into account that blood is an extremely complex dispersion of cells in a liquid phase known as plasma. The gene vector would be exposed to electrolytes, hormones, blood proteins, enzymes and many other blood components. It is especially concerning the presence of nucleases, a ubiquitous type of enzyme capable of hydrolyzing the phosphodiester bonds of the DNA strands. Therefore, the carrier must protect DNA from degradation by serum nucleases.

Furthermore, the physiological ionic strength corresponds to approximately 150 mM of NaCl. The interactions between DNA and most of the condensing agents are highly dependent on the salt concentration, as previously explained. Accordingly, the stability of the carrier should be tested at biologically relevant conditions. Aggregates might cause partial or complete occlusion of blood vessels or capillaries, a process known as embolization. Although some embolic nanomaterials have been designed to deliberately
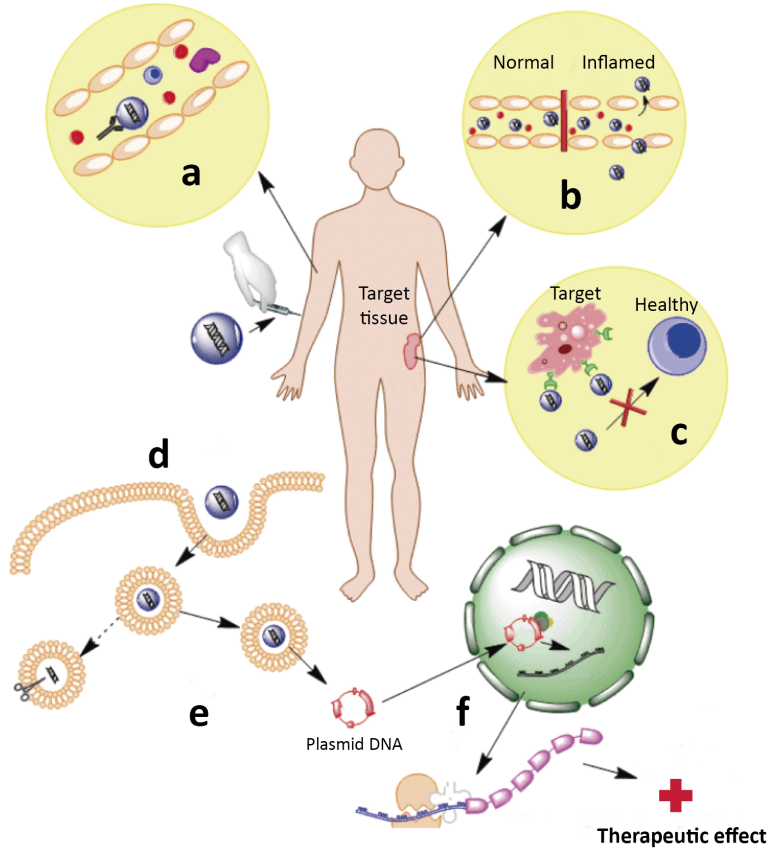
Figure 1.6: Diagram of the biological barriers to gene delivery upon intravenous administration.

block blood vessels[69], it is generally an undesirable side effect that should be controlled.

Unfortunately for our purpose, the immune system is in charge of the rapid clearance of exogenous elements from the bloodstream which can occur within minutes. The complement system is usually activated the first time that the carrier is inoculated. This primitive part of the immune system is composed by a group of proteins that trigger a biochemical cascade aimed at the removal of pathogens. The non-specific adsorption of the so-called opsonins onto the surface of the particle may activate the complement system and receptor-mediated phagocytosis occurs. Worse still, cell-mediated immunity might be stimulated by the complement system

causing allergy to the injected material, which will be specifically recognized if ever injected again[70,71]. In order to avoid the adsorption of plasma proteins, neutral polymers such as polyethyleneglycol (PEG) have been extensively used, usually grafted to the condensing agents, in order to improve the circulatory half-life of the carrier[72,73].

b) Extravasation

The internal surface of the blood vessels is covered by a cell monolayer called endothelium that serves as a semipermeable barrier between circulating blood and tissues. Unless the targeted cell type is precisely the endothelium, the DNA carrier will have to extravasate from the blood stream into the disease site. Under normal circumstances the threshold limit is approximately 3 nm in radius[74] owing to the tight endothelial junctions. However, the blood vessels in the vicinity of solid tumors or inflammation sites are structurally different and present a larger pore size. Consequently, particles smaller than 500 nm (preferentially under 150 nm) in diameter will be extravasated due to the phenomenon known as *enhanced permeation and retention*[75] (EPR). The EPR effect has been used for passive targeting, since the carriers can only access to damaged tissues[76].

c) Specific targeting

Typically, it is assumed that positively charged carriers will facilitate inter-action with cell membranes, which are slightly negatively charged. While this is true and it works well for *in vitro* experiments, positively charged carriers bind nonspecifically to any cell, damaged or not, limiting their use *in vivo*. On the other hand, neutral or anionic vectors may be completely unable to enter the cells at all. A specific ligand bound to the carrier might mediate a receptor-ligand uptake, increasing the efficiency and reducing the side-effects. Targeting strategies for gene delivery usually are based on the covalent coupling of specific ligands to the condensing agent. The RGD (arginine-glycine-aspartic acid) peptide motif[77], transferrin[78], the epidermic growth factor (EFG)[79], folic acid[80,81], or specialized antibodies[82] are just some of the investigated ligands.

Our first studies with colloidal systems for therapeutic delivery were done with a cationic polymer, chitosan, covalently modified with folic acid[80]. We demonstrated that the uptake of the nanocapsules coated with the

chitosan-folate was increased due to the presence of a specific ligand, and they were internalized via folate receptor, since the blockage of the receptor decreased the uptake (Fig. 1.7).
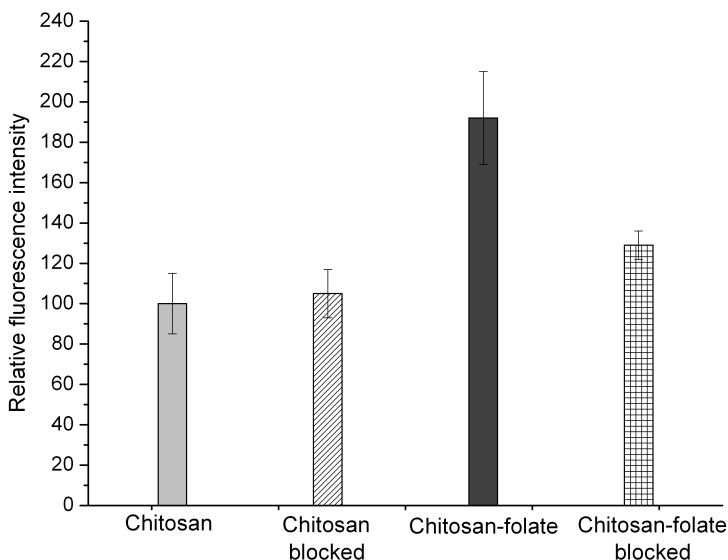
Figure 1.7: Relative fluorescent intensity of MCF-7 cells when incubated for 4 h with Red Nile loaded nanocapsules coated with chitosan (light gray) and chitosan-folate (dark gray). The patterned columns represent experiments in which the membrane folate receptors had been previously blocked with free folic acid.

d) Endocytosis

Although some vectors, especially those including lipids, can enter cells via fusion with the plasma membrane, the majority of the non-viral vectors studied appears to enter via endocytosis, whether they bear specific ligands or not. The different endocytic routes known in mammalian cells[83] are schematized in Figure 1.8. Since phagocytosis is restricted to specialized cells, by endocytosis we are usually referring to pinocytosis. In this process, the material is progressively enclosed by a small portion of the cell membrane, which first invaginates and then pinches off to form an endocytic vesicle containing the DNA carrier[2]. Not all of these mechanisms are completely understood yet, but some pathways have been identified during the uptake

of non-viral vectors. The most common are clathrin-dependent, caveolae mediated and macropinocytosis[84].

In the absence of targeting strategies, the entry is generally said to be by adsorptive endocytosis. The uptake can be modulated by tuning the nonspecific interactions between the vector and the cell membrane[85].

   - *Electrostatic interactions*: Proteoglycans are a type of protein present on the cell surface grafted to negatively charged glycosaminoglycans (GAGs) exposed to the extracellular space. The electrostatic interaction between positively charged DNA carriers and proteoglycans is believed to mediate internalization, although the mechanism is unclear.

   - *Hydrophobic interactions*: The cell membrane is composed by a bilayer of phospholipids. It is plausible to think that lipophilic modifications of the condensing agents might enhance the adsorption of the particle to the membrane, fomenting endocytosis[86]. While lots of studies show increased transfection when hydrophobic substituents are added[87], further investigation on the specific interaction particle-membrane would help to clarify its relevance.

   - *Cell penetrating peptides (CPPs)*[88]: Some viruses have proteins capable of penetrate the cell membrane and facilitate translocation. Sequences of 5-40 aminoacids belonging to those proteins have been identified and they are known as CPPs. The peptides are amphipathic and positively charged and the uptake is not clear yet, but it is believed that the lysosomal route (explained below) might be avoided, which would be a huge advantage.

e) Endosomal escape

Depending on the entry pathway, the endocytic vesicle containing the DNA carrier might eventually fuse with lysosomes[89], which are vesicles containing digestive enzymes. Once the fusion takes place, the pH inside the vesicle is acidified a couple of units and the contained material is degraded by the proteases, lipases, DNases, etc. which are conveniently active only at acidic pH, avoiding the risk of self-destruction. Consequently, escape from the endosomes is essential for efficient transfection[90]. This step is usually considered the bottleneck of gene delivery.

Several strategies have been investigated to achieve endosomal release of the non-viral vectors:
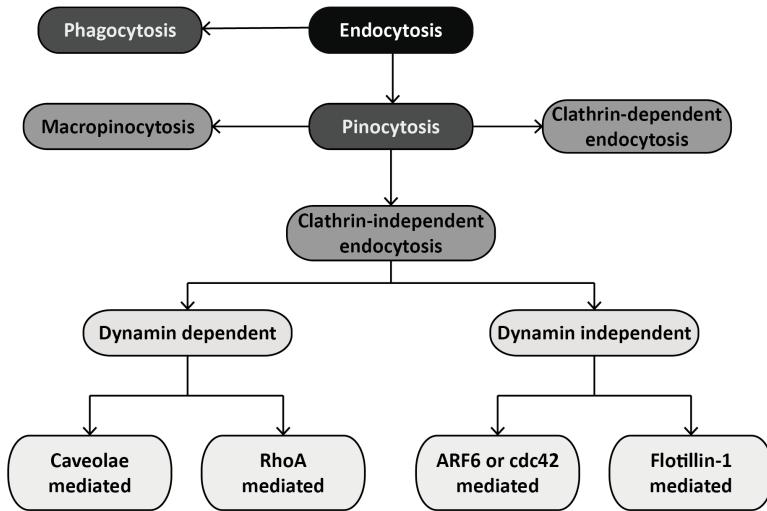
Figure 1.8: Scheme of the endocytic pathways in mammalian cells.

- *Proton sponge*[91, 92]: This strategy is based on the buffering capacity of the condensing material, and it is usually referred to polymers. The membrane proton pump ATPase actively introduces protons into the vesicle followed by the passive entry of the corresponding Cl^- anions. The protonable groups of the polymers will trap the protons and the pH is maintained, due to their high buffering capacity. Consequently, both protons and chloride anions will be continuously entering, increasing the osmotic pressure of the compartment. Water influx will swell the endosomes and its content is eventually released to the cytosol[93]. Some of the studied polymers known to escape from the endosome through this mechanism are polyethyleneimine (PEI), polyamidoamine (PAMAM), imidazol derivatives, etc.

- *Lysosomotropic agents*[94]: The strategy is similar to the proton sponge effect. Lysosomotropic is the name given to any substance that is accumulated and sequestered in the lysosomes by a mechanism of ion trapping. Typically these molecules are small, slightly hydrophobic and weakly basic. At physiological pH they are not ionized and passively diffuse across the membranes. Under the acidic environment of the lysosomes, they acquire charge and cannot diffuse freely. Its accumulation raises the osmotic pressure and the endosome is destabilized. Chloroquine and sucrose are an example of lysosomotropic agents that have proven to improve the

transfection efficiency *in vitro*[95].

- *pH-sensitive liposomes or fliposomes*[96]: It has been observed that some lipids are capable of forming stable bilayers at physiological pH, but under acidic conditions a flip-flop mechanism occurs. As a consequence of the structural change, the membrane is destabilized and the cargo is released in the cytosol[97].

- *Fusogenic peptides*[98]: Synthetic fusogenic peptide sequences have been created by mimicking the endosomal escape mechanism of some viruses. It consists basically on the fusion of the DNA carrier with the membrane of the endosome by using the peptide. Sequences derived from the hemoaglutinine (HA) of the influenza virus have been investigated showing a significant improvement of the transfection efficiency[99].

Regardless the strategy used to escape from the endosome, once the gene vector finally reaches the cytosol, it is exposed to a reducing environment. The pH acidification of the endosome and the intracellular reducing conditions are environmental parameters that can be further exploited to activate specific functions and create an efficient and dynamic "artificial virus"[65].

f) Transfer into the nucleus

Plasmid DNA needs to be transferred into the nucleus of the cell, where the corresponding messenger RNA (mRNA) will be synthesized and exported back to the cytosol. The proposed entry mechanisms are exposed below:

- *Mitosis*: The nuclear envelope is absent during cell division in order to allow chromosomal segregation. It can be deduced that transfection would be more efficient in rapidly dividing cells, taking advantage of the cell cycle. This has been observed in several studies[100].

- *Nuclear Pore Complexes*: The interchange of materials between the nucleus and the cytosol occurs through the Nuclear Pore Complexes (NPCs). Those protein structures are highly selective and they are implicated in both active and passive transport across the nuclear envelope[101]:

i) Passive transport: The NPCs allow the entry of molecules with a diameter up to 10 nm without energy consumption. Even if the DNA were still condensed, these apertures are extremely small,

which makes this mechanism unlikely, especially for high molecular weight plasmids.

ii) Active transport: There are many proteins that functions inside the nucleus, such as the DNA polymerases. Since they are synthesized in the cytosol, there has to be a mechanism that involves targeting and specific transport across the nuclear envelope. The import of those proteins is specified by short sequences of aminoacids known as nuclear localization sequences (NLSs). The mechanism is ATP-dependent and the NPCs diameter can reach 30 nm in diameter. Consequently, covalent attachment on NLS peptides to the condensing agent or the DNA itself will help the nuclear import of the exogenous genetic material[102, 103].

- *Other*: A low percentage of exogenous DNA is always found in the nucleus after transfection. It can be deduced that there exist other entry mechanisms still unknown.

1.3   Bibliography

[1] A.Y. Grosberg. How two meters of DNA fit into a cell nucleus: Polymer models with topological constraints and experimental data. *Polymer Science Series C*, 54(1):1–10, 2012.

[2] B. Alberts, A. Johnson, J. Lewis, M. Raff, K. Roberts, and P. Walter. *Molecular Biology of the Cell. 4th edition.* Garland Science, New York, 2002.

[3] K. Struhl. Fundamentally Different Logic of Gene Regulation in Eukaryotes and Prokaryotes. *Cell*, 98(1):1 − 4, 1999.

[4] Y. Lorch, B. Maier-Davis, and R.D. Kornberg. Mechanism of chromatin remodeling. *Proc. Natl. Acad. Sci.*, 107(8):3458–3462, 2010.

[5] M. Miller, M. Brinkworth, and D. Iles. Paternal DNA packaging in spermatozoa: more than the sum of its parts? DNA, histones, protamines and epigenetics. *Reproduction*, 139:287–301, 2010.

[6] L.R. Brewer, M. Corzett, and R. Balhorn. Protamine-Induced Condensation and Decondensation of the Same DNA Molecule. *Science*, 286(5437):120–123, 1999.

[7] J. DeRouchey, B. Hoover, and D.C. Rau. A Comparison of DNA Compaction by Arginine and Lysine Peptides: A Physical Basis for Arginine Rich Protamines. *Biochemistry*, 52(17):3000–3009, 2013.

[8] V.A. Bloomfield. DNA condensation. *Curr. Opin. Struct. Biol.*, 6:334–41, 1996.

[9] F.H. Crick. The genetic code. *Sci. Am.*, 215(4):66–74, 1962.

[10] E.T. Kool. Preorganization of DNA: Design principles for improving nucleic acid recognition by synthetic oligonucleotides. *Chem. Rev.*, 97(5):1473–1488, 1997.

[11] J.D. Watson and F.H. Crick. Molecular structure of nucleic acids; a structure for deoxyribose nucleic acid. *Nature*, 171:737–738, 1953.

[12] A.and Lavelle C. Carrivain, P.and Cournac, J. Lesne, A.and Mozziconacci, F. Paillusson, L. Signon, J. M. Victor, and M. Barbi. Electrostatics of DNA compaction in viruses, bacteria and eukaryotes: functional insights and evolutionary perspective. *Soft Matter*, 8:9285, 2012.

[13] V. A. Kabanov and A. B. Zezin. Soluble interpolymeric complexes as a new class of synthetic polyelectrolytes. *Pure Appl. Chem.*, 56:343–354, 1984.

[14] R. Duncan and M.J. Vicent. Polymer therapeutics-prospects for 21st century: The end of the beginning. *Adv. Drug Delivery Rev.*, 65(1):60 – 70, 2013.

[15] Y. Yue, F. Jin, R. Deng, J. Cai, Y. Chen, M.C.M. Lin, H.F. Kung, and C. Wu. Revisit complexation between DNA and polyethylenimine - effect of uncomplexed chains free in the solution mixture on gene transfection. *J. Control. Release*, 155:67–76, 2011.

[16] E. Ramsay, J. Hadgraft, J. Birchall, and M. Gumbleton. Examination of the biophysical interaction between plasmid DNA and the polycations, polylysine and polyornithine, as a basis for their differential gene transfection in-vitro. *Int. J. Pharm.*, 210(1â€"2):97 – 107, 2000.

[17] J. Haensler and F.C. Szoka. Polyamidoamine cascade polymers mediate efficient transfection of cells in culture. *Bioconjugate Chem.*, 4(5):372–379, 1993.

[18] F. Amaduzzi, F. Bomboi, A. Bonincontro, F. Bordi, S. Casciardi, L. Chronopoulou, M. Diociaiuti, F. Mura, C. Palocci, and S. Sennato. Chitosan–DNA complexes: Charge inversion and DNA condensation. *Colloids Surf., B*, 114(0):1 – 10, 2014.

[19] S.C. De Smedt, J. Demeester, and W.E. Hennink. Cationic polymer based gene delivery systems. *Pharm. Res.*, 17:113–26, 2000.

[20] H. Eliyahu, Y. Barenholz, and A.J. Domb. Polymers for DNA delivery. *Molecules*, 10:34–64, 2005.

[21] Andre Estevez-Torres and Damien Baigl. DNA compaction: fundamentals and applications. *Soft Matter*, 7:6746–6756, 2011.

[22] O.E. Philippova, T. Akitaya, I.R. Mullagaliev, A.R. Khokhlov, and K. Yoshikawa. Salt-Controlled Intrachain/Interchain Segregation in DNA Complexed with Polycation of Natural Origin. *Macromolecules*, 38:9359–9365, 2005.

[23] A. Zinchenko, K. Yoshikawa, and D. Baigl. Compaction of Single-Chain DNA by Histone-Inspired Nanoparticles. *Phys. Rev. Lett.*, 95:7–10, 2005.

[24] V.A. Bloomfield. DNA condensation by multivalent cations. *Biopolymers*, 44:269–82, 1997.

[25] L.C. Gosule and J.A. Schellman. Compact form of DNA induced by spermidine. *Nature*, 259(5541):333–335, January 1976.

[26] L.C. Gosule and J.A. Schellman. DNA condensation with polyamines: I. Spectroscopic studies. *J. Mol. Biol.*, 121(3):311 – 326, 1978.

[27] J. Widom and R.L. Baldwin. Cation-induced toroidal condensation of DNA. *J. Mol. Biol.*, 144:431–453, 1980.

[28] A. Zinchenko, V.G. Sergeyev, K. Yamabe, S. Murata, and K. Yoshikawa. DNA compaction by divalent cations: structural specificity revealed by the potentiality of designed quaternary diammonium salts. *ChemBioChem*, 5:360–368, 2004.

[29] A. A. Ouameur and H.-A. Tajmir-Riahi. Structural analysis of DNA interactions with biogenic polyamines and cobalt(iii)hexamine studied by fourier transform infrared and capillary electrophoresis. *J. Biol. Chem.*, 279:42041–54, 2004.

[30] A. Y. Grosberg, I. Y. Erukhimovitch, and E. I. Shakhnovitch. On the theory of psi-condensation. *Biopolymers*, 21(12):2413–2432, 1982.

[31] L. S. Lerman. A transition to a compact form of DNA in polymer solutions. *Proc. Natl. Acad. Sci. U.S.A.*, 68(8):1886—1890, August 1971.

[32] V. V. Vasilevskaya, A. R. Khokhlov, Y. Matsuzawa, and K. Yoshikawa. Collapse of single DNA molecule in poly(ethylene glycol) solutions. *J. Chem. Phys.*, 102(16):6595–6602, 1995.

[33] G. Kleideiter and E. Nordmeier. Poly(ethylene glycol)-induced DNA condensation in aqueous/methanol containing low-molecular-weight electrolyte solutionsi. Theoretical considerations. *Polymer*, 40(14):4013 − 4023, 1999.

[34] E. Dauty and J.-P. Behr. Monomolecular condensation of DNA by cationic detergents. *Polym. Int.*, 52:459–464, 2003.

[35] R.S. Dias, A.A.C.C. Pais, M.G. Miguel, and B. Lindman. DNA and surfactants in bulk and at interfaces. *Colloids Surf., A*, 250:115–131, 2004.

[36] K. Hayakawa, J.P. Santerre, and J. C.T. Kwak. The binding of cationic surfactants by DNA. *Biophys. Chem.*, 17(3):175 − 181, 1983.

[37] S.M. Mel'nikov and K. Yoshikawa. First-order phase transition in large single duplex DNA induced by a nonionic surfactant. *Biochem. Biophys. Res. Commun.*, 230(3):514 − 517, 1997.

[38] P. L. Felgner and G. M. Ringold. Cationic liposome-mediated transfection. *Nature*, 337(6205):387–388, January 1989.

[39] M. Macarrone, L. Dini, L. D. Marzio, A. D. Giulio, A. Rossi, G. Mossa, and A. Finazzi-Agró. Interaction of DNA with cationic liposomes: Ability of transfecting lentil protoplasts. *Biochem. Biophys. Res. Commun.*, 186(3):1417 – 1422, 1992.

[40] B. Sternberg, F. L. Sorgi, and L. Huang. New structures in complex formation betweenDNA and cationic liposomes visualized by freeze-fracture electron microscopy. *FEBS Letters*, 356(2–3):361 – 366, 1994.

[41] N.S. Templeton, D.D. Lasic, P.M. Frederik, H.H. Strey, D.D. Roberts, and G.N. Pavlakis. Improved DNA: liposome complexes for increased systemic delivery and gene expression. *Nat Biotech*, 15(7):647–652, July 1997.

[42] S. Huebner, B. J. Battersby, R. Grimm, and G. Cevc. Lipid-DNA complex formation: Reorganization and rupture of lipid vesicles in the presence of DNA as observed by cryoelectron microscopy. *Biophys. J.*, 76(6):3158–3166, 1999.

[43] G. Luque-Caballero, A. Martín-Molina, A.Y. Sánchez-Trevino, M.A. Rodríguez-Valverde, M.A. Cabrerizo-Vílchez, and J. Maldonado-Valderrama. Using AFM to probe the complexation of DNA with anionic lipids mediated by Ca2+: the role of surface pressure. *Soft Matter*, 10:2805–2815, 2014.

[44] M. R. Mozafari and V. Hasirci. Mechanism of calcium ion induced multilamellar vesicle-DNA interaction. *J. Microencapsulation*, 15(1):55–65, 1998.

[45] S. Khiati, N. Pierre, S. Andriamanarivo, M.W. Grinstaff, N. Arazam, F. Nallet, L. Navailles, and P. Barthél'emy. Anionic Nucleotide-Lipids for In Vitro DNA Transfection. *Bioconjugate Chem.*, 20(9):1765–1772, 2009.

[46] P.J. Hagerman. Flexibility of DNA. *Annu. Rev. Biophys. Biophys. Chem.*, 17(1):265–286, 1988.

[47] S. Geggier and A. Vologodskii. Sequence dependence of DNA bending rigidity. *Proc. Natl. Acad. Sci.*, 107(35):15421–15426, 2010.

[48] Z. Reich, R. Ghirlando, and A. Minsky. Nucleic Acids Packaging Processes: Effects of Adenine Tracts and Sequence-Dependent Curvature. *J. Biomol. Struct. Dyn.*, 9(6):1097–1109, 1992.

[49] D. Ben-Amotz and R. Underwood. Unraveling water's entropic mysteries: A unified view of nonpolar, polar, and ionic hydration. *Acc. Chem. Res.*, 41(8):957–967, 2008.

[50] G.S. Manning. Limiting laws and counterion condensation in polyelectrolyte solutions i. colligative properties. *J. Chem. Phys.*, 51:924, 1969.

[51] R.W. Wilson and V.A. Bloomfield. Counterion-induced condensation of deoxyribonucleic acid. A light-scattering study. *Biochemistry*, 18(11):2192–2196, 1979.

[52] M.T. Record Jr, T.M. Lohman, and P. Haseth. Ion effects on ligand-nucleic acid interactions. *J. Mol. Biol.*, 107(2):145 – 158, 1976.

[53] F. Oosawa. Interaction between parallel rodlike macroions. *Biopolymers*, 6(11):1633–1647, 1968.

[54] A. Yu. Grosberg, T. T. Nguyen, and B. I. Shklovskii. The physics of charge inversion in chemical and biological systems. *Rev. Mod. Phys.*, 74:329–345, 2002.

[55] I. Rouzina and V.A. Bloomfield. Macroion attraction due to electrostatic correlation between screening counterions. 1. mobile surface-adsorbed ions and diffuse ion cloud. *J. Phys. Chem.*, 100(23):9977–9989, 1996.

[56] T. T. Nguyen, I. Rouzina, and B. I. Shklovskii. Reentrant condensation of DNA induced by multivalent counterions. *J. Chem. Phys.*, 112(5):2562–2568, 2000.

[57] E.E. Meyer, K.J. Rosenberg, and J. Israelachvili. Recent progress in understanding hydrophobic interactions. *Proc. Natl. Acad. Sci.*, 103(43):15739–15746, 2006.

[58] S. Filippov, C. Konak, P. Kopeckova, L. Starovoytova, M. Spirkova, and P. Stepanek. Effect of hydrophobic interactions on properties and

stability of DNA-polyelectrolyte complexes. *Langmuir*, 26(7):4999–5006, Apr 2010.

[59] S.M. Mel'nikov, V.G. Sergeyev, and K. Yoshikawa. Transition of double-stranded DNA chains between random coil and compact globule states induced by cooperative binding of cationic surfactant. *J. Am. Chem. Soc.*, 117:9951–9956, 1995.

[60] Y.S. Mel'nikova, S.M. Mel'nikov, and J.E. Löfroth. Physico-chemical aspects of the interaction between DNA and oppositely charged mixed liposomes. *Biophys. Chem.*, 81:125–41, 1999.

[61] D. Ibraheem, A. Elaissari, and H. Fessi. Gene therapy and DNA delivery systems. *Int. J. Pharm.*, 459(1–2):70 – 83, 2014.

[62] S.A. Rosenberg, P. Aebersold, K. Cornetta, A. Kasid, R.A. Morgan, R. Moen, E.M. Karson, M.T. Lotze, J.C. Yang, S.L. Topalian, M.J. Merino, K. Culver, A.D. Miller, R. M. Blaese, and W. F. Anderson. Gene transfer into humans - immunotherapy of patients with advanced melanoma, using tumor-infiltrating lymphocytes modified by retroviral gene transduction. *N. Engl. J. Med.*, 323(9):570–578, 1990. PMID: 2381442.

[63] T. Friedmann. Human gene therapy: an immature genie, but certainly out of the bottle. *Nat. Med.*, 2(2):144–147, 1996.

[64] H. Boulaiz, J.A. Marchal, and J. Prados. Non-viral and viral vectors for gene therapy. *Cell. Mol. Biol.*, pages 3–22, 2005.

[65] E. Wagner. Strategies to improve DNA polyplexes for in vivo gene transfer: will "artificial viruses" be the answer? *Pharm. Res.*, 21:8–14, 2004.

[66] F. Martin, M. G. Toscano, M. Blundell, C. Frecha, G.K. Srivastava, M. Santamaria, A.J. Thrasher, and I.J. Molina. Lentiviral vectors transcriptionally targeted to hematopoietic cells by WASP gene proximal promoter sequences. *Gene Ther.*, 12(8):715–723, March 2005.

[67] R. O'Doherty, U. Greiser, and W. Wang. Nonviral methods for inducing pluripotency to cells. *BioMed Research International*, 2013:6, 2013.

[68] N. Montserrat, E. Garreta, F. González, J. Gutiérrez, C. Eguizábal, V. Ramos, S. Borrós, and J.C. Izpisua-Belmonte. Simple generation of human induced pluripotent stem cells using poly-beta-amino esters as the non-viral gene delivery system. *J. Biol. Chem.*, 286:12417–28, 2011.

[69] X. Chen, H. Lv, M. Ye, S. Wang, E. Ni, F. Zeng, C. Cao, F. Luo, and J. Yan. Novel superparamagnetic iron oxide nanoparticles for tumor embolization application: Preparation, characterization and double targeting. *Int. J. Pharm.*, 426(1–2):248 – 255, 2012.

[70] M.A. Dobrovolskaia, P. Aggarwal, J.B. Hall, and S.E. McNeil. Preclinical studies to understand nanoparticle interaction with the immune system and its potential effects on nanoparticle biodistribution. *Mol. Pharmaceutics*, 5:487–95, 2008.

[71] M.A. Dobrovolskaia and S.E. McNeil. Immunological properties of engineered nanomaterials. *Nat. Nanotechnol.*, 2:469–78, 2007.

[72] J.W. Hong, J.H. Park, K.M. Huh, H. Chung, I.C. Kwon, and S.Y. Jeong. PEGylated polyethylenimine for in vivo local gene delivery based on lipiodolized emulsion system. *J. Control. Release*, 99:167–76, 2004.

[73] Y. Wang, P. Chen, and J. Shen. A facile entrapment approach to construct PEGylated polyplexes for improving stability in physiological condition. *Colloids Surf., B*, 58:188–96, 2007.

[74] D. Mehta and A.B. Malik. Signaling mechanisms regulating endothelial permeability. *Physiol. Rev.*, 86(1):279–367, 2006.

[75] K. Greish. Enhanced Permeability and Retention (EPR) Effect for Anticancer Nanomedicine Drug Targeting. In Stephen R. Grobmyer and Brij M. Moudgil, editors, *Cancer Nanotechnology*, volume 624 of *Methods in Molecular Biology*, pages 25–37. Humana Press, 2010.

[76] R. Duncan. Polymer conjugates for tumour targeting and intracytoplasmic delivery. the EPR effect as a common gateway? *Pharm. Sci. Technol. Today*, 2(11):441 – 449, 1999.

[77] F.M. Mickler, Y. Vachutinsky, M. Oba, K. Miyata, N. Nishiyama, K. Kataoka, C. Bräuchle, and N. Ruthardt. Effect of integrin targeting and PEG shielding on polyplex micelle internalization studied by live-cell imaging. *J. Control. Release*, 156:364–73, 2011.

[78] D.R. Somani, S.and Blatchford, O. Millington, M.L. Stevenson, and C. Dufés. Transferrin-bearing polypropylenimine dendrimer for targeted gene delivery to the brain. *J. Control. Release*, 188(0):78 – 86, 2014.

[79] Z. Yin, N. Liu, M. Ma, L. Wang, Y. Hao, and X. Zhang. A novel EGFR-targeted gene delivery system based on complexes self-assembled by EGF, DNA, and activated PAMAM dendrimers. *Int. J. Nanomedicine*, 7:4625–35, 2012.

[80] A. Rata-Aguilar, P. Sanchez-Moreno, A. B. Jódar-Reyes, A. Martín-Rodríguez, H. Boulaiz, J. A. Marchal-Corrales, J. M. Peula-García, and J. L. Ortega-Vinuesa. Colloidal stability and "in vitro" antitumor targeting ability of lipid nanocapsules coated by folate-chitosan conjugates. *J. Bioact. Compat. Polym.*, 27:388–404, 2012.

[81] H. Cheng, J.-L. Zhu, X. Zeng, Y. Jing, X.-Z. Zhang, and R.-X. Zhuo. Targeted gene delivery mediated by folate-polyethylenimine-block-poly(ethylene glycol) with receptor selectivity. *Bioconjugate Chem.*, 20:481–7, 2009.

[82] J.Y. Bae, M. Mie, and E. Kobatake. Targeted Gene Delivery via PEI Complexed with an Antibody. *Appl. Biochem. Biotechnol.*, 168(8):2184–2190, 2012.

[83] D. Vercauteren, R.E. Vandenbroucke, A.T. Jones, J. Rejman, J. Demeester, S.C. De Smedt, N.N. Sanders, and K. Braeckmans. The Use of Inhibitors to Study Endocytic Pathways of Gene Carriers: Optimization and Pitfalls. *Mol. Ther.*, 18(3):561–569, March 2010.

[84] L.K. Medina-Kauwe, J. Xie, and S. Hamm-Alvarez. Intracellular trafficking of nonviral vectors. *Gene Ther.*, 12(24):1734–1751, August 2005.

[85] S.Y. Wong, J.M. Pelet, and D. Putnam. Polymer systems for gene delivery-Past, present, and future. *Prog. Polym. Sci.*, 32(8–9):799 – 837, 2007.

[86] V. Incani, A. Lavasanifar, and H. Uludag. Lipid and hydrophobic modification of cationic carriers on route to superior gene vectors. *Soft Matter*, 6:2124–2138, 2010.

[87] Z. Liu, Z. Zhang, and Y. Zhou, C.and Jiao. Hydrophobic modifications of cationic polymers for gene delivery. *Prog. Polym. Sci.*, 35:1144–1162, 2010.

[88] I.R. de Figueiredo, J.M. Freire, L. Flores, A.S. Veiga, and M.A.R.B. Castanho. Cell-penetrating peptides: A tool for effective delivery in gene-targeted therapies. *IUBMB Life*, 66(3):182–194, 2014.

[89] I.A. Khalil, K. Kogure, H. Akita, and H. Harashima. Uptake Pathways and Subsequent Intracellular Trafficking in Nonviral Gene Delivery. *Pharmacol. Rev.*, 58(1):32–45, 2006.

[90] N. Wattiaux, R.and Laurent, S. W.-D. Coninck, and M. Jadot. Endosomes, lysosomes: their implication in gene transfer. *Adv. Drug Delivery Rev.*, 41(2):201 – 208, 2000.

[91] J.-P. Behr. The Proton Sponge: a Trick to Enter Cells the Viruses Did Not Exploit. *Chimia*, 51(1-2):34–36, 1997.

[92] S. Yang and S. May. Release of cationic polymer-DNA complexes from the endosome: A theoretical investigation of the proton sponge hypothesis. *J. Chem. Phys.*, 129:185105, 2008.

[93] W. Liang and J. K. W. Lam. Endosomal Escape Pathways for Non-Viral Nucleic Acid Delivery Systems. In Brian Ceresa, editor, *Molecular Regulation of Endocytosis.* InTech, 2012.

[94] C.D. Duve, T.D. Barsy, B. Poole, A. Trouet, P. Tulkens, and F. Van Hoof. Lysosomotropic agents. *Biochem. Pharmacol.*, 23(18):2495 – 2531, 1974.

[95] K. Ciftci and R.J. Levy. Enhanced plasmid DNA transfection with lysosomotropic agents in cultured fibroblasts. *Int. J. Pharm.*, 218(1–2):81 – 92, 2001.

[96] A. V. Samoshin, I. S. Veselov, V. A. Chertkov, A. A. Yaroslavov, G. V. Grishina, N. M. Samoshina, and V. V. Samoshin. Fliposomes: new amphiphiles based on trans-3,4-bis(acyloxy)-piperidine able to perform a pH-triggered conformational flip and cause an instant cargo release from liposomes. *Tetrahedron Lett.*, 54(41):5600 – 5604, 2013.

[97] Y. Xu and F.C. Szoka. Mechanism of DNA Release from Cationic Liposome/DNA Complexes Used in Cell Transfection. *Biochemistry*, 35(18):5616–5623, 1996.

[98] E. Wagner. Application of membrane-active peptides for nonviral gene delivery. *Adv. Drug Delivery Rev.*, 38(3):279 – 289, 1999.

[99] E. Wagner, C. Plank, K. Zatloukal, M. Cotten, and M. L. Birnstiel. Influenza virus hemagglutinin HA-2 N-terminal fusogenic peptides augment gene transfer by transferrin-polylysine-DNA complexes: toward a synthetic virus-like gene-transfer vehicle. *Proc. Natl. Acad. Sci.*, 89(17):7934–7938, 1992.

[100] S. Brunner, T. Sauer, S. Carotta, M. Cotten, M. Saltik, and E. Wagner. Cell cycle dependende of gene transfer by lipoplex, polyplex and recombinant adenovirus. *Gene Ther.*, 7:401–407, 2000.

[101] F. Melchior and L. Gerace. Mechanisms of nuclear protein import. *Curr. Opin. Cell Biol.*, 7(3):310 – 318, 1995.

[102] Z. Yang, Z. Jiang, Z. Cao, C. Zhang, D. Gao, X. Luo, X. Zhang, H. Luo, Q. Jiang, and J. Liu. Multifunctional non-viral gene vectors with enhanced stability, improved cellular and nuclear uptake capability, and increased transfection efficiency. *Nanoscale*, 6:10193–10206, 2014.

[103] M.A. Zanta, P. Belguise-Valladier, and J.-P. Behr. Gene delivery: A single nuclear localization signal peptide is sufficient to carry DNA to the cell nucleus. *Proc. Natl. Acad. Sci.*, 96(1):91–96, 1999.

2

METHODOLOGY

The second chapter is dedicated to the description of the materials, protocols and techniques used along this dissertation.

Contents

2.1 Materials

2.1.1 Plasmid DNA

Plasmid DNA was chosen for this thesis due to its unique properties. These circular and double-stranded DNA molecules are usually found naturally in bacteria and they are replicated independently from the chromosomal DNA. Using restriction enzymes, an exogenous gene of interest can be inserted in the sequence and the plasmid can be used for both replication and expression. Accordingly, plasmid DNA can be easily amplify by using competent bacteria and it can also be used to transfect mammalian cells, where the corresponding protein of interest will be expressed. Two plasmids with different biological applications, pEGFP and pRevTre have been used and a detailed description is provided below.

2.1.1.1 *pEGFP*

Reporter genes are frequently used to determine the efficiency of transfection of any gene delivery system. They must provide an easily identifiable or measurable characteristic to the cells expressing it. A convenient reporter for monitoring transfection efficiency is the green fluorescent protein (GFP). When excited by blue or UV light, the protein emits bright green fluorescence light. GFP is typically detected by fluorescence microscopy or flow cytometry. Genes encoding green fluorescent proteins have been cloned from various organisms such as the jellyfish Aequorea Victoria. To facilitate their use as reporters, several GFP variants have been developed and they are commercially available. That is the case of EGFP-C1 which is encoded in the pEGFP-C1 plasmid from Clontech (see Map in Figure 2.1) used in this work. It was kindly provided by Dr. Márquez (Molecular Biology and Biochemistry, University of Málaga, Spain). The plasmid confers resistance to kanamycin (30 μg/mL) to E. coli hosts and its size is 4.7 kbp.
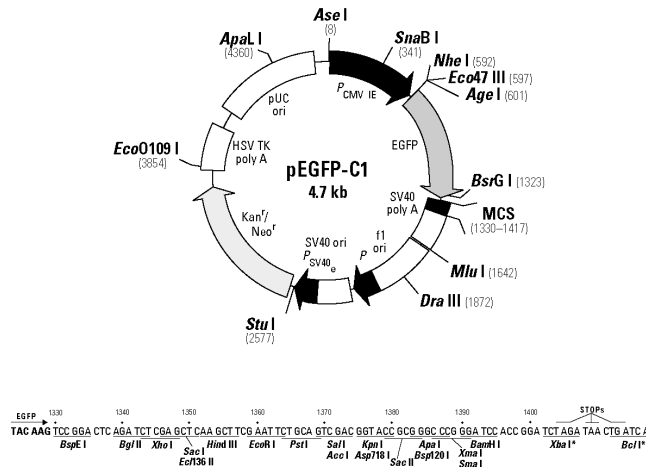
Figure 2.1: Restriction map and multiple cloning sites of pEGFP-C1 (Clontech)

2.1.1.2   *pRevTre-gef*

The majority of the plasmids are intended for transient transfection. This means that the exogenous gene will not be integrated into the genome nor replicated. However, it is possible to use the machinery of naturally occurring retroviruses to integrate a gene of interest into a host cell. And this is the aim of the RevTet-On system (Clontech), that allows the production of stable cell lines with a tetracycline-inducible gene expression system. It is based on the creation of retroviral vectors capable of infecting a wide range of mammalian cells. The gene of interest can be inducibly expressed at high levels in response to varying concentrations of the tetracycline derivative doxycycline (Dox). For that purpose, three elements are needed: the pRevTet-On plasmid, which contains the reverse tetracycline-controlled transactivator (rtTA) , the pRevTre plasmid, which contains the gene of interest, and a cell line capable of producing the retrovirus, such as the Retropack PT67.

In our case, the gene of interest is the gef gene, found in Escherichia coli DNA, which encodes a small (50 amino acids) protein related to cell-killing functions[1]. It was inserted in the pRevTre by Dr. Boulaiz at the Human Anatomy and Embriology Department (IBIMER) of the University of Granada (Spain). The corresponding pRevTre-gef plasmid DNA, with an approximate size of 6.5 kbp was kindly provided by Dr. Boulaiz. The map
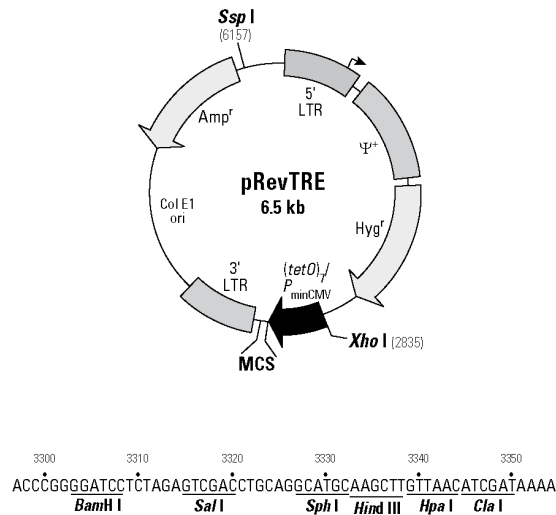
Figure 2.2: Restriction map and multiple cloning sites of pRevTre (Clontech)

of the plasmid can be seen in Figure 2.2. The plasmid confers resistance to ampicillin (50 μg/mL) to E. coli hosts.

2.1.1.3   Bacterial transformation

Bacteria are normally used to store and replicate plasmid DNA, even those designed for use in mammalian cells. For this reason, plasmids include in their sequences a bacterial origin of replication and an antibiotic resistance gene to be used as selectable marker.

Some bacteria strains have been genetically modified to be more easily transformed with exogenous plasmids. This is the case of Top10 or DH5α. Under specific chemical or electrical treatments, bacteria become 'competent', which means that they are more susceptible to transformation.

Transformed DH5α containing the pRevTre-gef were provided by Dr. Boulaiz. To store and amplify the pEGFP plasmid, the competent Escherichia Coli Top10 host strain (Microbiology Department, UGR) was transformed with the heat shock method described below .

The circular region of Whatman filter paper containing the spotted DNA was cut out and placed inside a 1.5 mL microfuge tube. The sample was

allowed to dilute in 100 μL of MilliQ water for 2 hours at room temperature. An aliquot of 10 μL of the plasmid solution was then pipetted into a glass tube placed on ice and 100 μL of previously thawed competent Top10 were added without further mixing. The bacteria were incubated on ice for 20 minutes, followed by heat shock at 42°C for 2 minutes. The tube was returned to ice for another couple of minutes and 1 mL of 2xYT medium was added to allow recovery in a shaking incubator at 37°C for 1 hour. Aliquots of the cell suspension were plated on 2xYT-agar + kanamycin (50 μg/mL) selective plates and incubated overnight at 37°C. Transformant colonies were grown in liquid 2xYT medium for storage and amplification.

2.1.1.4   *Plasmid DNA amplification*

500 μL of the transformed bacteria containing the plasmid were inoculated into 10 mL of 2xYT sterile medium containing antibiotic (50 μg/mL ampicillin for pRevTre-gef or 50 μg/mL of kanamycin for pEGFP) and incubated at 37°C overnight. The next day, aliquots of 5 mL of the cultured cells were added into 1 L of antibiotic-medium in 2L erlenmeyers capped with sterilized hydrophobic cotton plugs to avoid contaminations. The flasks were allowed to grow overnight at 37°C in a shaking incubator.

The transformed E.coli were harvested by centrifugation at 5000g for 5 minutes and the supernatant was discarded. According to the manufacturer's protocol (Figure 2.3), the pellet was subjected to a modified alkaline-SDS lysis and the obtained lysate was cleared by filtration. The binding solution and the silica membrane in the presence of high salts help to the capture of DNA, which can be washed thoroughly. The DNA was finally eluted in endotoxin-free water and it is ready to be used or stored at -20°C.

Experienced User Protocol

❑ **Preparation**:
- Add 3.0 mL RNase A to the Resuspension Solution (600 mL)
- Add 800 mL of 95–100% Ethanol to Wash Solution 2 (200 mL); should additional quantities be needed, add 300 mL of 95–100% Ethanol to Wash Solution 2 (75 mL)
- Chill the Neutralization Solution.

1 Harvest Bacteria

❑ Pellet **2000 mL** of an overnight culture at $5000 \times g$, 10 minutes. Discard supernatant.

2 Prepare Column

❑ Place a Gigaprep Binding Column onto a 45 mm neck bottle (1000 mL).
❑ Add **100 mL** of Column Preparation Solution to Gigaprep Binding Column, apply vacuum and allow it to pass through.

3 Resuspend & Lyse Bacteria

❑ Resuspend cells in **100 mL** of Resuspension RNase Solution. Pipette up and down or vortex to mix.
❑ Add **100 mL** of Lysis Solution and gently invert 10–12 times to mix. Do not vortex. Allow to clear, 3–5 minutes.

4 Prepare Cleared Lysate

❑ Add **100 mL** of Neutralization Solution to the lysed cells and gently shake 10–12 times to mix.
❑ **Empty** entire bag of Lysate Clearing Agent into lysate and gently shake several times to mix. **Incubate 5 minutes at RT.**
❑ Attach the Lysate Filter to a 45 mm neck bottle ($\geq$500 mL).
❑ Add lysate to assembled Lysate Filter and apply the vacuum to clear the lysate of cell debris.
❑ Add **100 mL** of Binding Solution to cleared lysate and swirl to mix.

5 Bind Plasmid DNA to Column

❑ Add cleared lysate to prepared Gigaprep Binding Column, apply vacuum, and allow all lysate to pass through.

6 Wash to Remove Contaminants

❑ Add **40 mL** of EndoCleaning Solution to the Gigaprep Binding Column and allow it to pass through.
❑ Add **150 mL** of Wash Solution 1 to the Gigaprep Binding Column and allow it to pass through.
❑ Add **200 mL** of Wash Solution 2 to the Gigaprep Binding Column and allow it to pass through.
❑ Leave the vacuum on for 25–35 minutes to dry the Gigaprep Binding Column.

7 Elute Purified Plasmid DNA

❑ Attach the Gigaprep Binding Column to another sterile Endo-Free 45 mm neck bottle (150–250 mL).
❑ Add **30 or 50 mL** of Endotoxin-Free Water to Gigaprep Binding Column, **wait 1-2 minutes** and apply vacuum for 2–3 minutes.
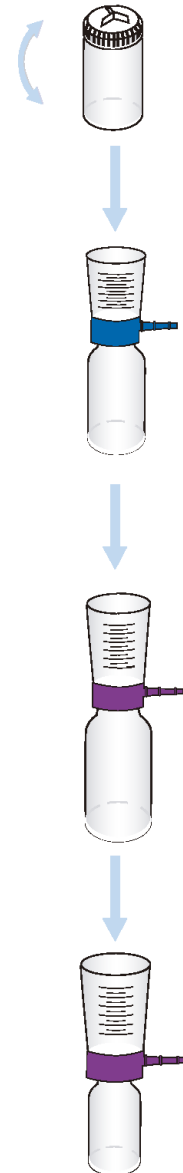
Figure 2.3: Manufacturer's protocol for plasmid amplification. GenElute is a Trademark of Sigma Aldrich Co.

2.1.1.5 *DNA concentration and quantitation*

The ethanol precipitation protocol was followed when a higher concentration of DNA was required. 200 μL of original DNA solution were pipetted into a 2 mL centrifuge tube along with 22 μL of sodium acetate 3M solution and 488 μL of 100% ethanol cold. The solution was thoroughly mixed and incubated on ice for 20 minutes. The DNA was then pelleted by centrifugation at 14000 rpm for 15 minutes at 4°C. The supernatant is discarded and the pellet is washed with 1 mL of 70% ethanol. After 10 minutes of centrifugation, the ethanol is removed and the pellet is air dried. Overdried pellets will take longer to dissolve. The DNA can be resuspended in a volume lower than the original of the required solvent.

DNA concentration is commonly estimated by absorbance at 260 nm (A$_{260}$), wavelength at which the DNA shows maximum absorption due to the aromatic nitrogen bases. Direct measurements of A$_{260}$ can be converted to concentration using the Lambert-Beer law:

$$A = \varepsilon \cdot l \cdot c \qquad\qquad (2.1)$$

where A is the absorbance, ε is the molar extinction coefficient, which for double-stranded DNA is known to be 0.020 mL/($\mu g \cdot cm$), l is the light pathway and c is the concentration(in the units corresponding to ε). Care should be taken to use UV-transparent cuvettes and to keep the A$_{260}$ readings within the linear range (generally 0.1-1). The stock DNA concentration will be obtained multiplying by the dilution factor.
The purity of the DNA solution is routinely checked by reading the absorbance at 280 nm, a wavelength typical of proteins. The ratio A_{260}/A_{280} is kept between 1.7-2.0 in good-quality samples.

2.1.2 Poly(β-aminoester)s synthesis

The poly(β-amino ester)s (pβAEs) used in this dissertation were synthesized by Nathaly Segovia at the Dr. Borrós' group (Material Engineering GEMAT-IQS, University of Ramon Llull, Barcelona). The two-step synthesis

procedure has been previously described[2–4]. Briefly, hexane-1,6-diyl diacrylate was polymerized with 4-amino-1-butanol in a 1.2:1 molar ratio, yielding poly-5-amino-1-pentanol-co-1,4-butanediol diacrylate. 1,3-diaminopropane and 1,3-diaminopentane were added separately to the acrylate-terminated polymer to form B1 and B2 polymer respectively (Structures can be seen in Figure 3.1).

In the case of B3-SS, an equal molar mixture of hexane-1,6-diyl diacrylate and disulfanediylbis(ethane-2,1-diyl) diacrylate was used along with the 4-amino-1-butanol to obtain the acrylate-terminated polymer. 2-methylpentane-1,5-diamine was added to form B3-SS polymer. (Structure can be seen in Figure 4.1)

Each resulting amino-terminated polymer was purified by precipitation in 100 mL of diethyl ether and dried under vacuum. The chemical structure of the polymers was confirmed by 1H NMR. The average molecular weight of the polymers, as confirmed by MALDI-TOF spectra, is 2 kDa in the case of B1 and B2, while the chain length of the B3-SS is slightly longer with 3 kDa. B1 and B2 polymers were used in Chapter 3 and B3-SS was studied in Chapter 4.

2.1.3 | C18-PAMAM synthesis

The dendrimers used in Chapter 5 were kindly provided by Prof. Santoyo (Organic Chemistry Department, University of Granada). Generation 2 PAMAM dendrimer (PAMAM-G2) was purchased from Aldrich. The incorporation of the C18 chain to PAMAM G2 was done by Alicia Megía and the detailed synthesis procedure was previously published.[5]. Briefly, the original bromide functionality of 1-bromooctadecane was replaced by the vinyl sulfonyl group. The obtained vinyl sulfone derivative (0.15 mM, tetrahydrofurane (THF) 15 mL) was added to a solution of PAMAM-G2 (0.3 mM, milliQ-water 15 mL). The mixture was magnetically stirred at room temperature for 1 day. Then the solvent (THF) was evaporated under reduced pressure and the water was freeze-dried. The product was used directly and the correspoding structures can be seen in Figure 5.1. Commercially available reagents and solvents were used as purchased without further purification.

| 2.1.4 | Polyaminoamides synthesis |

The i-shaped polyaminoamides (pAAs) used in Chapter 6 were kindly pro-
vided by Prof. Ernst Wagner (Department Pharmazie, Ludwig-Maximilians-
Universität, München, Germany) and they were synthesized by Claudia
Scholz.

The polymer synthesis is based on the formation of amide bonds using
unnatural or natural aminoacids as monomers. The first monomer is
covalently attached to resin beads in order to retain the polymer on the
solid-phase. The by-products and reagents are easily removed by filtration.
In the final step, the polymer is cleaved from the beads, obtaining a purified
and sequence-defined product.

In this case, a fmoc-Cys(trt)-Wang resin was used to support the whole
synthesis. Protecting fmoc groups were sequentially cleaved with piperidine
and the corresponding monomer was added and incubated until Kaiser test
indicates complete conversion. A double-protected lysine residue was used
to attach two fatty acids to the linear polyaminoamide. After thorough
washing, the resin was treated with a trifluoroacetic solution for cleavage.
The precipitate was collected by centrifugation and lyophilized. The detailed
synthesis is explained by Schaffert et al.[6]. The structure of the three
polymers used can be seen in Figure

| 2.1.5 | Solutions, buffers and media |

Formulation buffer solutions	
HEPES 50 mM pH 7, 10 mL	• 119.2 mg HEPES acid • Adjust pH to 7 with NaOH • H_2O added to 10 mL

HEPES 5 mM pH 7.4, 10 mL	• 11.9 mg HEPES acid • Adjust pH to 7.4 with NaOH • H_2O added to 10 mL
HEPES 20 mM pH 7.4, 10 mL	• 47.7 mg HEPES acid • Adjust pH to 7.4 with NaOH • H_2O added to 10 mL
Acetic acid stock 0.5 M, 25 mL	• 0.72 mL acetic acid • H_2O added to 25 mL
Sodium acetate stock 0.5 M, 25 mL	• 1.025 g sodium acetate • H_2O added to 25 mL
Acetate buffer 50 mM pH 5, 10 mL	• 0.33 mL acetic acid stock solution 0.5M • 0.67 mL sodium acetate stock solution 0.5M • Check pH 5 • H_2O added to 10 mL
Bacterial culture media	
2xYT medium, 2 L	• 62 g 2xYT powder • Heat with frequent agitation and boil if necessary • Adjust pH to 7.4 with NaOH • H_2O added to 2 L; autoclave • Add corresponding antibiotic solution

Ampicillin solution 2000X 100 mg/mL, 10 mL	• 1 g ampicillin sodium salt • H_2O added to 10 mL; sterilized by filtration *Note: Aliquots must be stored in a freezer at -20 ℃*
Kanamycin solution 2000X 100 mg/mL, 10 mL	• 1 g kanamycin sulfate • H_2O added to 10 mL; sterilized by filtration *Note: Aliquots must be stored in a freezer at -20 ℃*
2xYT agar, 250 mL	• 7.75 g 2xYT powder • H_2O added to 250 mL • 5 g agar; autoclave • Place it into a water bath, 55℃ • Add corresponding antibiotic solution • Pour into Petri dishes
DNA concentration	
Acetate buffer 3M pH 5.2, 10 mL	• 2.46 g sodium acetate • Adjust pH to 5.2 with glacial acetic acid • H_2O added to 10 mL *Note: It takes a while to fully dissolve*
Solutions for electrophoresis	

TBE buffer 10X, 250 mL	• 27 g Tris base • 13.75 g boric acid • 10 mL 0.5 M EDTA pH 8.0 • Adjust pH to 7.6 • H_2O added to 250 mL
EDTA 0.5 M pH 8.0, 10 mL	• 1.8612 g EDTA • Adjust pH to 8.0 • H_2O added to 10 mL *Note: It may be necessary to raise the pH to dissolve EDTA powder*
Commercial gel loading buffer	• 0.05 % bromophenol blue • 40 % sucrose • 0.1 M EDTA pH 8.0 • 0.5 % SDS
Homemade gel loading buffer	• 40 % sucrose • Formulation buffer or Milli-Q water
GelRed 3X solution, 250 mL	• 75 μL stock GelRed 10000x in water • H_2O added to 250 mL
DNAse I solution 1000 units, 1 mL	• 50 % glycerol • 10 mM Tris-HCl, pH 7.5 • 10 mM $CaCl_2$ • 10 mM $MgCl_2$
DNAse I 10X reaction buffer, 1 mL	• 200 mM Tris-HCl, pH 8.3 • 20 mM $MgCl_2$
DNAse I stop solution, 1 mL	• 50 mM EDTA

HeLa cells culture	
Dulbecco's Phosphate buffered saline (PBS), 50 mL	• Without $MgCl_2$ and $CaCl_2$ • 0.48 g PBS • H_2O added to 50 mL; autoclave
Homemade phosphate buffered saline (PBS), 1 L	• Without $MgCl_2$ and $CaCl_2$ • 8 g NaCl (137 mM) • 0.2 g KCl (2.7 mM) • 1.44 g Na_2HPO_4 (10 mM) • 0.24 g KH_2PO_4 (2 mM) • Adjust pH to 7.4 with NaOH or HCl • H_2O added to 1 L; filter sterilized
Culture media, 150 mL	• 133.5 mL Dulbecco's Modified Eagle Medium (DMEM) • 15 mL fetal bovine serum (FBS) • 1.5 mL non-essential aminoacid solution (100X) • Autoclave
Trypsin-EDTA solution 0.25 % 1L	• 2.5 g porcine trypsin • 0.2 g EDTA
MTT solution 5 mg/mL, 5 mL	• 25 mg Thiazolyl blue formazan powder • 5 mL PBS *Note: Keep in darkness*
Formazan solubilizing solution, 20 mL	• 10 mL DMSO • 10 mL isopropanol

2.2   Formation of the complexes

The ideal buffer solution would keep the physiological pH and the minimum concentration of buffering compound. Some modifications were done for each system, based on the solubility of the polymers and their buffering capacity.

2.2.1   pβAE polyplexes formation

2.2.1.1   B1 and B2 polyplexes

DNA working solution, containing a plasmid concentration of 20 μg/mL, was obtained by diluting it in HEPES 50 mM solution buffered at pH 7. Polymer stock solutions were prepared in DMSO solvent at a concentration of 100 mg/mL. Working dilutions of each polymer were prepared prior to each use in HEPES buffer 50 mM, pH 7. The DNA solution was added to an equal volume of the polymer solution (containing the desired concentration) and immediately mixed by thorough pipetting. The complexes were allowed to self-assemble at room temperature for 30 min. The ratio polymer/DNA was expressed as weight ratio (w/w). pRevTre plasmid was used for all the experiments, except for the transfection studies, where we used pEGFP due to the need of a reporter gene, not present in the pRevTre.

2.2.1.2   B3-SS polyplexes

DNA working solution, containing a plasmid concentration of 20 μg/mL, was obtained by diluting it in HEPES 50 mM solution buffered at pH 7 or acetate buffer 50 mM, pH 5. Polymer stock solution was prepared in DMSO solvent at a concentration of 100 mg/mL. Working dilutions of the polymer were prepared prior to each use in the corresponding buffer (pH 5 or pH 7). The DNA solution was added to an equal volume of the polymer solution (containing the desired concentration) and immediately mixed by thorough pipetting. The complexes were allowed to self-assemble at room

temperature for 30 min. The ratio polymer/DNA was expressed as weight ratio (w/w) and the plasmid used was pEGFP.

2.2.2   Dendriplexes formation

DNA working solution at 20 μg/mL was prepared in HEPES 5 mM pH 7.4. Dendrimer stock solutions were prepared in a mixture of DMSO:water (1:2) at a concentration of 20 mg/mL. Working dilutions of each dendrimer were prepared prior to each use in HEPES buffer 5 mM at pH 7.4. The DNA solution was added to an equal volume of the dendrimer solution (containing the desired concentration) and immediately mixed by thorough pipetting. The complexes were allowed to self-assemble at room temperature for 30 min. The ratio between DNA and dendrimer was expressed as Z=N/P (the ratio between protonable nitrogen residues of the dendrimer and DNA phosphate-groups), and the plasmid used was pEGFP.

2.2.3   pAA polyplexes formation

DNA working solution at 20 μg/mL was prepared in HEPES 20 mM pH 7.4. Polymer stock solutions were prepared in HEPES 20 mM pH 7.4 at a concentration of 20 mg/mL. Working dilutions of each polymer were prepared prior to each use in the same buffer solution. The DNA was added to an equal volume of the polymer solution (containing the desired concentration) and immediately mixed by thorough pipetting. The complexes were allowed to self-assemble at room temperature for 30 min. The ratio between DNA and polymer was expressed as Z=N/P (the ratio between protonable nitrogen residues of the polymer and DNA phosphate-groups) and the plasmid used was pEGFP.

| 2.2.4 | DNA retardation by EMSA |

Formation of polyplexes was confirmed by gel retardation using the electrophoretic mobility shift assay (EMSA). This is a common technique used to characterize DNA complexes. EMSA is based on the observation that complexes migrate through a gel more slowly than naked DNA. In its free form, DNA slips through the holes in the lattice formed by agarose while the complexes are retarded or even stopped.

The agarose gel was prepared by suspending 1%(w/v) powder agarose in TBE buffer 1X. The solution is placed in an Erlenmeyer flask lightly stoppered with a glass marble and microwaved until the solution becomes clear and no crystals remain. It is recommended to stop and swirl every 10 seconds. Once the solution has cooled to 50-55 ^{o}C it is poured into the corresponding casting tray containing the comb and allowed to cool completely. Bubbles must be exploded with a pipette tip. The solidified gel should be submerged in the running buffer TBE 1X to avoid drying.

DNA concentration must be kept above 80 ng per well in order to be visualized correctly. In our case, 200 ng of DNA per well were used and complexes were formed at corresponding ratios in a maximum volume of 10 μL. Since the gel is immersed in the buffer solution, the density of the samples shall be increased so they sink into the well. Commercial loading solutions contain bromophenol blue, which is a tracking dye that migrates in the same direction as DNA at a rate corresponding to a small fragment of 500 bp. However, its negative charge may interfere in the mobility of the complexes, so a homemade loading buffer has been used instead, consisting of sacarose 40%(w/v) in the same buffer used for condensation. 2 μL are added to each sample before loading them into the wells. One of the wells is loaded with DNA and the commercial loading solution with bromophenol blue in order to use the dye line as an indicator of the running time. The gel is run at 100 V, taking into account that the DNA will move toward the positive electrode (red). Once the electrophoresis had finished, the gel is stained in a 3X GelRed^{TM} solution (Labnet biotécnica, Madrid) for 20 minutes and destained in water for another 10 minutes in order to clear the background. The obtained bands are visualized on a UV illuminator and photographed for posterior analysis.

2.2.5 Hydrodynamic diameter by DLS

The average hydrodynamic diameter of the complexes was determined by cumulant analysis of dynamic light scattering (DLS) using a Zetasizer NanoZeta ZS device (Malvern Intruments Ltd, U.K.) working at 25°C with a He-Ne laser beam (633 nm), and using a scattering angle of 173°. For data analysis, the viscosity (0.8905 mPa/s) and refractive index (1.333) of pure water at 25°CC were used. Results are given as mean values of three runs of 60 s duration each. All measurements were carried out in duplicates at 25°C.

The cumulants analysis of the device gives two values, a mean value for the size, and the Polydispersity Index (PDI). The PDI is a parameter that indicates the heterogeneity of the sizes of the sample. When obtained from cumulant analysis, as in the case of the Malvern device, its ranges are 0-1, being 0 complete uniformity. The Z-average size can only be used to compare results with samples measured in the same dispersant, by the same technique, i.e. by Dynamic Light Scattering (DLS). In our case, we use this value to compare between samples prepared under the same conditions and same dispersant, but sometimes this size does not correspond to a real diameter since the systems might be polydisperse. If the polydispersity is over 0.5, a distribution analysis should be used to determine the peak positions. Intensity distributions were obtained from the manufacturer's software. Error bars correspond to standard deviation.

2.2.6 Size distribution by NTA

The Nanoparticle Tracking Analysis (NTA) technique combines light scattering and Brownian motion to calculate the size of the particles in suspension. By using a high-sensitivity CMOS camera (30 frames per second), mounted on a conventional microscope, a video of the particles moving under Brownian motion is recorded.

The NTA software identifies the centre of each particle and determines its two-dimensional position frame by frame. The x and y coordinates along
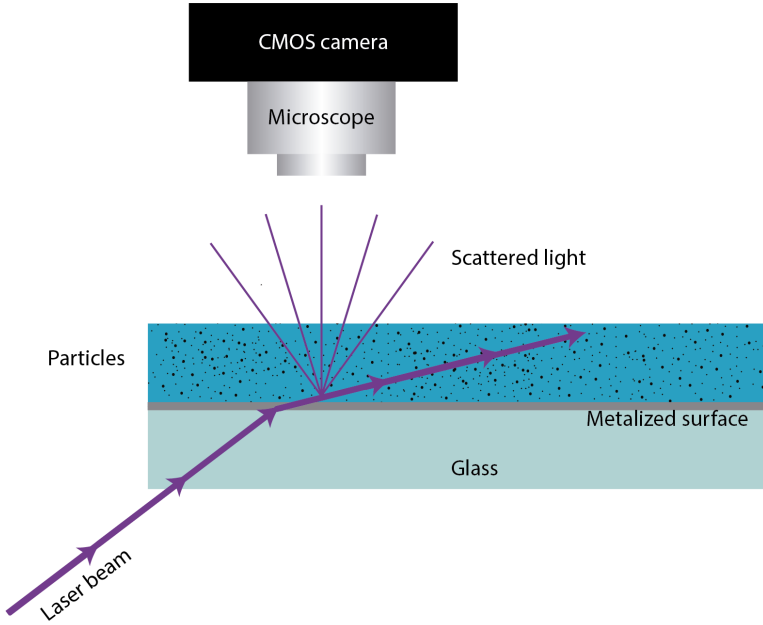
Figure 2.4: Schematic representation of the Nanosight set-up.

with the lag time $(\tau = \frac{1}{30}s)$ between frames are used to calculate the average distance moved by each particle in the x and y direction, i.e. the mean squared displacement (MSD) of the particles.

$$MSD = \langle [\overline{r_{xy}(t+\tau)} - \overline{r_{xy}(t)}]^2 \rangle \qquad (2.2)$$

being r_{xy} the vector that defines the position of the particle.

The sphere-equivalent hydrodynamic diameter (d_h) can be calculated through the particle diffusion coefficient (D) using the Stokes-Einstein equation (2.3). Since the Brownian motion occurs in three dimensions, but the device takes into account only two, the MSD has been adjusted.

$$\frac{MSD}{4t} = D = \frac{TK_b}{3\pi\nu d_h} \qquad (2.3)$$

where T is the temperature, K_b is the Boltzmann's constant, t is the time and ν is the viscosity of the solvent.

This results in a particle size distribution of high resolution, since the

particles are measured one by one. The advantages and drawbacks of this technique compared to usual DLS studies have been extensively contrasted in a paper reported by Filipe et al[7].

For NTA experiments, polyplexes were used at a final DNA concentration of 0.05 μg/mL by diluting the polyplexes with the formulation buffer. NTA measurements were performed with a NanoSight LM10-HS(GB)FT14 (NanoSight, Amesbury, UK), equipped with a sample chamber with a 404-nm laser and a high-sensitivity CMOS camera. The samples were injected in the sample chamber with sterile syringes (BD Discardit II, New Jersey, USA). All samples were measured three times for 60 s with manual shutter, gain, brightness, and threshold adjustments at 25^oC. The video images of the particles were captured and analysed by the NTA 2.3 image analysis software (NanoSight, Salisbury, UK).

2.2.7 Electrophoretic mobility

Electrophoresis[8] is the movement of charged colloidal particles or poly-electrolytes, immersed in a liquid and under the influence of an external electric field (E) that will determine their electrophoretic velocity (v_e). If the field is uniform, the relationship between both parameters will be linear, and the coefficient of proportionality is known as electrophoretic mobility, $\mu_e(m^2s^{-1})$.

$$v_e = \mu_e E \tag{2.4}$$

The electrophoretic mobility is related to the effective surface charge of the particles, and it is expressed as possitive if the particles move to the negative electrode and vice versa. μ_e was measured by the technique of laser Doppler electrophoresis with a Zetasizer NanoZeta ZS (Malvern Instruments Ltd, Worcestershire, UK) using folded capillary cells. All the measurements were carried out in duplicates at 25^oC.

The morphology of some of the complexes was investigated by transmission electron microscopy (TEM). Freshly prepared polyplexes at a DNA concentration of 8 μg/mL were deposited on Formvar/carbon coated copper grids and allowed to settle for 5 minutes at room temperature. The complexes were stained by the addition of 2% uranyl acetate solution and the excessive liquid was soaked down. The grid was air-dried for 30 minutes at room temperature and the images were collected at the Center of Scientific Instruments of the University of Granada in a LIBRA 120 PLUS electron microscope, Carl Zeiss SMT.

2.3 Stability of the complexes

2.3.1 Temporal stability

The durability of the complexes was evaluated by monitoring the evolution of the hydrodynamic diameter with time. Typically, an increase in the particle size is understood as aggregation. But since our particles are interpolyelectrolyte complexes (IPEC), swelling due to disassembly shall also be considered. We have used static light scattering, this is, the mean scattered intensity, to elucidate whether the size increase corresponds to aggregation or disassembly. The mean count rate expressed as kilocounts per second (kcps) will increase if aggregation takes place. On the other hand, when disassembly and swelling occur, the refractive index of the particles decreases and becomes similar to that of the solvent, resulting in a decrease of the mean count rate.

The SLS and DLS data were recorded simultaneously for each sample using a Zetasizer NanoZeta ZS device (Malvern Intruments Ltd, UK) working at 25°C with a He-Ne laser beam (633 nm) and using a scattering angle of 173°. Complexes were prepared as previously described, being the final DNA concentration 8 μg/mL.

| 2.3.2 | Colloidal stability: Effect of salinity |

Colloidal stability against NaCl concentration was analysed by using a Beckman DU 7400 spectrophotometer (Beckman, Fullerton, USA), setting the wavelength at 380 nm. Equal volumes (0.3 mL) of salt (NaCl) and particle solutions were mixed into the scattering cell, and the absorbance was recorded for 120 s in each experiment. If particles aggregate, the turbidity of the sample increases in a linear way during the first seconds. The initial slopes of the absorbance versus time curves (dAbs/dt) serve to determine the stability ratio "W", also called Fuchs factor, which is a parameter broadly used in colloidal stability studies. It can be experimentally derived from equation 2.5

$$W = \frac{(dAbs/dt)f}{(dAbs/dt)s} \qquad (2.5)$$

in which (dAbs/dt)f corresponds to the fastest coagulation regime, and (dAbs/dt)s is the slope for slower coagulation kinetics. The stability factor is a measurement of the average number of collisions that must suffer two colliding particles before they are kept definitively stuck. In this sense, if W =1 the system is totally unstable, while W = ∞ means total stability. Detailed information about experimental calculation of "W" can be found in bibliography[9, 10]. The analysis of the stability factor of colloidal systems versus salinity may be useful to determine the overall hydrophobic/philic character of the particle surface. In addition, it serves to get information about the electrical state of the surface. For hydrophobic charged surfaces, the well-known DLVO theory predicts a progressive loss of stability upon salt addition. Once the aggregation process reaches their maximum kinetics –at that salt concentration known as CCC (critical coagulation concentration)– the system remains unstable even for higher salt concentrations added. However, for partially hydrophilic charged surfaces, a restabilization mechanism may appear at moderate or high salinity conditions. This stabilization process comes from the action of the so-called hydration forces, which are structural short-range repulsive forces that arise from the overlapping of the structural water and the hydrated-ion layers that surround the hydrophilic particles. Detailed information can be consulted in specific

references[11–13].

To sum up, if a particle is hydrophilic, a repulsive potential barrier appears when two particles approach each other to collapse in a high salt concentration medium. This barrier slows down the aggregation process, eventually being completely avoided. It is known as critical stabilization concentration (CSC) the minimum salt concentration necessary to make this repulsive barrier appear. Generally, the CCC value gives information about the effective surface charge of the particle (complementing the zeta-potential data), while the CSC informs about the hydrophilic character of the surface. The higher the CCC data, the higher the surface charge. However, the higher the CSC, the lower the hydrophilicity of the particles. That is, a hydrophilic surface needs a lower salt concentration to create a protective structural shell of water and ions around it to prevent the contact with another similar surface. In this sense, the CSC values become a good criterion to quantitatively classify colloidal particles with regard to their hydrophobic/philic character.

2.3.3 │ DNAse I digestion

Deoxyribonucleases (DNAses) are the enzymes that hydrolyze the phospho-diester bonds within the DNA backbone. If the enzyme removes nucleotides exclusively at the end of the chain, it is called exonuclease. Conversely, endonucleases cleave the nucleic acid chains in the interior. Deoxyribonuclease I (DNAse I) is a non-specific (without regard to sequence) endonuclease capable of hydrolyze single and double stranded DNA, and it is widely used in Molecular Biology.

When polyplexes are exposed to nucleases, the enzyme can only cleave the DNA portions that are accessible from the outward. Therefore, DNAse I digestion may unveil details on DNA location and accessibility in the complex. Polyplexes were exposed to DNAse I under standard conditions with recommended buffers (20 mM Tris-HCl, pH 8.3, 2 mM $MgCl_2$). After polyplex formation, they were incubated with 5 IU of DNase per μg of DNA for periods of time from 1 minute to 75 minutes. Naked DNA was completely degraded in approximately 1 minute when incubated with the

same amount of DNAse I. The enzymatic reaction was terminated by the addition of 1 μL of Stop Solution (50 mM EDTA). The DNA was then separated from the polymers by incubating with SDS 1% and heparin overnight. Without further purification, samples were electrophoresed on a 1% (w/v) agarose gel at 100 V for 40 minutes. After GelRed staining, the gel was photographed under UV.

2.3.4 Stability upon dilution

Dilution might be a stress mechanism[14] usually suffered by self-assembled systems, but not always considered. Information regarding the complex stability after dilution would be useful for physicochemical studies of the polyplexes as well as for biological purposes, since they have to be diluted into a complex medium. In order to evaluate the effect of dilution on our polyplexes, changes in size were monitored after a dilution of 1:200 from the original formulation. NTA was chosen as a suitable technique for our purpose due to the possibility of analyzing different size populations of highly diluted systems.

2.3.5 Stability under reducing conditions

The polymer B3-SS contains disulfide bonds, which are reversible under reducing conditions. The destabilization of the polymer is expected to trigger the disassembly of the complex and, consequently, DNA should be released. Polyplexes formed with B3-SS as previously described were exposed to the reducing agent β-mercaptoethanol (β-ME). 1 μL of β-ME were added to 10 μL of the complexes and incubated at 37°C for 2 hours. Each sample was mixed with 2 μL of homemade loading buffer and electrophoresed on a 1% (w/v) agarose gel at 100 V for 40 minutes. After GelRed staining, the gel was photographed under UV and the results were compared to untreated complexes.

2.4   *In vitro* activity of the complexes

2.4.1   Interaction with a cell membrane model

Lipid membrane models can be used to elucidate the interaction of nanocarriers with the phospholipids of biological membranes. These studies might help to design and develop more efficient delivery systems[15].

Phospholipid monolayers can be formed at the air/water interface and they are generally stable and well-defined. The interaction with colloidal delivery systems has been investigated by means of (a) adsorption kinetics of the materials onto the interface, (b) surface dilatational rheology studies, and (c) adsorption isotherms.

2.4.1.1   *Adsorption kinetics*

We determined the interfacial tension as a function of time for different systems in order to study their kinetics of adsorption onto a dipalmitoylphopshpatidyl choline (DPPC) monolayer.
The surface characterization of the mixed system has been made in the OCTOPUS. This is a Pendant Drop Surface Film Balance equipped with a subphase multi-exchange device fully designed and assembled at the University of Granada (patent submitted P201001588) and described in detail in the bibliography[16]. The detection and calculation of surface area and surface tension is done with the DINATEN software, based on Axisymmetric Drop Shape Analysis (ADSA)[17].

An HEPES solution droplet is formed first at the tip of the double coaxial capillary. By deposition with a microsyringe a fixed amount of DPPC dissolved in chloroform is spread onto the drop surface to provide a surface pressure of 20 mN/m. After evaporation of the solvent and equilibration of the surface pressure, the buffer subphase is exchanged by simultaneously injecting the new solution and extracting the bulk subphase[18, 19]. After complete exchange of the subphase we monitor the surface pressure at constant surface area for 20 minutes.

The surface tension of the clean surface was measured before every experiment, in order to confirm the absence of surface-active contaminants, yielding values of $72.5 \pm 0.5 \; mN/m$ at 20ºC.

2.4.1.2 *Surface dilatational rheology*

Dilatational rheology quantifies the viscoelastic response of the interfacial layer to a dilatational deformation. With the pendant drop technique, changes in the interfacial area are induced by injecting and extracting liquid at a controlled rate, and the interfacial tension is simultaneously calculated by DINATEN. This gives information about the structure, intermolecular interactions and molecular rearrangement during deformation processes.

The interfacial elasticity (E') quantifies the stiffness of an interface when subjected to a dilatational compression and expansion. Accordingly, it was defined by Gibbs as the relationship between the change in the interfacial tension ($d\gamma$) and the change in the interfacial area (d lnA):

$$E' = \frac{d\gamma}{d \ln A} = \frac{d\gamma}{(dA/A)} \tag{2.6}$$

On the other hand, interfacial viscosity (η) characterizes the resistance of the interfacial tension to change upon gradual deformation of the interfacial area. Consequently, it is time-dependent and it can be expressed as:

$$\eta = \frac{d\gamma}{(d \ln A/dt)} \tag{2.7}$$

Typically, materials exhibit both, elastic and viscous behavior. The change in the interfacial tension is expressed as the sum of both contributions. By using 2.6 and 2.7:

$$d\gamma = E'(dA/A) + \eta \frac{(dA/A)}{dt} \tag{2.8}$$

The interfacial material functions can be developed[20], finally obtaining:

$$E' = \frac{\gamma_a}{(A_a/A)} cos(\delta) \tag{2.9}$$

$$\eta = \frac{\gamma_a}{(A_a/A)} sin(\delta) \cdot \omega^{-1} \qquad (2.10)$$

where A_a is the area amplitude, δ is the phase angle, γ_a is the tension amplitude and ω is the angular frequency.

Both parameters, E' and η were calculated with the image analysis program CONTACTO. Once the subphase exchange with the corresponding solution was completed, the drop was subjected to dilatational deformation by imposing cycles of 10 oscillations at different frequencies. The reproducibility of the experiments was tested by performing at least three replicate measurements. The surface tension of the clean surface was measured before every experiment, in order to confirm the absence of surface-active contaminants, yielding values of $72.5 \pm 0.5\ mN/m$ at 20^oC.

2.4.2 | Transfection studies

With the aim of testing the capability of the complexes to efficiently deliver the plasmid DNA into the nucleus, *in vitro* assays were performed. The pEGFP plasmid was used in all cases in order to evaluate the expression of the reporter Green Fluorescent Protein (GFP).

2.4.2.1 *Cell culture*

Human cervix carcinoma HeLa cell line was purchased from the Cell Bank of the Center of Scientific Instruments of the University of Granada. The cultured cells were grown in DMEM (Sigma-Aldrich, Milwaukee, USA) supplemented with 1% non-essential amino acids and 10% fetal bovine serum (FBS), at 37^oC and 5% CO_2.

For cell passaging, culture medium is removed and the adherent cells were washed twice with sterile PBS without calcium and magnesium. 2 mL of trypsin-EDTA solution was added and incubated for 5 minutes at 37^oC. In order to stop the reaction, 8 mL of DMEM were added and cells were sedimented by centrifugation at 1000g for 5 minutes. Pellet was resuspended

in 10 mL of culture medium and cells were counted using a Neubauer counter chamber according to the established procedure.

2.4.2.2   Transfection procedure

HeLa cells were seeded into 24-well plates at a density of 100 000 cells/well. After 24 h, culture medium was replaced with 400 μL fresh serum-free DMEM. DNA complexes (polyplexes or dendriplexes) at the desired polymer/DNA ratios in 100 μL of corresponding buffer containing 0,5 μg pDNA were added to each well and incubated at 37°C for 40 minutes. The transfection medium was replaced with supplemented DMEM (10% FBS, 1% non-essential aminoacids) and cells were incubated for further 24 hours. Subsequently, cells were washed twice with 500 μL PBS, detached with trypsin/EDTA solution and taken up in PBS. GFP expression was evaluated at the Center of Scientific Instruments of the University of Granada by flow cytometry(BECTON DICKINSON FACSCanto II). Cells transfected with polyethyleneimine (PEI) at a N/P ratio of 6 were used as positive control.

2.4.2.3   MTT toxicity assay

The MTT (3-[4,5-dimethylthiazol-2-yl]-2,5 diphenyl tetrazolium bromide) colorimetric assay is based on the conversion of MTT into formazan crystals by living cells, which determines mitochondrial activity. For the majority of cell lines the total mitochondrial activity is related to the number of viable cells, and consequently this assay is widely used to evaluate the *in vitro* cytotoxic effects of substances on cells.[21]

NAD(P)H-dependent cellular oxidoreductase enzymes reduce the yellow MTT to insoluble formazan, which has a purple color. Solvation of formazan crystals produces a colored solution that can be quantified by measuring absorbance at 570 nm.

HeLa cells were seeded into 96-well plates at a density of 10 000 cells/well. After 24 h, culture medium was replaced with 80 μL fresh DMEM. pDNA complexes at desired ratios in corresponding buffer containing 100 ng pDNA were added to each well and incubated at 37°C for 40 minutes. The transfection medium was replaced with supplemented DMEM (10% FBS, 1% non-essential aminoacids) and cells were cultured for further 24 h.

Culture media was replaced with 100 μL of fresh media and then 50 μL of MTT reagent (5 mg/mL in PBS) was added to each well. Following a 4 hour incubation at 37°C, medium was replaced with 100 μL/well of solvent (50% DMSO, 50% isopropanol).

Absorbance at 570 nm was read at the Center of Scientific Instruments of the University of Granada in a Nanoquant Infinite M200 Pro (Tecan) analyzer. Untreated cells were used as positive control (100% viable).

2.5   Bibliography

[1] H. Boulaiz, J. Prados, J.A. Marchal, A.M. García, L. Álvarez, C. Melguizo, E. Carrillo, J.L. Ramos, and A. Aránega. Transfection of MS-36 melanoma cells with gef gene inhibits proliferation and induces modulation of the cell cycle-. *Cancer Sci.*, 94(6):564–568, 2003.

[2] G.T. Zugates, W. Peng, A. Zumbuehl, S. Jhunjhunwala, Y.H. Huang, R. Langer, J.A. Sawicki, and D.G. Anderson. Rapid optimization of gene delivery by parallel end-modification of poly(beta-amino-amino ester)s. *Mol. Ther.*, 15:1306–1312, 2007.

[3] J. Green, G. Zugates, N. Tedford, Y.H. Huang, L. Griffith, D. Lauffenburger, J. Sawicki, R. Langer, and D. Anderson. Combinatorial modification of degradable polymers enables transfection of human cells comparable to adenovirus. *Adv. Mater.*, 19:2836–2842, 2007.

[4] N. Montserrat, E. Garreta, F. González, J. Gutiérrez, C. Eguizábal, V. Ramos, S. Borrós, and J.C. Izpisua-Belmonte. Simple generation of human induced pluripotent stem cells using poly-beta-amino esters as the non-viral gene delivery system. *J. Biol. Chem.*, 286:12417–28, 2011.

[5] J. Morales-Sanfrutos, A. Megia-Fernandez, F. Hernandez-Mateo, M.D. Giron-Gonzalez, R. Salto-Gonzalez, and F. Santoyo-Gonzalez. Alkyl sulfonyl derivatized PAMAM-G2 dendrimers as nonviral gene delivery vectors with improved transfection efficiencies. *Org. Biomol. Chem.*, 9:851–64, 2011.

[6] D. Schaffert, C. Troiber, and E. Wagner. New sequence-defined polyaminoamides with tailored endosomolytic properties for plasmid DNA delivery. *Bioconjugate Chem.*, 2012.

[7] V. Filipe, A. Hawe, and W. Jiskoot. Critical evaluation of Nanoparticle Tracking Analysis (NTA) by NanoSight for the measurement of nanoparticles and protein aggregates. *Pharm. Res.*, 27:796–810, 2010.

[8] A. V. Delgado, F. González-Caballero, R. J. Hunter, L. K. Koopal, and J. Lyklema. Measurement and interpretation of electrokinetic phenomena. *J. Colloid Interface Sci.*, 309(2):194 – 224, 2007. Elkin 06, International Electrokinetics Conference, June 25-29, Nancy, France.

[9] T. López-León, M.J. Santander-Ortega, J.L. Ortega-Vinuesa, and D. Bastos-González. Hofmeister effects in colloidal systems: influence of the surface nature. *J. Phys. Chem. C*, 112(41):16060–16069, 2008.

[10] J.M. Peula-García, J.L. Ortega-Vinuesa, and D. Bastos-González. Inversion of hofmeister series by changing the surface of colloidal particles from hydrophobic to hydrophilic. *J. Phys. Chem. C*, 114(25):11133–11139, 2010.

[11] R. M. Pashley. Hydration forces between mica surfaces in aqueous electrolyte solutions. *J. Colloid Interface Sci.*, 80(1):153–162, 1981.

[12] N.V. Churaev and B.V. Derjaguin. Inclusion of structural forces in the theory of stability of colloids and films. *J. Colloid Interface Sci.*, 103(2):542–553, 1985.

[13] J.A. Molina-Bolívar and J. L. Ortega-Vinuesa. How proteins stabilize colloidal particles by means of hydration forces. *Langmuir*, 15(8):2644–2653, 1999.

[14] T. Miller, A. Hill, S. Uezguen, M. Weigandt, and A. Goepferich. Analysis of immediate stress mechanisms upon injection of polymeric micelles and related colloidal drug carriers: implications on drug targeting. *Biomacromolecules*, 13:1707–18, 2012.

[15] C. Peetla, A. Stine, and V. Labhasetwar. Biophysical interactions with model lipid membranes: Applications in drug discovery and drug delivery. *Mol. Pharmaceutics*, 6(5):1264–1276, 2009. PMID: 19432455.

[16] J. Maldonado-Valderrama, J. A. Terriza, Holgado, A. Torcello-Gómez, and M. A. Cabrerizo-Vilchez. In vitro digestion of interfacial protein structures. *Soft Matter*, 9:1043–1053, 2013.

[17] D.Y. Kwok, D. Vollhardt, R. Miller, D. Li, and A. W. Neumann. Axisymmetric drop shape analysis as a film balance. *Colloids Surf., A*, 88(1):51 − 58, 1994. A collection of papers presented at the 67th Colloid and Surface Science Symposium of the Colloid and Surface Science Division of the American Chemical Society.

[18] H. A. Wege, J.A. Holgado-Terriza, and M.A. Cabrerizo-Vílchez. Development of a constant surface pressure penetration langmuir balance based on Axisymmetric Drop Shape Analysis. *J. Colloid Interface Sci.*, 249(2):263 − 273, 2002.

[19] J. Maldonado-Valderrama, T. Torcello-Gómez, A.and del Castillo-Santaella, J.A. Holgado-Terriza, and M.A. Cabrerizo-Vílchez. Subphase exchange experiments with the pendant drop technique. *Adv. Colloid Interface Sci.*, (0):–, 2014.

[20] A. Torcello-Gómez. *Application of interfacial properties of polymeric surfactants in physiological processes for biomedical and nutraceutic purposes.* PhD thesis, University of Granada., 2012.

[21] J. van Meerloo, G.J.L. Kaspers, and J. Cloos. Cell Sensitivity Assays: The MTT Assay. In *Cancer cell culture. Methods and Protocols.*, chapter 20, pages 237–245. Humana Press, 2011.

3

PβAE/DNA COMPLEXES: INFLUENCE OF ALKYL CHAINS

In this third chapter, the role of short hydrophobic chains in the properties of poly(β-aminoester)/DNA complexes is analyzed.

Contents

3.1   Background and motivation

Poly(β-amino ester)s[?, 1–3](pβAEs) are a class of degradable cationic polymers containing tertiary amines in their backbones. The synthesis is based on the conjugate addition of bis(secondary amine) monomers to diacrylate esters[1]. These polymers degrade spontaneously into nontoxic small molecule byproducts due to the hydrolysis of the ester bonds. P(β)AEs have the ability to assemble plasmid DNA into nanometer-scale polymer/DNA complexes. The interaction between both positively and negatively charged polymers have been described extensively in literature, being mainly electrostatic, and it is influenced by several parameters such as pH, added salt and its nature, molecular weight and charge density[4–7].

On the other hand, hydrophobic interactions are rarely considered in the formation and behavior of the so-called polyplexes. Many hydrophobic modifications have been reported due to the improvement of internalization of the complexes when long hydrophobic chains interact with the cell membrane[8, 9] and some systematic physicochemical studies have been reported[10, 11]. However, fewer papers are focused on the influence of short hydrophobic moieties ˘ which do not improve transfection efficiency by themselves ˘ on the formation and final properties of the polyplexes. We have selected two different p(β)AEs, referred to as B1 and B2, that differ in the presence (or absence) of a short hydrophobic ethyl group in both ends. Their structures can be seen in Figure 3.1.

The aim of this chapter is to determine the influence of those small hydrophobic moieties on the compaction of the plasmid DNA pRevTre-gef and the subsequent effect on the colloidal properties of the complexes and their transfection ability. B1 and B2 polymers have an average molecular weight of 2kDa and an approximate number of (primary, secondary and tertiary) amino groups per molecule of 10, which are values low enough to evaluate possible hydrophobic contributions that would be masked if electrostatic interactions were stronger.
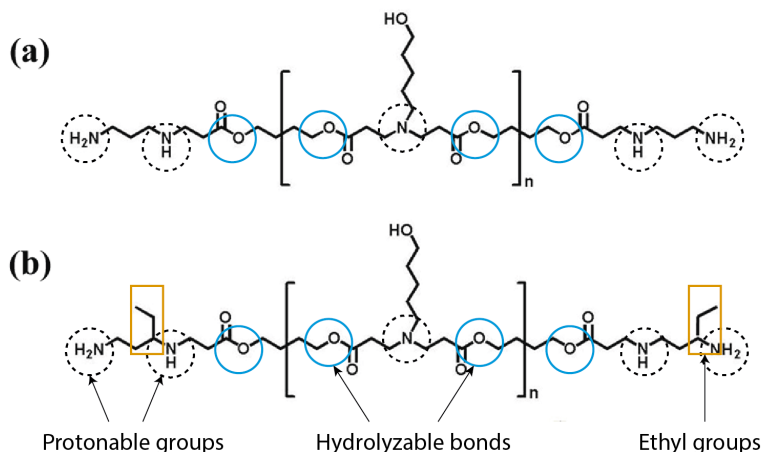
Figure 3.1: Chemical structures of poly(β-amino ester)s B1 (a) and B2 (b). The ester bounds are circled in blue, the protonable groups in dashed black and the ethyl groups are highlighted in orange.

3.2 Results and discussion

3.2.1 DNA condensation

DNA condensation by polycations is usually studied as a function of the relative proportion between the charges of both polymers the so-called N/P ratio. Unfortunately, we do not know the exact number of amino groups in our polymers and we decided to use a weight ratio (w/w) instead. Several authors encountered the same issue when working with poly(β-amino ester)s and the w/w ratio was also used[12].

In a first step, we evaluated if the alkyl chains present in the B2 polymer but not in B1 have an influence on the DNA condensation process. B1 and B2 poly(β-amino ester)s were mixed at different weight ratios (polymer/DNA) with a semidilute[13] solution of plasmid DNA. Solutions were always prepared in HEPES buffer 50 mM pH 7 maintaining pH and ionic strength constant due to their influence on the final properties of the system[14].

Once the incubation took place, an electrophoretic mobility shift assay

(EMSA) was carried out, as shown in Figure 3.2. When DNA is associated with the polymer, its mobility is reduced and eventually it is retained in the well. Comparing Figures 3.2a and 3.2b, a first difference between the two polymers is found. A weight ratio of 10 is enough to completely retain all DNA with B1, while the minimum concentration of B2 required is ten-fold higher. EMSA studies evaluate the presence of free DNA in the sample, but nothing can be said about the complexes formed (if any). This is why the average diameter and electrophoretic mobility of the samples were measured with a Malvern Nanosizer ZS at different weight ratios and the results are shown in Figures 3.3a and 3.3b. In Figure 3.3a we cannot
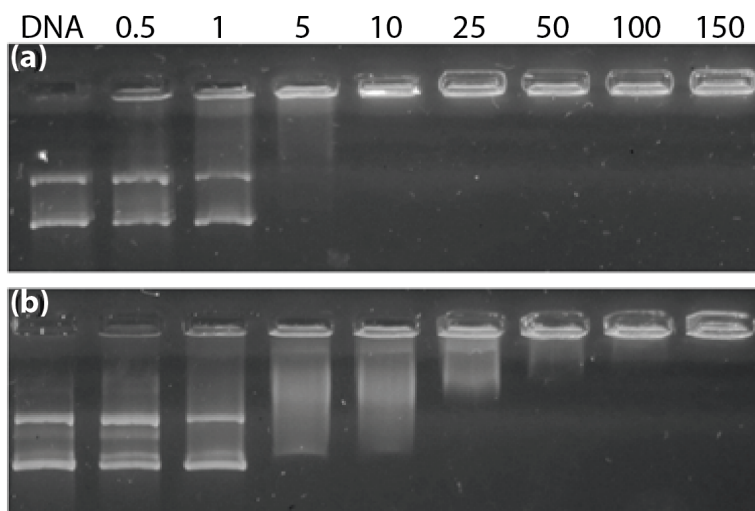
Figure 3.2: Electrophoresis mobility shift assay of polyplexes B1/DNA (a) and B2/DNA (b) at different weight ratios. Lane 1, naked DNA; lanes 2-9, weight ratios 0.5, 1, 5, 10, 25, 50, 100 and 150.

find significant differences on the size of the polyplexes formed with B1 and B2. An unstable solution mixture appears when low concentration of polymer is used. Further addition of B1 or B2 leads to size reduction of the complexes. The hydrodynamic diameter is finite and equals to 100 nm above polymer/DNA ratios of 50 for both polymers, which is a size suitable for efficient cellular uptake[15].

On the contrary, in Figure 3.3b fundamental differences are found. From 0 to 25 w/w, B1 polyplexes have electrophoretic mobility values slightly higher than those of B2. When charge inversion occurs, aggregates are

found with both polymers as expected. However, B2 polyplexes formed at w/w of 50 or higher present increased electrophoretic mobility compared to B1 polyplexes in contrast to what happened before the intersection point. It can be deduced that the binding affinity of the B2 polymer to DNA is somehow enhanced above a critical point, close to 50 w/w.

If we analyze the EMSA study for B2, free DNA is seen at some of the w/w ratios over the critical point, being 150 the first w/w ratio at which DNA is completely retained. The intersection point found in the electrophoretic mobilities along with the EMSA studies suggest a cooperative binding of B2 polycations, which preferentially bind to preformed DNA polyplexes rather than to free DNA chains. Consequently, there would be a range of B2 weight ratios (approximately 25-100) where coexistence of free DNA chains and compacted particles are found. The presence of such a cooperative effect on the condensation of DNA has been described in many systems[16, 17]. Since this phenomenon was not observed with the B1 polymer, which retains all DNA above w/w 10, the explanation must be related to the difference in their molecular structures, i.e. the alkyl chains.

The inclusion of the ethyl groups increases the hydrophobicity of the polymer B2. Hence, an attractive polymer-polymer hydrophobic interaction should be considered. This force would gain in importance over a critical point[10] and it would favor attachment of B2 to existing polyplexes giving rise to particles with a higher surface charge, as experimentally corroborated by electrophoretic mobility data (see Fig. 3.3b). Accordingly, if we consider the weight ratios between 25 and 100, we will find a mixture of fully condensed particles strongly charged and uncomplexed DNA with B2 in contrast to a homogeneous population of condensed particles with a lower surface charge with B1.

3.2.2   Temporal stability

From our studies on DNA compaction it was clear that the process was different for both polymers, but when the weight ratio was high enough, the size of the formed particles was similar. Thus, it is of interest to analyze if there exist differences in their temporal stability, since an optimal balance of
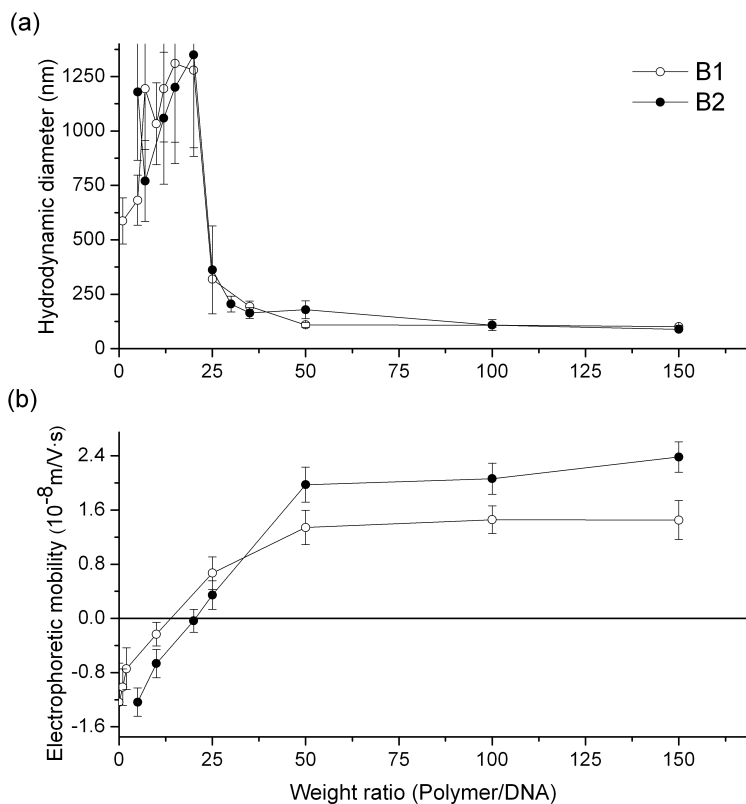
Figure 3.3: (a) Average hydrodynamic diameter and (b) average electrophoretic mobility, at various weight ratios of B1 (○) and B2 (●) polyplexes.

durability and release of DNA should be achieved.[18]. The temporal stability of the polyplexes in the same medium used for compaction –HEPES buffer 50 mM pH 7– is shown in Figure 3.4. Three different types of complexes were prepared for these studies using 50, 100 and 150 w/w polymer/DNA ratios for both polymers. It should be noted, though, that 50 w/w polyplexes became unstable in such a short time that further analysis was pointless. The presented results are, therefore, referred to the 100 and 150 w/w cases. Along this chapter we will name these complexes as B1-100, B2-100, B1-150 and B2-150.

According to the size data (Fig. 3.4a) the particle size increases in few hours reaching an extremely high mean diameter. The increase in size given by DLS measurements may be caused by two different phenomena: aggregation
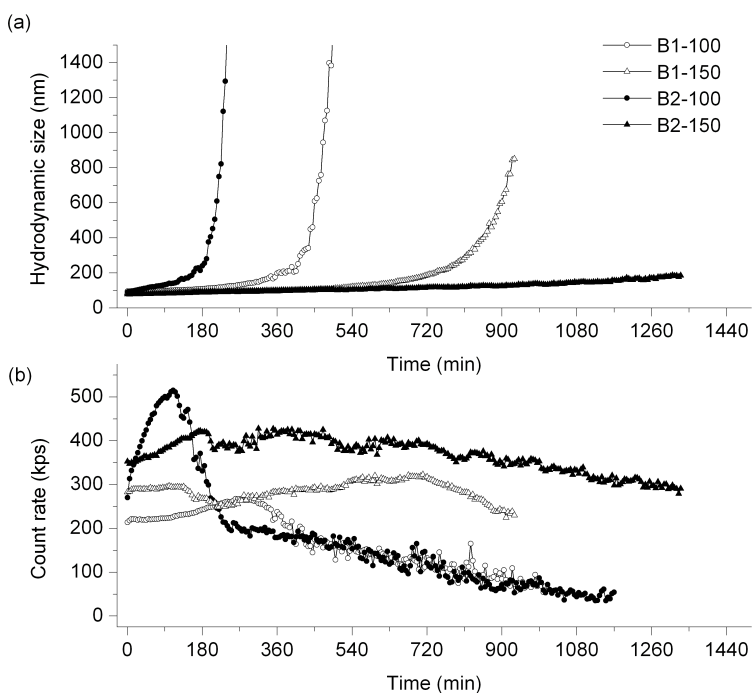
Figure 3.4: Temporal evolution of hydrodynamic diameter (a) and light scattering intensity (b) of polyplexes B1-100 (○), B2-100 (●), B1-150 (△) and B2-150 (▲) by DLS.

or swelling of the complexes. We have used static light scattering to solve which of these two situations occurs. Figure 3.4b gives information about the intensity of the light scattered by the colloidal suspension. Aggregation will be distinguishable as an increase in the scattered light. On the contrary, if particles swell, the scattered light will diminish with time, as the refractive index of the polyplexes would tend to be similar to that of the solvent during the swelling process.

Both processes will be triggered by polymer hydrolysis. As observed by Kim et al.[19], once the polyplex is formed, the initial degradation occurs at the surface, leaving the inner polymer protected from cleavage, which prolongs the degradation rate. A hydrophilic environment would facilitate water penetration into the system, accelerating the polymer degradation while the presence of hydrophobic moieties may slow down the hydrolysis rate[20].

In the w/w 100 case, the lower amount of polymer used presents faster degradation kinetics. On the one hand, B1 due to its higher hydrophilicity allows the access of water into the complex, leading to a swelling mechanism. The polymer is equally exposed in the inner and the outer part of the polyplex and the degradation rate becomes homogeneous, leading to disassembly instead of aggregation. This is confirmed in Figure 3.4b, where the B1-100 complexes show an almost constant light scattering intensity during the first 5 hours, and then such intensity decreases slowly.

On the other hand B2, due to its hydrophobic units, can only be degraded on the polyplex surface, as water access into the particle is hindered. The hydrolysis of the outer poly(β-amino ester) layer would release polymer fragments to the aqueous phase. This loss of positive charges[21] reduces the charge density of the particles, which would tend to aggregate according to the DLVO theory. The light intensity scattered by the B2-100 complexes (Fig. 3.4b) increases significantly during the first hour, indicating aggregation. The sudden drop found after the maximum would be caused by a precipitation process in which large "scattering" aggregates disappear from the bulk as sediments, remaining smaller aggregates and/or individual original particles.

The stability found with higher polymer concentrations (150 w/w, Fig. 3.4) means that neither aggregation nor disassembly due to ester-bond hydrolysis occurs during (at least) the first 10 hours. It seems that for both B1 and B2 cases, a high polymer load is translated into a better crosslinking between chains, generating polyplexes in which the condensing polymer is protected more effectively against degradation. Moreover, in the case of B2-150 the size of the polyplexes remains constant during almost 24 hours, suggesting a protective shell made of B2 molecules stabilized by polymer/polymer hydrophobic forces. It is then clear that despite having similar initial size, the structure and temporal stability of the systems are completely different.

| 3.2.3 | DNA accessibility |

Temporal stability has shown different behavior of the polyplexes depending on the polymer type and the weight ratio. It is of interest to elucidate the disposition of DNA within the complex during the studied dynamic processes. When polyplexes are exposed to nucleases, the enzyme only acts on the DNA segments that protrude outwards from the particle, leaving unaltered the DNA chains in the interior of the complex. Consequently, DNAse digestion may provide a lead on the accessibility and location of DNA. Polyplexes were incubated with DNAse I for periods of time from
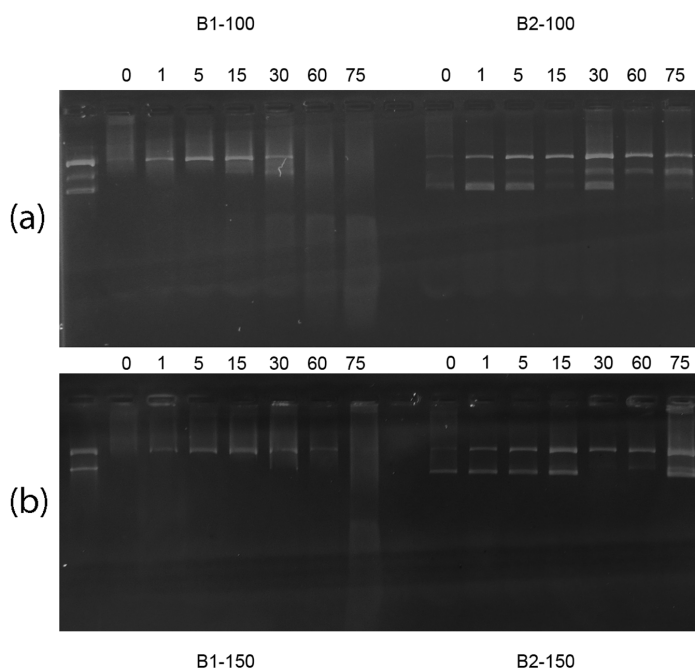
Figure 3.5: Gel electrophoresis assay for the protection ability against DNase I digestion. Polyplexes of B1 and B2 at a weight ratio of 100 (a) or 150 (b). Lane 1, naked DNA in absence of DNAse I; time of incubation with DNAse in minutes is indicated above each lane.

1 to 75 minutes and analysed by agarose gel electrophoresis, as shown in Figure 3.5. It should be noted that DNAse digestion is carried out at 37ºC, which might accelerate the dynamic processes observed at room

temperature. DNA smearing can be seen after 30 minutes in the case of B1-100 (Fig. 3.5a) or 75 minutes for B1-150 (Fig. 3.5b), indicating partial DNA degradation. We have seen that B1 polyplexes progressively swell due to hydrolysis of the polymer. DNA becomes accessible during that process, since it is degraded by the nucleases after 30-75 minutes (depending on the w/w ratio) but not before.

In contrast, for B2 polyplexes, as observed in Figure 3.5, little-to-no evidence of DNA degradation is found. In the case of B2-100, aggregation takes place during the experiment and DNase cannot access to DNA inside those aggregates, remaining intact. However, in the case of B2-150, the polymer would form a protective shell with the DNA located in the inner part of the particle structure. This phenomenon is in accordance with the temporal stability found for B2-150.

3.2.4 Colloidal stability versus salinity

The analysis of the colloidal stability of the polyplexes versus salinity is useful to determine the overall hydrophobic/philic nature of the particle surface, which would be helpful to confirm the protective polymer-polymer shell proposed for B2. Figure 3.6 shows the stability factor "W" of the polyplexes as a function of NaCl concentration. Polyplexes with a weight ratio of 100 were not used in this colloidal stability studies by salinity due to its lower temporal stability. The corresponding CCC (critical coagulation concentration) and CSC (critical stabilization concentration) can be calculated from the graph. The CCC values (450 mM for B1 and 470 mM for B2) correlate properly with the electrophoretic mobility data shown in Figure 3.3b, since the value given by the B1 polymer is lower than that of B2. That is, the surface charge density of the B2 polyplexes is higher than that of the B1 ones, due to the higher concentration of B2-polymer molecules on the particle. Besides, the CCC values of both systems are far above the physiological salt concentration, that is, both of them would be potentially useful in cell culture media or *in vivo* experiments from a colloidal point of view.

The CSC values (455 mM for B1 and 520mM for B2) also confirm the dif-
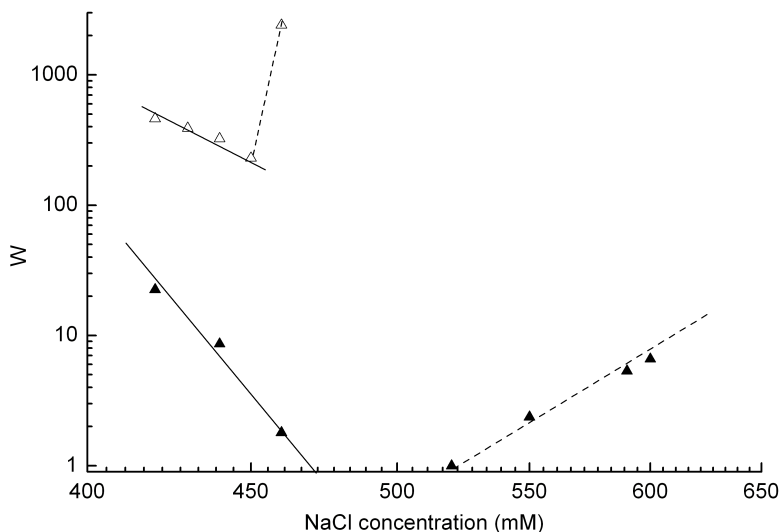
Figure 3.6: Stability factor (W) as a function of NaCl concentrations of polyplexes B1-150 ($\triangle$) and B2-150 ($\blacktriangle$).

ferent hydrophobic/philic nature of the B1 and B2 polymers. B1 polyplexes show a lower CSC value as well as slower aggregation kinetics (higher W values) than those of B2, indicating the presence of a hydration barrier around them that somehow obstructs the particle aggregation. Note that a restabilization mechanism by hydration forces appears in the B1 complexes before the classical DLVO barrier disappears by further salt addition. This gives aggregation kinetics extremely low even at its corresponding CCC (that occurs at 450 mM of NaCl). The higher CSC value for the B2 polyplexes as well as the lack of such a hydration barrier at 500 mM of NaCl confirms that the overall surface of these particles is much more hydrophobic than that of the B1 complexes. This fact is completely plausible considering the chemical structures of both polymers (Fig. 3.1).

3.2.5 | Stability upon dilution

Dilution[22–24] might be a stress mechanism usually suffered by self-assembled systems, but not always considered. Information regarding the polyplex stability after dilution would be useful for physicochemical studies as well

as for biological purposes, since they have to be diluted into a complex medium. Dilution might trigger a change in the entropy of the sample. In order to find a new state of minimum free energy, some polymer would be desorbed. This is only possible if the number of charges per molecule of polymer is low, thus the electrostatic attraction to DNA is not high enough to prevent desorption.

In order to evaluate the effect of dilution on our polyplexes, changes in size were monitored after a dilution of 1:200 from the original formulation with and without excess of free polymer. NTA was chosen as a suitable technique for our purpose due to the possibility of analyzing different size populations of highly diluted systems. In Figures 3.7a and 3.7c we observe that dilution
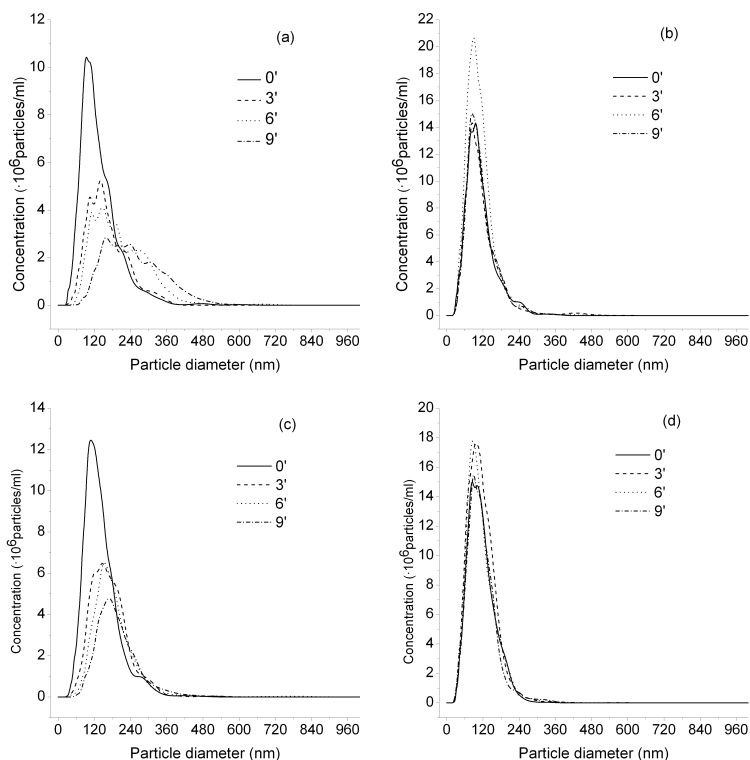
Figure 3.7: Temporal evolution of the size distribution of polyplexes after dilution 1:200 in HEPES 50 mM, pH 7. B1-150 diluted in formulation buffer (a), B1 150 diluted in formulation buffer with an excess of free B1 (b), B2-150 diluted in formulation buffer (c), and B2-150 diluted in formulation buffer with an excess of free B2 (d).

in formulation buffer leads to a fast aggregation process. The particles aggregate in barely 10 minutes, appearing as a broad distribution of different populations in size with an augmented polydispersity index. Due to the polymer desorption caused by dilution, the surface charge density diminishes, and consequently, aggregation takes place. The remaining polymer is still able to maintain the DNA condensed, as individual particles are found in the sample. Otherwise, polyplexes would be disassembled and we could not detect any particle in solution.

According to phase transition equilibrium, if the bulk was previously saturated with free polymer, desorption from the polyplexes should be avoided. Figures 3.7b and 3.7d show the stability of the complexes upon dilution after some excess of the corresponding polymer is added to the buffer solution. Aggregation is avoided confirming that our systems are firmly subjected to an adsorption/desorption equilibrium.

3.2.6 Transfection efficiency and toxicity

To examine the ability of our polyplexes to efficiently deliver plasmid DNA into cells, polyplexes were prepared with pEGFP-C1 plasmid, which encodes the Green Fluorescent Protein (GFP). The percentages of transfected HeLa cells and their relative viability are shown in Figure 3.8. It is concerning the high toxicity induced by the polyplexes, achieving values of 60% at the highest weight ratio independently of the polymer used. The poly(β-amino ester)s are rapidly degraded in aqueous solution and consequently they were expected to have no adverse effects when used to deliver DNA. The toxicity is probably induced by the free polymer present in all polyplex formulation, and not by the polyplexes themselves, as explained by Yue et al.[25]. Therefore, purification of the polyplexes would be advised in order to increase cell survival.

According to Figure 3.8, the number of cells positive for GFP increase with the weight ratio for both polymers as expected. However, it is noticeable that at w/w 25 and w/w 50, B2 polyplexes are significantly more efficient than the B1 counterparts. There exists a cooperative effect in B2 binding, but not for B1 as previously explained. When we use low quantities of
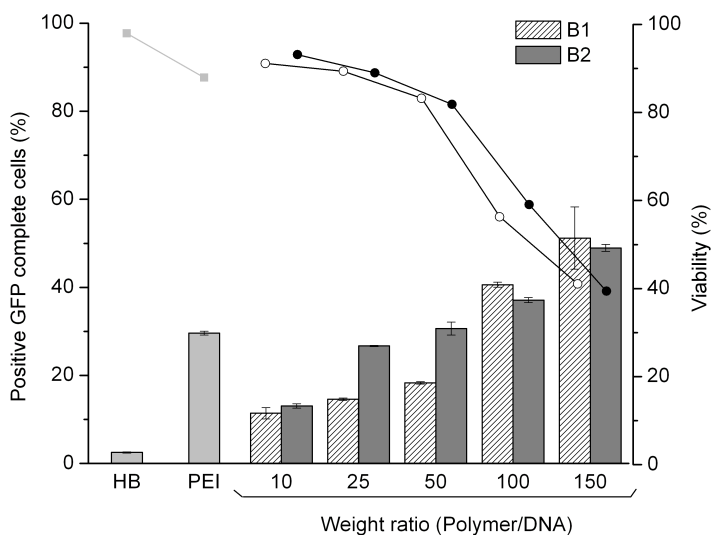
Figure 3.8: Transfection efficiency (bars) and relative viability (circles). HeLa cells were transfected with B1 or B2 polyplexes at the indicated weight ratios. HEPES buffer was used as negative control and PEI polyplexes at N/P = 6 were considered positive control (light gray bars and symbols). B1 (patterned bars, ○) , B2 (gray bars, ●).

polymer to condense DNA we obtain (a) B2 polymer: a mixture of fully condensed particles strongly charged and uncomplexed DNA and (b) B1 polymer: a homogeneous population of condensed particles with a lower surface charge.

Therefore, at low w/w ratios,the compact particles formed with B2 correspond to a higher effective weight ratio as a result of the cooperative binding of the polymer. Consequently their transfection efficiency is better than that of B1 particles, which contain fewer polymer chains per particle. On the other hand, at high weight ratios, all DNA is condensed in both systems and we did not find significant differences on their transfection ability. This means that the short alkyl chains do not seem to interact with cell membranes, as expected from their length.

Some conclusions about the use of this polymers can be drawn from evaluating together the transfection efficiency, toxicity and temporal stability.

If the desired transfection experiment requires long periods of time, high weight ratios need to be used, as they show the higher temporal stability (Fig. 3.4). In this case, both polymers present similar transfection efficiency and toxicity, but B2-150 would be chosen for being the most stable formulation. On the other hand, if the transfection experiment is carried out in short times, the temporal stability is not an issue. Therefore, low weight ratios shall be selected based on the toxicity values. Seeing the transfection studies, B2 would be chosen again due to its efficiency.

3.3   Conclusions

Two degradable linear poly(β-amino ester)s that differ slightly in their backbone structure have been used to form polyplexes with plasmid DNA. The terminal ethyl groups in the B2 molecules provided hydrophobic fragments that are responsible for a cooperative binding of free polymer to pre-formed B2-DNA polyplexes. This extra accumulation of B2 polymer gave rise to particles with a higher surface charge but also more hydrophobic than those of B1, as corroborated by the CSC values and aggregation kinetics.

The hydrolysis of these polymers is responsible for both processes of aggregation and disassembly of the polyplexes. Among all the formulations tested in this work, B2-150 polyplexes were the most stable in solution, maintaining a size of 100 nm up to 24 hours. Moreover, the hydrophobic polymer-polymer interactions exhibited exclusively by B2 form a protective shell around the polyplexes providing extended protection of the cargo against enzymatic digestion.

As a result of the low number of charges per molecule of our polymers, there is equilibrium between the polymer in the complex and that dissolved in the bulk that can be easily displaced by dilution causing polymer desorption. That partial desorption of the polymer makes the surface charge density of the particle diminish, and consequently, aggregation takes place.

The short hydrophobic moieties do not improve the efficiency of transfection by themselves as expected. However, they have a significant effect on the condensation process and the subsequent properties of the formed systems.

Consequently, B2 polyplexes would be chosen for transfection experiments requiring short and long time periods.

3.4   Bibliography

[1] D.M. Lynn and R. Langer. Degradable poly(β-amino-amino esters): Synthesis, characterization, and self-assembly with plasmid DNA. *J. Am. Chem. Soc.*, 122(44):10761–10768, 2000.

[2] D.G. Akinc, A.and Anderson, D.M. Lynn, and R. Langer. Synthesis of poly(beta-amino ester)s optimized for highly effective gene delivery. *Bioconjugate Chem.*, 14:979–88, 2003.

[3] D.G. Anderson, A. Akinc, N. Hossain, and R. Langer. Structure/property studies of polymeric gene delivery using a library of poly(beta-amino esters). *Mol. Ther.*, 11:426–34, 2005.

[4] E. Ramsay, J. Hadgraft, J. Birchall, and M. Gumbleton. Examination of the biophysical interaction between plasmid DNA and the polycations, polylysine and polyornithine, as a basis for their differential gene transfection in-vitro. *Int. J. Pharm.*, 210(1â€"2):97 − 107, 2000.

[5] E. Lai and J.H. van Zanten. Monitoring DNA/Poly-l-Lysine Polyplex Formation with Time-Resolved Multiangle Laser Light Scattering. *Biophys. J.*, 80(2):864–873, 2001.

[6] S.Y. Wong, N. Sood, and D. Putnam. Combinatorial evaluation of cations, pH-sensitive and hydrophobic moieties for polymeric vector design. *Mol. Ther.*, 17:480–90, 2009.

[7] K. Romoren, S. Pedersen, G. Smistad, A. Evensen, and B.J. Thu. The influence of formulation variables on in vitro transfection efficiency and physicochemical properties of chitosan-based polyplexes. *Int. J. Pharm.*, 261:115–127, 2003.

[8] V. Incani, A. Lavasanifar, and H. Uludag. Lipid and hydrophobic modification of cationic carriers on route to superior gene vectors. *Soft Matter*, 6:2124–2138, 2010.

[9] D. De Paula, M.V.L.B. Bentley, and R.I. Mahato. Hydrophobization and bioconjugation for enhanced siRNA delivery and targeting. *RNA*, 13:431–56, 2007.

[10] S. Filippov, C. Konak, P. Kopeckova, L. Starovoytova, M. Spirkova, and P. Stepanek. Effect of hydrophobic interactions on properties and stability of DNA-polyelectrolyte complexes. *Langmuir*, 26(7):4999–5006, Apr 2010.

[11] M. Kurisawa, M. Yokoyama, and T. Okano. Transfection efficiency increases by incorporating hydrophobic monomer units into polymeric gene carriers. *J. Control. Release*, 68:1–8, 2000.

[12] D.G. Anderson, D.M. Lynn, and R. Langer. Semi-Automated Synthesis and Screening of a Large Library of Degradable Cationic Polymers for Gene Delivery. *Angew. Chem., Int. Ed.*, 42(27):3153–3158, 2003.

[13] H. Kuramochi and Y. Yonezawa. Formation of large DNA aggregates induced by spermidine. *J. Biosci. Bioeng.*, 92:183–5, 2001.

[14] M. Ogris, P. Steinlein, M. Kursa, K. Mechtler, R. Kircheis, and E. Wagner. The size of DNA/transferrin-PEI complexes is an important factor for gene expression in cultured cells. *Gene Ther.*, 5:1425–33, 1998.

[15] M.P. Desai, V. Labhasetwar, E. Walter, R.J. Levy, and G.L. Amidon. The mechanism of uptake of biodegradable microparticles in Caco-2 cells is size dependent. *Pharm. Res.*, 14(11):1568–73, 1997.

[16] Andre Estevez-Torres and Damien Baigl. DNA compaction: fundamentals and applications. *Soft Matter*, 7:6746–6756, 2011.

[17] R.S. Dias, O. Innerlohinger, J.and Glatter, M.G. Miguel, and B. Lindman. Coil-globule transition of DNA molecules induced by cationic surfactants: a dynamic light scattering study. *J. Phys. Chem. B*, 109:10458–63, 2005.

[18] C.L. Grigsby and K.W. Leong. Balancing protection and release of DNA: tools to address a bottleneck of non-viral gene delivery. *J. R. Soc. Interface*, 7 Suppl 1:S67–82, 2010.

[19] H.J. Kim, M.S. Kwon, J.S. Choi, B.H. Kim, J.K. Yoon, K. Kim, and J.S. Park. Synthesis and characterization of poly (amino ester) for slow biodegradable gene delivery vector. *Bioorg. Med. Chem.*, 15:1708–15, 2007.

[20] J.and Raval A. Engineer, C.and Parikh. Review on Hydrolytic Degradation Behavior of Biodegradable Polymers from Controlled Drug Delivery System. *Trends Biomater. Artif. Organs*, 25(2):79–85, 2011.

[21] L. Wan, Y. You, Y. Zou, D. Oupicky, and G. Mao. DNA release dynamics from bioreducible poly(amido amine) polyplexes. *J. Phys. Chem. B*, 113:13735–41, 2009.

[22] J. Widom and R.L. Baldwin. Cation-induced toroidal condensation of DNA. *J. Mol. Biol.*, 144:431–453, 1980.

[23] T. Miller, A. Hill, S. Uezguen, M. Weigandt, and A. Goepferich. Analysis of immediate stress mechanisms upon injection of polymeric micelles and related colloidal drug carriers: implications on drug targeting. *Biomacromolecules*, 13:1707–18, 2012.

[24] S. He, P.G. Arscott, and V.A. Bloomfield. Condensation of DNA by multivalent cations: experimental studies of condensation kinetics. *Biopolymers*, 53:329–41, 2000.

[25] Y. Yue, F. Jin, R. Deng, J. Cai, Y. Chen, M.C.M. Lin, H.F. Kung, and C. Wu. Revisit complexation between DNA and polyethylenimine - effect of uncomplexed chains free in the solution mixture on gene transfection. *J. Control. Release*, 155:67–76, 2011.

4

PβAE/DNA COMPLEXES: INFLUENCE OF DISULFIDE BONDS AND pH

In this forth chapter the influence of reducible disulfide bonds and condensation pH on the properties and biological activity of poly(β-aminoester)/DNA complexes is evaluated.

Contents

4.1   Background and motivation

In the previous chapter we introduced poly(β-amino ester)s, in which the cleavage of the ester bonds is non-specific and kinetically controlled. In this forth chapter some bioreducible disulfide bonds have been introduced into a poly(β-amino ester) referred to as B3, obtaining the polymer B3-SS (Figure 4.1). These bonds are cleaved rapidly in the subcellular space by glutathione and thioredoxin reductases.Therefore, the purpose of this modification is to gain a better control on the release of the DNA, promoted by the reduction-responsive cleavage in the cytoplasm. There are numerous studies in which
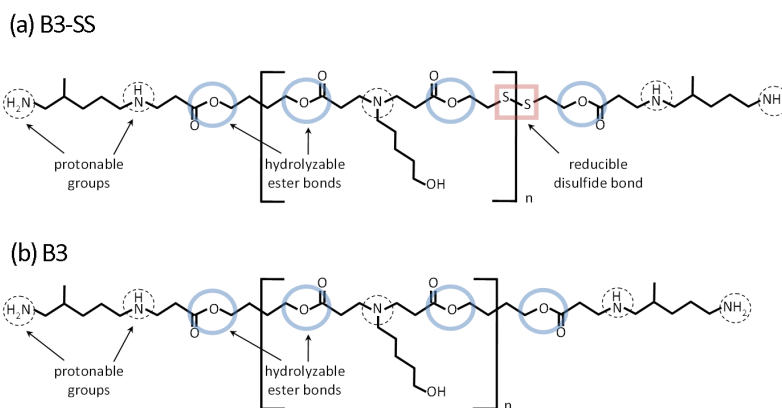
Figure 4.1: Chemical structures of poly(β-amino esters) B3-SS (a) and B3 (b). The ester bounds are circled in blue, the protonable groups in dashed black and the disulfide bond is highlighted in red.

different types of reducible materials have shown transfection activities comparable to or even better than commercially available formulations[1–4] but fewer papers are, to our knowledge, dedicated to a dual rupture strategy based on both reducible and hydrolyzable groups[5–7].

In line with our previous work, a physiological pH value was initially chosen to form the polyplexes. Unfortunately, a first handicap arose as soon as the B3-SS was dissolved in pH 7, since its intrinsic solubility in neutral aqueous media was extremely low. Aggregates of defined size around 150 nm appeared spontaneously regardless if the DNA plasmid was previously added or not during the synthesis procedure, as shown in Figure 4.2. Several studies

on poly(β-amino ester)s have encountered this issue before and polyplexes are routinely formulated in acetate buffer at pH 5 making the amino groups in the polymer molecules be more charged[8–10]. In our case, the pH change was immediately translated into an almost complete solubilization of the polycation (see Fig. 4.2).

 This fact led us to question the influence of the condensation pH on the
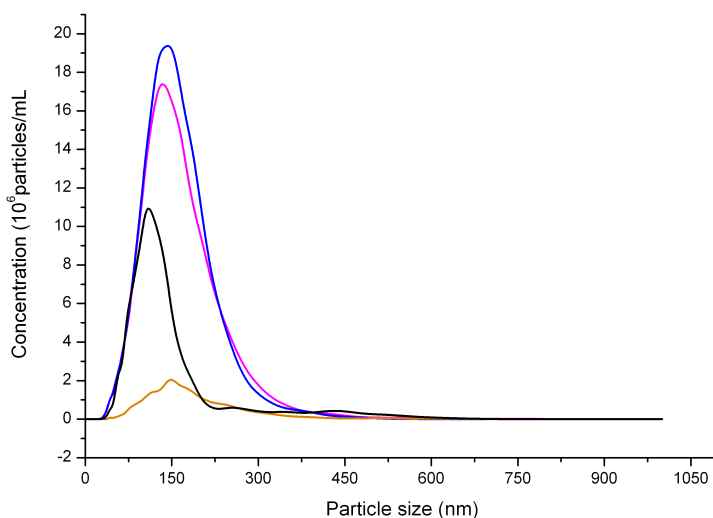
Figure 4.2: Size distribution by NTA of B3-SS at pH 7 (magenta line), complexes of DNA/B3-SS at pH 7 , w/w=50 (blue line), B3-SS at pH 5 (orange line) and complexes of DNA/B3-SS at pH 5, w/w=50 (black line).

final transfection activity of the complexes, taking into account that the final pH will always be almost neutral for biological purposes.

The objectives of this chapter are consequently redefined as follows: (a) to determine if the transfection efficiency could be improved by adding disulfide bonds to the polymer backbone, and (b) to evaluate the influence of formulation pH, i.e. 5 or 7, on the colloidal properties and *in vitro* activity of the polyplexes.

4.2   Results and discussion

4.2.1   DNA condensation

DNA condensation was evaluated using B3-SS at different concentrations, keeping constant the pEGFP plasmid concentration ($8 \mu g DNA/mL$) in a semidilute regime at the two established values of pH: 5 and 7. The weight/weight ratio was used again in this chapter to express the ratio of polymer/DNA. Figures 4.3a and 4.3b show the average diameter of the formed polyplexes as well as their electrophoretic mobility values, both obtained with the device Malvern NanoZS.

At low polycation concentrations, there is no charge reversal, and the solution mixture is formed by free DNA molecules and supramolecular structures with only few cationic polymers interacting with DNA. At those ratios at which charge cancellation occurs, large aggregates are found. Further addition of polymer finally leads to positively charged particles with a compact size. The main difference between both experimental conditions is the minimum concentration of polycation necessary to induce DNA condensation: 10 w/w at pH 5 and 15 w/w at pH 7. Under the acidic environment, the polycation presents higher positive charge, due to the protonation of more amino groups from its backbone. This has an influence on the solubility of the polymer and on its interaction with DNA. This means that at pH 5, a higher amount of polymer is available to condense DNA, due to its higher solubility, and the charge reversal is more efficient, since the polycation has more positive charges. Nevertheless, irrespective the pH value fixed for condensation (5 or 7) the particle diameter resulted always under 200 nm.

The DLS results shown in Figure 4.3 were corroborated with gel electrophoretic mobility shift assays (EMSA), as seen in Figures 4.4a and 4.4c. Free DNA chains are still found in w/w ratios lower than 25 at pH 7, while at pH 5 a completed condensation is achieved for 10 w/w values. From these results we concluded that despite the polymer alone aggregates at pH 7, when dissolved from the stock in DMSO to HEPES buffer in presence of DNA, polyplexes are formed and DNA can be efficiently condensed.
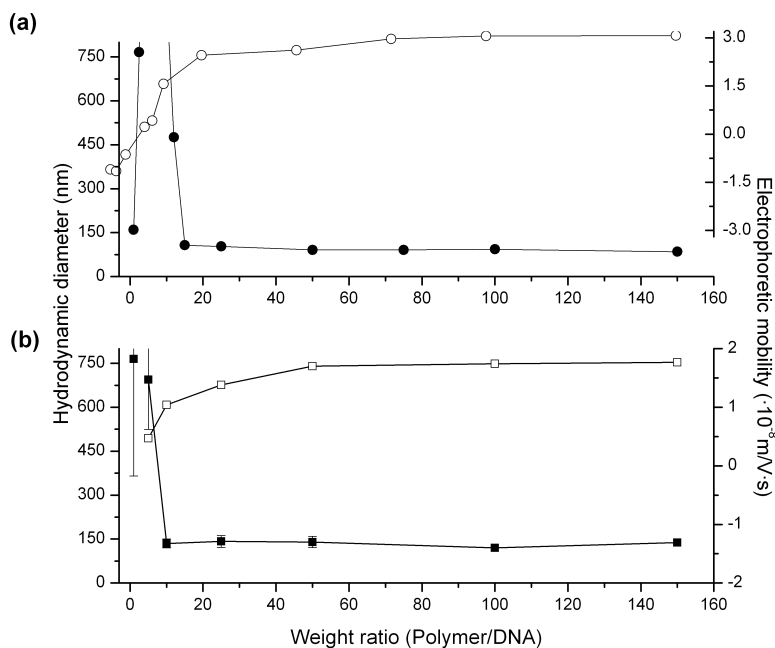
Figure 4.3: (a) Average hydrodynamic diameter (●) and electrophoretic mobility (○) at pH 7 and (b) average hydrodynamic diameter (■) and electrophoretic mobility (□) at pH 5, of B3-SS polyplexes at various weight ratios.

4.2.2 Induction of DNA release under reducing conditions

One of the aims of this chapter is to evaluate if the incorporation of disulfide bonds into the polymer backbone improves the transfection efficiency of the formed polyplexes. The strategy is based on the reversibility of the disulfide bonds, which are stable under non-reducing environments, but are cleaved by exposure to reducing agents. The destabilization of the polymer triggers the disassembly of the complex and consequently DNA should be released.

We performed EMSA studies after the exposure of our polyplexes to the reducing agent β-mercaptoethanol (β-ME). The results for both pH values are shown in Figure 4.4. Figures 4.4a and 4.4c represent the condensation ability of the B3-SS polymer at pH 5 and pH 7 respectively, and they were

commented in the previous section. On the other hand, Figures 4.4b and 4.4d show the influence of β-ME on the polyplexes. When compared to the
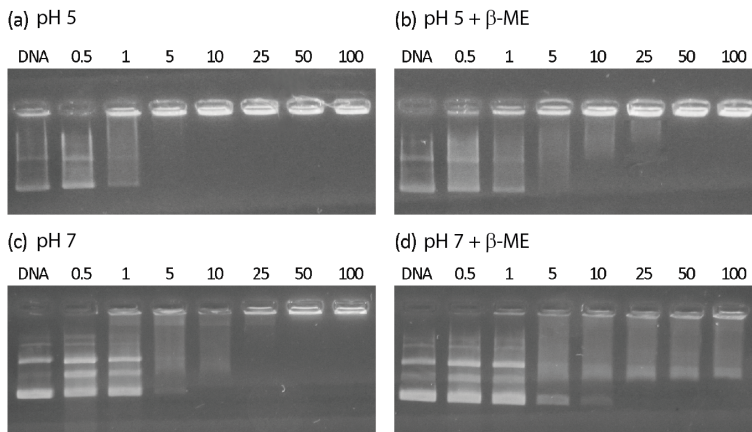
Figure 4.4: Electrophoresis mobility shift assay of B3-SS polyplexes at weight ratios polymer/DNA indicated above each lane. (a) B3-SS at pH 5, (b) B3-SS at pH 5 after 2 hours of incubation with β-ME at 37ºC, (c) B3-SS at pH 7 and (d) B3-SS at pH 7 after 2 hours of incubation with β-ME at 37ºC.

non-reducing conditions, it is clear that DNA was partially released from the complexes as a consequence of the disulfide cleavage. At pH 7, free DNA is observed even at the higher w/w ratio studied. On the other hand, at pH 5 DNA is moderately released only at low w/w ratios, 10 and 25.

Chen[11] et al. demonstrated that degradation of poly(β-amino ester)s is extremely sensitive to the pH, above all if pendant primary amino groups are present in their chemical structure. These authors showed that amino-containing polyesters degrade much more rapidly in basic solutions than in acidic conditions. They defend that the ester degradation is mainly contributed by an intramolecular/intermolecular amidation mechanism instead of purely hydrolysis of ester bonds in the polymer. The protonation of pendant primary amino groups in acidic solutions inhibits the amino intra/intermolecular nucleophilic attack to the ester linkage and significantly decreases the degradation rate. Our B3-SS polymer also possesses such a type of pendant primary amino groups (see Fig. 4.1), and consequently we can infer that its hydrolysis will be pH-dependent. It should be noted that the number of hydrolyzable ester bonds is considerably higher than that of disulfide bonds.

Considering all above-mentioned aspects, the results shown in Fig. 4.4, can be explained as follows: When exposed to β-ME for two hours at 37 °C, at pH 5 only the disulfide bonds are reversed and that does not seem to be enough to disassembly the polyplexes at high w/w. On the other hand at pH 7, not only the disulfide bonds are cleaved, but also the explained ester break-up mechanism catalyzed by the presence of the amino groups occurs, accelerating the degradation process, and consequently releasing DNA.

4.2.3 Temporal stability

The spontaneous hydrolysis of the ester groups of poly(β-amino ester)s is bound to have a direct impact on the stability in solution of the complexes obtained with DNA. This can be an advantage for their application in biological systems, as the DNA is eventually released and the polymers are degraded into shorter chains that should be easier to metabolize. On the other hand, if the stability is too low, it may be difficult to work with those complexes, and storage becomes unthinkable. The temporal stability of the polyplexes must be analyzed in order to find the optimal conditions. We used dynamic light scattering (DLS) to evaluate the changes in size of w/w 50 polyplexes with time, and static light scattering (SLS) for the evolution of scattered light intensity, and the results are shown in Figures 4.5a and 4.5b respectively. The mean size obtained with DLS is the diameter that an equivalent spherical particle would have in solution. This means that if various populations are present, and/or the particles are non-spherical, the size given by the device is an approximation, which is useful for comparison but might be unreal. With regard to the SLS results, the scattered light intensity will increase in case of aggregation and drop if the particles swell or precipitate.

It is clear from Figure 4.5a that B3-SS polyplexes are more stable at pH 5. The particles keep their size relatively constant during the whole experiment. However at pH 7, the size of the complexes starts to increase as early as two hours after condensation. As foreseen, the explanation is related to the hydrolysis of the ester bonds. The hydrolysis rate depends on several parameters and the most important one is the pH. At pH 5 the hydrolysis is slowed down and it seems to have no influence over the size of the complexes

(a)

(b)
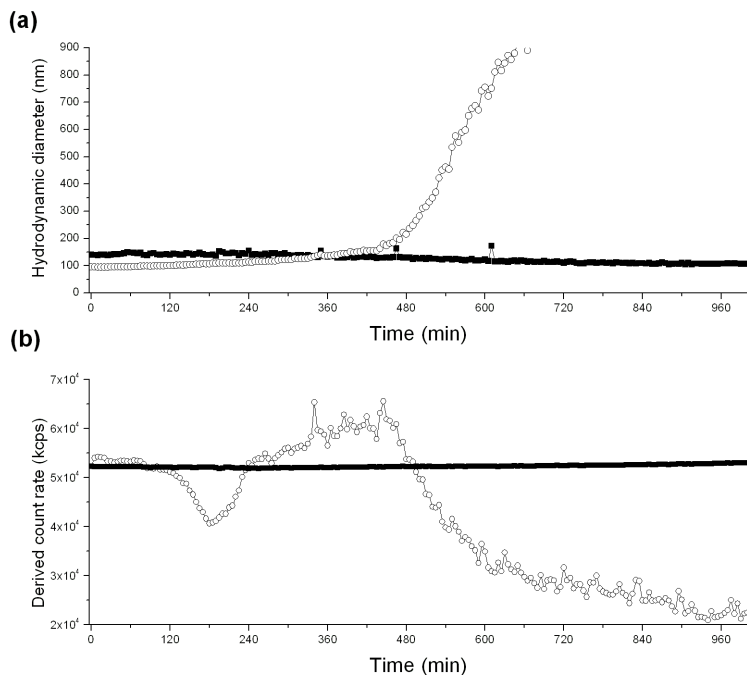
Figure 4.5: Temporal evolution of hydrodynamic diameter (a) and light scattering intensity (b) of w/w 50 B3-SS polyplexes at pH 7 (○) and pH 5 (■).

at least during the first 16 hours. In Figure 4.5b the scattered light intensity of the polyplexes at this pH is practically constant, which corroborates the stability of the system. However, the scattered light intensity corresponding to pH 7 apparently presents 4 different regimes:

i) 0 - 120 min. The scattered light remains constant and so is the size. The complexes are stable.

ii) 120 - 180 min. There is a drop in the scattered light and the size is slightly increased. Hydrolysis of the outer layer of the complexes takes place and polymer fragments are released. The system starts to disassemble and consequently it swells, diminishing the amount of scattered light.

iii) 180 - 450 min. Both the scattered light and the size increase. The loss of positive charges due to hydrolysis reaches a critical point where the charge density is not enough to keep the particles from aggregation according to

the classical DLVO theory. We found two different slopes in the scattered light, which might be associated to aggregation kinetics. Further studies should be done in that regard.

iv) 450 min - End. The scattered light decreases and the size increases quickly. The particles have formed large aggregates that precipitate. The device is not able to detect them resulting in diminution of the scattered light.

It is clear from these results that the pH is a determinant factor on the stability of this type of polyplexes, obtaining durable particles when the pH is kept acidic. This is a first step to obtain appropriate conditions for their manipulation and storage.

4.2.4   Colloidal stability versus salinity

The stability of the complexes upon addition of salt is necessary to understand their behaviour under physiological conditions, but it also serves to give a qualitative information about the hydrophobic/philic nature of the particles. The diameter of the complexes was obtained with the NTA technique, due to the low concentration needed. Sodium chloride was added to previously formed polyplexes and the size was measured after six minutes of exposure. The mean number-weighted diameter of the complexes against salt concentration for both pH values can be seen in Figure 4.6. The almost constant sizes of the complexes up to 200-250 mM of NaCl indicate that the particles can be exposed to the physiological concentration of salt (i.e. 150 mM). After that point, we find large aggregates, as predicted by the DLVO theory. In both cases restabilization by hydration forces is observed at 350-450 mM of salt which is a sign of the hydrophilicity of the complexes.

4.2.5   Transfection efficiency and toxicity

In order to fulfill the objectives of this chapter, the biological performance of the studied polyplexes should be evaluated. We carried out viability and *in vitro* transfection studies directed to answer our two main questions.
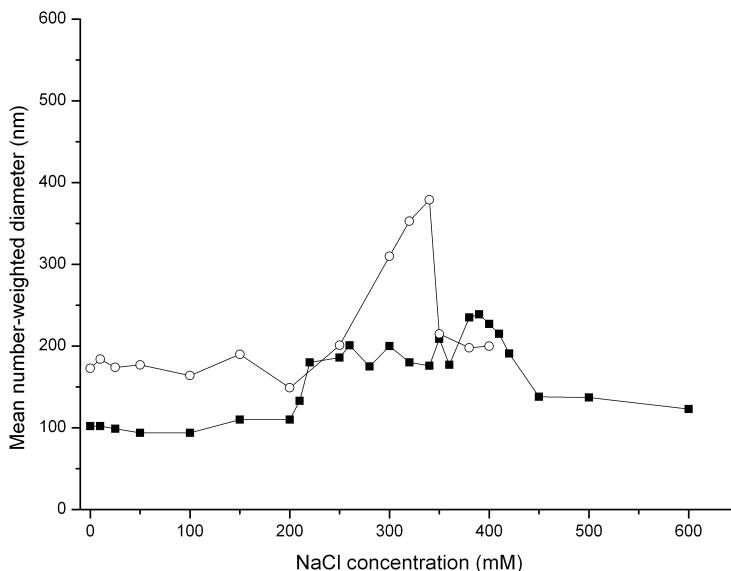
Figure 4.6: Mean number-weighted as a function of NaCl concentrations of w/w 50 B3-SS polyplexes at pH 5 (■) and pH 7 (○).

a) Influence of the disulfide bonds We needed control polyplexes without disulfide bonds to evaluate if the modification was useful. For that purpose we used a polymer, B3, which varies from B3-SS in the absence of disulfide bonds. The polyplexes formed with B3 are used as blank against its corresponding B3-SS counterparts. In Figure 4.7 we can see from the percentages of transfected cells that no significant difference is found due to the disulfide bonds. As deduced from the treatment with β-ME, the number of disulfide bond is not sufficient when compared to the number of ester groups, which are predominant and present in both B3-SS and B3 polymers.

b) Influence of the initial pH In all cases, polyplexes were added to the culture medium, which is at pH 7.4. The influence of the condensation pH can also be evaluated from Figure 4.7. The only significant difference is found at w/w 10, where the polyplexes condensed at pH 5 seem to be more efficient. According to the previous results, at this weight ratio polyplexes are formed at pH 5 but not at pH 7. The percentage of transfected cells is not influenced by the initial pH for the other weight ratios, which means
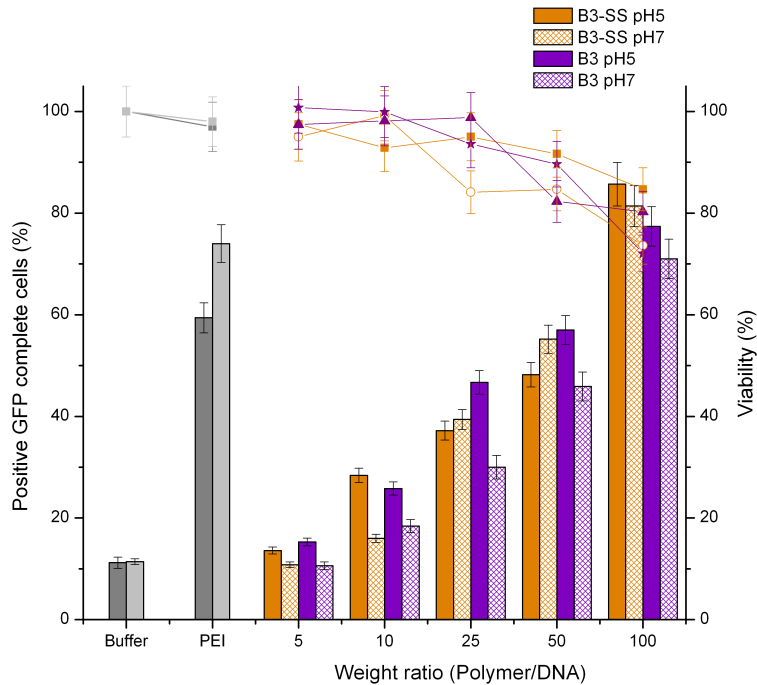
Figure 4.7: Transfection efficiency (bars) and relative viability (symbols). HeLa cells were transfected with B3-SS or B3 polyplexes at indicated weight ratios and pH. Buffers were used as negative control (gray) and PEI polyplexes at N/P = 6 were considered positive control (light gray). B3-SS pH 5 (Orange bars and squares) , B3-SS pH 7 (orange patterned bars and circles), B3 pH 5 (purple bars and triangles) and B3 pH 7 (purple patterned bars and stars).

that pH 5 can be used as working condition with no reduction of efficiency but with higher stability.

The viability of the complexes is kept above the 70% for the highest concentration used. Complexes of B3-SS at initial pH 5 seem to be slightly less toxic, probably due to better solubility.

4.3   Conclusions

A poly(β-amino ester) B3-SS containing disulfide bonds was used to condense DNA at two different values of pH, 5 and 7. Due to the higher protonation of the amino groups at pH 5, the minimum condensation ratio was lower than that observed at pH 7. Nevertheless, further addition of polymer led to positively charged particles under 200 nm in diameter at both pH values.

When exposed to a reducing agent, such as β-mercaptoethanol, the disulfide bonds are reversed. At pH 5, those breakages are not enough to release all DNA. On the contrary, at pH 7 the combined cleavage of disulfide and ester bonds results in disassembly of the polyplexes.

The stability in solution of the polyplexes is extremely dependent on the pH, owing to the hydrolysis of the ester bonds catalyzed by the pendant amino groups at neutral pH. As a result, complexes at the acidic pH are stable over a longer period of time.

The colloidal stability of the polyplexes at both pH values indicates that the particles can be exposed to the physiological salt concentration without aggregation. In both cases restabilization by hydration forces was observed.

Transfection efficiency was evaluated in HeLa cells and no significant differences were found on account of the disulfide bonds. The number of these environmentally responsive bonds was not sufficient to observe an increase in the *in vitro* activity, considering the predominance of ester groups present in both the control B3 and the B3-SS polymers. The viability of the complexes was kept above the 70% even for the highest concentration used.

Transfection was also analyzed as a function of the initial pH. The percentage of transfected cells was not significantly influenced by this parameter. Thus, we found three reasons to routinely use pH 5 to form B3-SS polyplexes: i) it favors the solubility of the polymer, ii) it increases the temporal stability of the complexes, which improves their storage, and iii) it does not reduce the transfection efficiency.

4.4 Bibliography

[1] M.X . Tang, C.T. Redemann, and F.C. Szoka. In vitro gene delivery by degraded polyamidoamine dendrimers. *Bioconjugate Chem.*, 7:703–14, 1996.

[2] D. Oupicky, A.L. Parker, and L.W. Seymour. Laterally stabilized complexes of DNA with linear reducible polycations: Strategy for triggered intracellular activation of DNA delivery vectors. *J. Am. Chem. Soc.*, 124(1):8–9, 2002. PMID: 11772047.

[3] W. Li, P. Zhang, K. Zheng, Q. Hu, and Y. Wang. Redox-triggered intracellular dePEGylation based on diselenide-linked polycations for DNA delivery. *J. Mater. Chem. B*, 1:6418–6426, 2013.

[4] H.C. Hwang, H.S.and Kang and Y.H. Bae. Bioreducible polymers as a determining factor for polyplex decomplexation rate and transfection. *Biomacromolecules*, 14(2):548–556, 2013. PMID: 23259985.

[5] G.T. Zugates, D.G. Anderson, S.R. Little, I.E.B. Lawhorn, and R. Langer. Synthesis of poly(β-amino ester)s with thiol-reactive side chains for DNA delivery. *J. Am. Chem. Soc.*, 128(39):12726–12734, 2006. PMID: 17002366.

[6] L. Zhang, Z. Chen, and Y. Li. Dual-degradable disulfide-containing PEI-Pluronic/DNA polyplexes: transfection efficiency and balancing protection and DNA release. *Int. J. Nanomedicine*, 8(1):3689—3701, 2013.

[7] C. Lin, T.M. Lammens, Z.Y. Zhong, H. Gu, M.C. Lok, X. Jiang, W.E. Hennink, J. Feijen, and J.F.J. Engbersen. Disulfide-containing poly(β-amino ester)s for gene delivery. *J. Control. Release*, 116(2):e79 − e81, 2006. Proceedings of the Ninth European Symposium on Controlled Drug Delivery.

[8] D.M. Lynn and R. Langer. Degradable poly(β-amino-amino esters): Synthesis, characterization, and self-assembly with plasmid DNA. *J. Am. Chem. Soc.*, 122(44):10761–10768, 2000.

[9] D.G. Akinc, A.and Anderson, D.M. Lynn, and R. Langer. Synthesis of poly(beta-amino ester)s optimized for highly effective gene delivery. *Bioconjugate Chem.*, 14:979–88, 2003.

[10] J. Kim, J.C. Sunshine, and J.J. Green. Differential polymer structure tunes mechanism of cellular uptake and transfection routes of poly(β-amino ester) polyplexes in human breast cancer cells. *Bioconjugate Chem.*, 25(1):43–51, 2014. PMID: 24320687.

[11] J. Chen, S.W. Huang, M. Liu, and R.X. Zhuo. Synthesis and degradation of poly(beta-aminoester) with pendant primary amine. *Polymer*, 48:675–681, 2007.

5

PAMAM/DNA COMPLEXES

In the fifth chapter an octadecyl sulfonyl PAMAM G2 was used to condense plasmid DNA. The influence of this modification at different levels was investigated by comparison with original PAMAM G2

Contents

5.1   Background and motivation

Dendrimers are polymers with unique properties, highlighting the perfectly defined and monodisperse structure (based on stepwise synthesis) and multiple terminal groups. These features make dendrimers useful for biomedical applications[1] as antimicrobial and antiviral drug, in tissue engineering, drug delivery, transfection and others[2–6]

When it comes to gene delivery, polyamido amines (PAMAM) are one of the most widespread dendrimers. PAMAM bears surface amino groups which facilitates the electrostatic interaction with the negatively charged DNA. Moreover, the buffering capacity of the internal amino groups is believed to facilitate endosomal escape due to the proton sponge effect. Haensler and Szoka[7] published the first gene delivery study using PAMAM to form a dendrimer-DNA complex (dendriplex). Many papers have followed, reaffirming the potential suitability of PAMAM for gene delivery[8,9].

However, in spite of their promising features, 20 years later dendriplexes have not been translated into the clinic. It is still a challenge to predict the in vivo behavior of synthetic vectors and there is a need for optimization and rational design of polymeric therapeutics[10]. Characterization of dendriplexes at the physicochemical, *in vitro* and *in vivo* levels[11–13] is essential to achieve the desirable outcome[14,15].

The original structure of PAMAM has been widely modified in literature. One example is the attachment of hydrophobic moieties. Aliphatic chains[16], steroids[17], hydrophobic aminoacids[18], or even organic fluorescent dyes[19] they all seem to agree on the improvement in transfection. In most cases this fact is ascribed to a facilitated interaction with cell membranes, even though it seems unlikely for some of the moieties used.

In this chapter we will discuss the implications of an aliphatic modification of PAMAM at different levels: (a) formation and stability of dendriplexes, (b) interaction with a cell membrane model and (c) transfection efficiency. For that purpose we have chosen an octadecyl modified PAMAM G2[20] (structure shown in Figure 5.1). The significant improvements in DNA condensation and transfection achieved by incorporation of a C18 alkyl chain to PAMAM G2 are described.

5.2 Results and discussion

5.2.1 DNA condensation

In a first approach, we studied the ability of PAMAM and C18-PAMAM G2 dendrimers (structures shown in Fig. 5.1) to condense DNA. The hydrodynamic diameter and surface charge at different Z were evaluated and the results are shown in Figure 5.2. It is important to note that the average size obtained by DLS is the diameter that an equivalent spherical particle would have in solution.

When low quantities of dendrimer are used, large aggregates appear in solution. Close to the neutralization point, aggregation of non-charged complexes occurs. If we increase Z we finally obtain particles of lower hydrodynamic diameter. The first difference we can observe is related to the average diameter of the particles. Much lower values are found when C18-PAMAM is used. The hydrophobic chain bound to C18-PAMAM contributes to better condensation of DNA, obtaining particles with an approximate average diameter of 80 nm. On the other hand, unmodified PAMAM yields bigger particles which become even bigger if we continue adding dendrimer.

In Figure 5.2b we can observe the electrophoretic mobility of the resulting complexes. Both curves are similar, as expected due to the low modification ratio, which barely changes the overall charge of the PAMAM dendrimers. The surface charge of the complexes remains constant and positive over an Z=5.

The intensity weighted size distributions of our complexes obtained from the DLS data as a function of Z for both dendrimers are shown in Figure 5.3. The evolution of the system upon progressive addition of dendrimer can be followed from top to the bottom. At the point of charge neutrality we find large aggregates of around 1 μm for both dendrimers. We will focus first on the solid lines in Figure 5.3, corresponding to dendriplexes of C18-PAMAM. In the region Z=5-12, it is evident the coexistence of two different populations[21]. On the one hand, we find a broad peak which

(a)

(b)
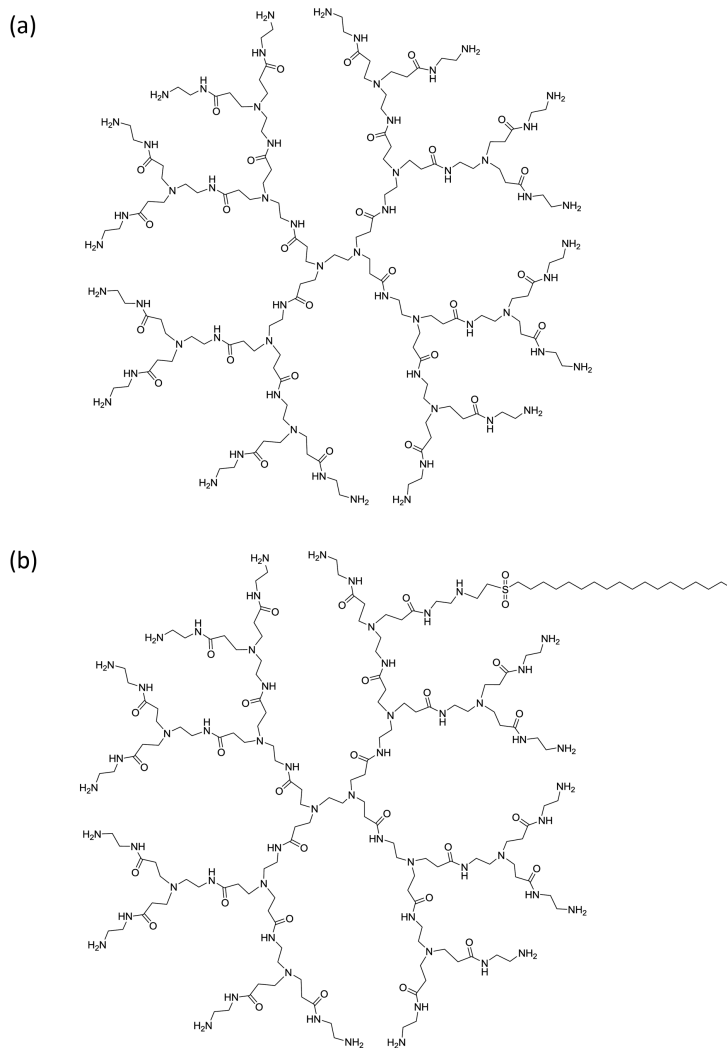
Figure 5.1: Chemical structures of (a) PAMAM G2 and (b) PAMAM G2 modified with a C18 alkyl sulfonyl chain (1:0.5) via aza-Michael addition(C18-PAMAM).

might correspond to a coil or extended conformation, with fluctuations as indicated by the width of the peak. On the other hand, we can see a narrower peak of more compact small particles that becomes predominant when increasing the dendrimer concentration. (Note that the x-axis scale is logarithmic).
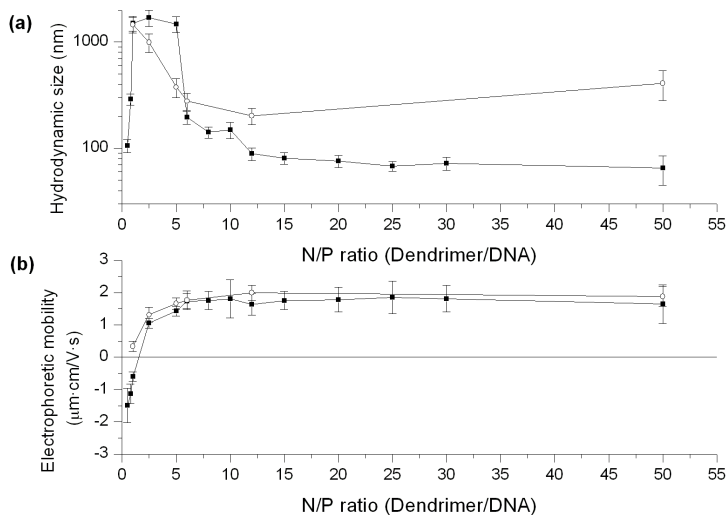
Figure 5.2: (a) Average hydrodynamic diameter and (b) average electrophoretic mobility, at various Z of PAMAM (○) and C18-PAMAM (■) dendriplexes.

If we observe now the dotted lines in Figure 5.3, that is, dendriplexes of PAMAM, some differences are found. We can also see coexistence, but both peaks are displaced into higher values. Besides, the proportion between the two populations remains basically constant even at high Z.

PAMAM dendrimers present primary amino groups on their surfaces, so they are positively charged at pH 7.4. Due to the negative charge of DNA, there will be electrostatic attraction between them, yielding to interpolyelectrolyte complexes (IPEC). In order to be used for gene delivery, the dendrimers should condense DNA into small particles able to pass more easily through the biological barriers. It is though not enough to obtain an IPEC, but the polymers must blend into more compact particles, presumably with a toroidal and/or rod shape in the case of second generation PAMAM[22,23]. According to our results, for both modified and unmodified PAMAM, interpolyelectrolyte complexes are formed with DNA. But only when the alkyl C18 chains are present, small compact and predominant particles are obtained.
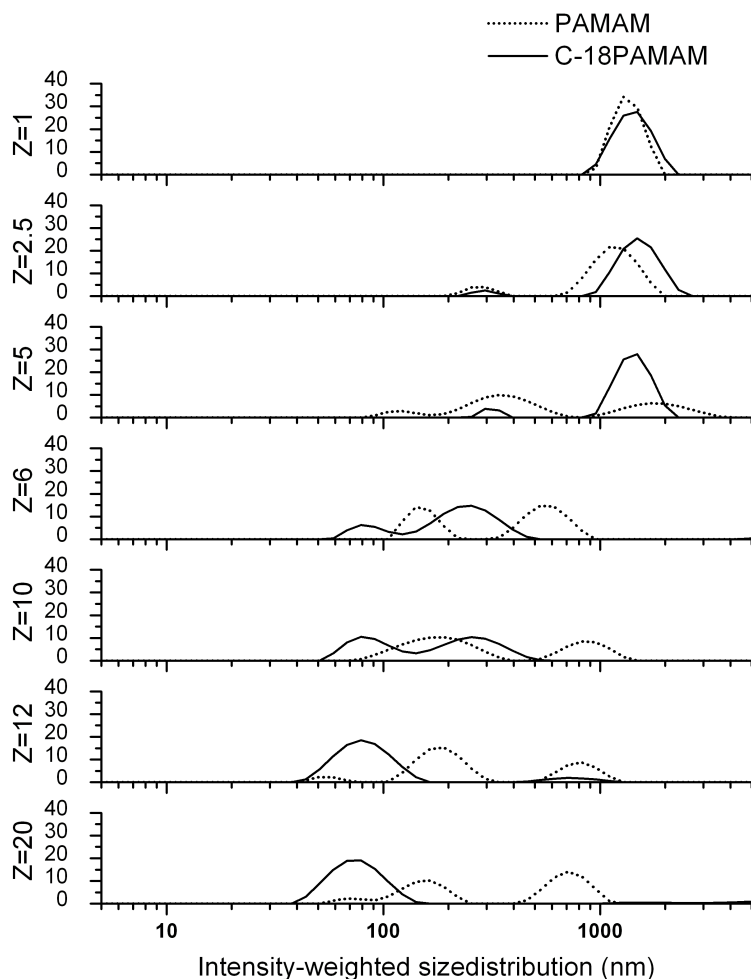
Figure 5.3: Intensity weighted distribution functions of PAMAM (dotted line) and C18-PAMAM (solid line) dendriplexes at various Z.

5.2.2 | Temporal stability

After analyzing particle size distributions, we decided to focus on Z=12, which is the lowest proportion we found with acceptable homogeneity of C18-PAMAM samples (percentage of intensity corresponding to compact particles over 80%). PAMAM and C18-PAMAM dendriplexes at Z=12 were allowed to evolve with time while we measured their diameter every

5 minutes. Figures 5.4a and 5.4b show the hydrodynamic diameter of the dendriplexes taken from the position of the main and secondary peaks of the intensity distribution given by the DLS device. (Note: Only the main and secondary peaks corresponding to intensity percentages higher than 20% are considered for clarity)
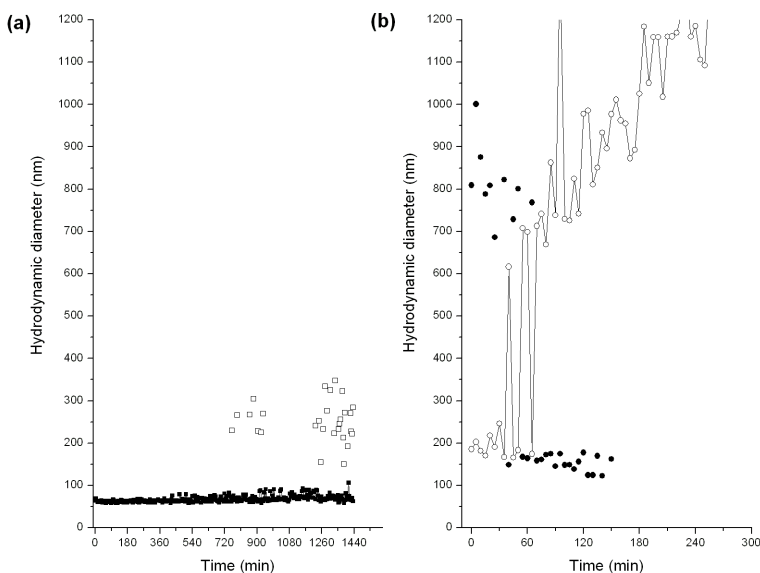
Figure 5.4: Temporal evolution of the mean diameters of the various peaks from the intensity distribution functions given by DLS of (a) C18-PAMAM dendriplexes, main peak ■, secondary peak □ and (b) PAMAM dendriplexes , main peak ○secondary peak ●at Z=12.

As observed in Figure 5.4a, C18-PAMAM dendriplexes have a hydrodynamic diameter of 60 nm and they are stable for at least 18 hours in formulation buffer. However, some aggregates of approximately 300-400 nm start to appear after 10 hours.

On the other hand, PAMAM dendriplexes, as seen in Figure 5.4b, present two peaks from the beginning corresponding to extended complexes and compact particles. It is easy to follow the evolution of both populations, which remain constant up to 40 minutes. At this point, bigger particles become predominant in terms of intensity, and their size starts to increase progressively. Two hours later the device is not able to detect any of the smaller particles, either because of their disappearance or due to the

impossibility of DLS to distinguish small (and scarce) particles when much bigger ones are present.

The increase in size might be caused by aggregation of the dendriplexes or decompaction of DNA. We have used static light scattering to solve which of these two situations occurs. Figure 5.5 gives information about the time evolution of scattered intensity. Aggregation will be distinguishable as an increase in the scattered light. On the contrary, if there is dissociation the scattered light intensity will drop.
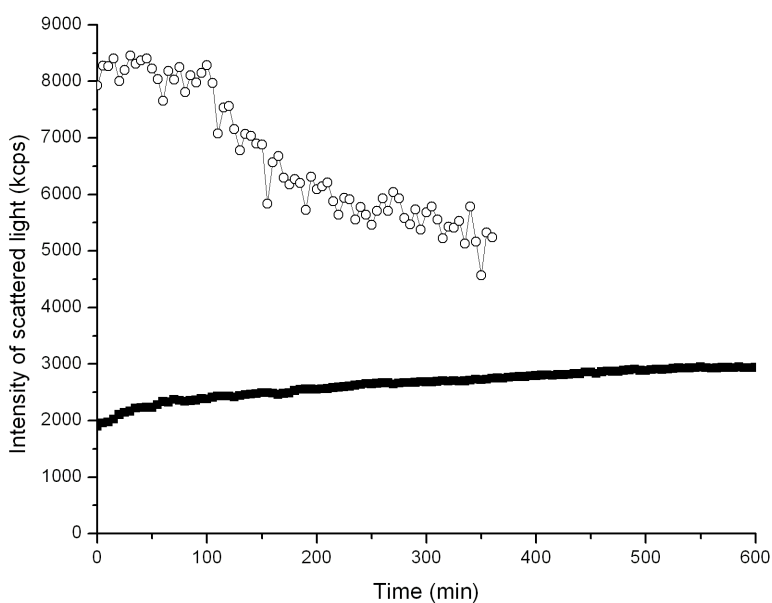
Figure 5.5: Temporal evolution of the intensity of light scattered by C18-PAMAM (■) and PAMAM (○) dendriplexes at Z=12.

It is clear from Figure 5.5 that the temporal behavior of both systems is different. In the case of PAMAM dendriplexes there is no appreciable change in the intensity during the first 100 minutes (after 30 minutes of condensation, this is, 130 minutes from mixing). After that, a fast decrease is observed, indicating disassembly due to morphological changes experienced by low generation PAMAM dendriplexes, as explained elsewhere[24]. From these results it is deduced that after mixing PAMAM G2 and DNA, an unstable state is reached and the system quickly evolves into a more stable configuration. But this instability can be avoided thanks to the added alkyl

chains in our C18-PAMAM. Despite the evident process of progressive slow aggregation deduced by the slight slope of the scattered light intensity (Fig. 5.5), the 60 nm population of C18-PAMAM dendriplexes remains unchanged for at least 20 hours (Fig. 5.4a). This is a huge improvement compared to original PAMAM.

5.2.3   Interaction with a cell membrane model

Once demonstrated that the PAMAM bearing alkyl chains with 18 carbon atoms improves the condensation of the DNA in the dendriplex due to hydrophobic forces, it is interesting to evaluate whether this modification also affects the interaction with a model cell membrane. We have evaluated both the adsorption kinetics of our dendriplexes onto a monolayer of zwitterionic lipid DPPC (dipalmitoylphosphatidylcholine) and the rheological properties of the mixed DPPC/dendriplex system. These experiments, which to our knowledge have not been performed before with dendriplexes, have been carried out in a pendant drop film balance implemented with subphase exchange so that the interaction can be analyzed in-situ and with minimal disturbance of the surface[25].

Figure 5.6a shows the time evolution of the surface pressure of a DPPC monolayer spread onto HEPES buffer following subphase exchange by dendriplex or HEPES solution at a surface pressure of $\pi = 20$ mN/m before exchange. Note that the data plotted in Figure 5.6a start after the subphase exchange had been completed so that the starting surface pressure is already different from 20 mN/m for the dendriplexes curves. A reference curve where we exchanged the drop subphase by the same buffer solution has been included in the figure for comparison. In this curve, the surface pressure remains constant at 20 mN/m. Exchange by PAMAM dendriplexes results in an increase in the surface pressure which is doubled in the case of C18-PAMAM complexes. The increase takes place during the exchange, as indicated by the different starting points of the curves, and it continues with time. The adsorption kinetics shows in both cases a small lag time after the exchange followed by a rapid increase of surface pressure reaching a steady state in 15 minutes. The small lag time recorded might indicate that the dendriplex sticks itself under the DPPC monolayer prior to penetrating

into the surface layer[26]. DPPC is a zwitteronic lipid that bears a positive
charge from the choline group and a negative charge from the phosphate.
At the air-water interface, the polar heads of the phospholipid are oriented
into the bulk so that the dendriplexes can interact electrostatically with
the phosphate group[27]. The increment of surface pressure shown in Figure
5.6a clearly indicates that both PAMAM and C18-PAMAM dendriplexes are
attracted onto the surface layer and penetrate into the phospholipid chains
but the effect is more noticeable when the alkyl chain is present.
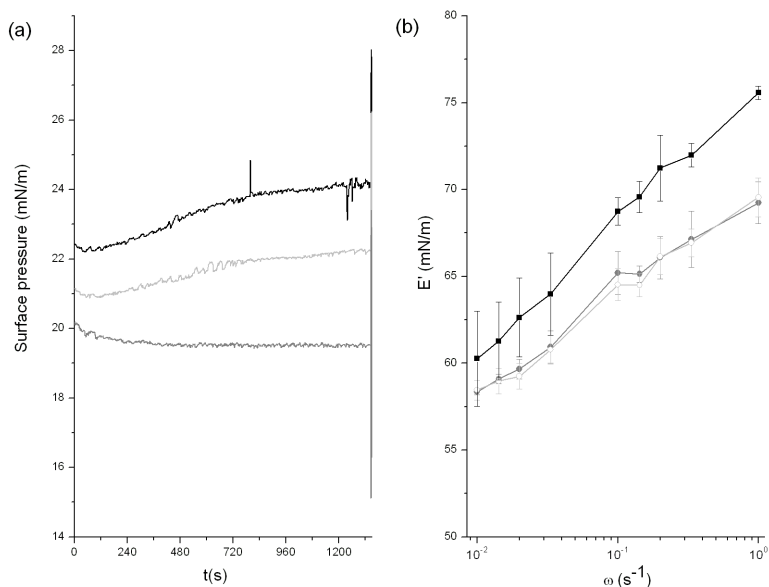
Figure 5.6: (a) Adsorption kinetics onto a DPPC monolayer at $\pi = 20$ mN/m
following subphase exchange with C18-PAMAM dendriplexes (black),with PA-
MAM dendriplexes (light gray) and with HEPES buffer (gray). (b) Dilatational
surface elasticity moduli as a function of frequency measured at the end of
curves plotted in (a). Subphase exchange of DPPC monolayer with C18-
PAMAM dendriplexes (black), with PAMAM dendriplexes (light gray) and with
HEPES buffer (gray).

Penetration of the dendriplexes into the lipid monolayer could result in alter-
ations of the lateral packing in the monolayer[28]. In order to investigate this
in more detail we measured the surface dilatational moduli of the adsorbed
dendriplexes onto the DPPC monolayer. This magnitude reflects inter-
and intramolecular interactions taking place at the surface and is sensitive
to molecular orientations and conformational transitions at the surface[29].

We measured the surface dilatational modulus at different frequencies of perturbation imposed to the oscillating drop. In all cases the viscous component of the dilatational modulus was very small and the systems appear predominantly elastic. Hence, Fig. 5.6b shows the elastic component of the surface dilatational modulus (E') of DPPC, DPPC/PAMAM dendriplex and DPPC/C18-PAMAM dendriplex. The oscillations were done at the end of each dynamic curve shown in Figure 5.6a.

Interestingly, Figure 5.6b shows that only the presence of the C18-PAMAM complexes significantly affects the dilatational elasticity of the surface layer. This suggests that the hydrophobic modification of C18-PAMAM not only implies a further penetration into the DPPC monolayer but also affects the packing state of the monolayer in contrast with PAMAM dendriplexes. According to Figure 5.3, PAMAM dendriplexes present an extended conformation (flexible), while C18-PAMAM condenses DNA into small particles (rigid). The increased stiffness observed with C18-PAMAM can be attributed to the presence of those rigid complexes at the surface. Also, the presence of the alkyl chains at the surface could promote molecular binding at the surface, hence resulting in a stiffer molecular assembly.

Figure 5.6b also shows that the dilatational elastic modulus increases with the oscillation frequency in all three curves as expected in the linear regime[30].However, this increase is more noticeable (higher slope) for the DPPC/C18-PAMAM dendriplex. Thus, the higher the frequency the more visible the differences are between the two dendrimers. According to López-Montero et al.[30], this behavior could be ascribed to the formation of lipid domains induced by the C18-PAMAM dendriplexes meaning that the interaction occurs locally at the surface in domains. Accordingly, despite the minor surface activity of the dendriplexes, C18-PAMAM dendriplexes seem to promote a local distortion of the phospholipid tails.

We have looked into two magnitudes of the mixed lipid/dendriplex. On the one hand, the dynamic adsorption curves in Fig. 5.6a demonstrate that C18-PAMAM dendriplexes have stronger affinity for phospholipids at the air-water interface than PAMAM complexes. On the other hand, only C18-PAMAM dendriplexes affect the rheological properties of the monolayer. Hence, at a low surface coverage of DPPC ($\approx$20 mN/m), PAMAM dendriplexes penetrate into the DPPC monolayer interacting with

the phospholipid molecules via electrostatic interactions. This mechanism barely affects the flexibility of the monolayer as measured by the dilatational elastic modulus. Conversely, C18-PAMAM dendriplexes penetrate into the DPPC monolayer interacting with the phospholipid molecules by a combined mechanism including electrostatic and hydrophobic interactions. The mechanism of DNA compaction of C18-PAMAM provides a stiffer system and the alkyl chain seems to induce lipid domains which could be significant for cellular uptake[31, 32].

5.2.4   Transfection efficiency and toxicity

The ultimate goal of our dendriplexes is to deliver efficiently plasmid DNA into cells. We used both systems at different Z to transfect HeLa cells with the GFP (Green Fluorescent Protein) encoding plasmid pEGFP. Figure 5.7 shows the percentage of complete cells that expressed green fluorescent protein after transfection with our dedriplexes and the viability of treated cells.

When Z is increased, so is the transfection efficiency of both systems. Between Z=1 and Z=5, the increase in the positive charge of the complexes (Fig. 5.2) favors the interaction with the negatively charged cell surfaces, which is a requirement for unspecific cellular uptake. However, if we focus on the C18-PAMAM we observe an augment in the percentage of transfected cells even when the charge of the complexes was constant; this is, from Z=5 to Z=20. This can be ascribed to the size distribution explained above (Fig. 5.3). When increasing Z, one small population was predominant, which is probably more efficient in delivering the plasmid[33].

If we compare now both systems, it is clear that the transfection efficiency of the C18-PAMAM dendriplexes is considerably enhanced. At the optimized Z=12, a three-fold increase in transfection was observed when the hydropho-bic chain was present. The incorporation of this alkyl chain influences the hydrophobicity, size and stability of the complexes, which contribute to their interaction with cells, as seen in the cell membrane model, resulting in this case in enhanced GFP expression.
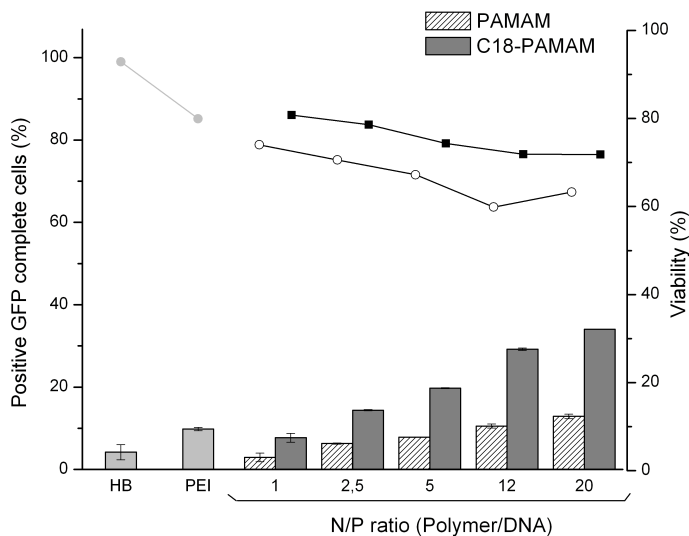
Figure 5.7: Transfection efficiency (bars) and relative viability (symbols). HeLa cells were transfected with PAMAM or C18-PAMAM dendriplexes at indicated Z. HEPES buffer was used as negative control and PEI polyplexes at Z=6 were considered positive control (light gray). PAMAM (Patterned bars, ○) , C18-PAMAM (gray bars, ■).

Cell viability is also shown in Figure 5.7. PAMAM dendriplexes are slightly more toxic than their modified C18-PAMAM counterparts. It is known that the cytotoxic effects of polycations are related to their interaction with the negatively charged cell membrane which leads to destabilization and even activation of intracellular signaling pathways[34]. When the polycation is bound to DNA, the toxicity is reduced if compared to the polycation itself. In our case, unmodified PAMAM G2 was not efficient in condensing DNA, and disassembly was found in a short time. This means that the concentration of free dendrimer is higher and explains the higher toxicity.

5.3   Conclusions

An alkyl-sulfonyl modified PAMAM G2 was investigated as gene vector and compared to unmodified PAMAM G2. The dendrimers were used to condense plasmid DNA and both modified and unmodified PAMAM formed interpolyelectrolyte complexes with DNA. Interestingly, incorporation of the C18 aliphatic chain helps to the condensation process via hydrophobic interactions resulting in a single population of small and compact complexes above Z=12. This is in contrast with the multiple coexistent conformations found for the entire range of Z studied with PAMAM.

The temporal stability of the dendriplexes was also influenced by the condensation process and consequently by the added alkyl chains. Complexes formed with C18-PAMAM were ten-fold more stable in solution than the original PAMAM dendriplexes, which disassembled in few hours.

The interaction of our dendriplexes with a model membrane was addressed by pendant drop tensiometry obtaining an augmented incorporation of C18-PAMAM complexes into a lipid layer. Moreover, the experimental results evidence that, at low surface coverage, the dilatational elasticity of the lipid monolayer is not affected by the presence of PAMAM dendriplexes whereas the C18-PAMAM dendriplexes increase the rigidity of the monolayer. The possible induction of lipid domains suggested by the interfacial rheology studies might have an effect on the internalization and should be further studied.

At the optimized N/P ratio of 12, a three-fold increase in transfection was observed when the hydrophobic chain was present. The incorporation of the octadecyl chains strongly influences the DNA condensation process modulating the size and stability of the complexes and their interaction with a model membrane, which results in better biological performance in vitro.

5.4   Bibliography

[1] M.A. Mintzer and M.W. Grinstaff. Biomedical applications of dendrimers: a tutorial. *Chem. Soc. Rev.*, 40:173–90, 2011.

[2] D.R. Somani, S.and Blatchford, O. Millington, M.L. Stevenson, and C. Dufés. Transferrin-bearing polypropylenimine dendrimer for targeted gene delivery to the brain. *J. Control. Release*, 188(0):78 – 86, 2014.

[3] J.M. Mccarthy, D. Appelhans, J. Tatzelt, and M.S. Rogers. Nanomedicine for prion disease treatment: new insights into the role of dendrimers. *Prion*, 7:198–202, 2013.

[4] L.M. Kaminskas, V.M. McLeod, G.M. Ryan, B.D. Kelly, J.M. Haynes, M. Williamson, D.J. Thienthong, N.and Owen, and C.J.H. Porter. Pulmonary administration of a doxorubicin-conjugated dendrimer enhances drug exposure to lung metastases and improves cancer therapy. *J. Control. Release*, 183(0):18 – 26, 2014.

[5] J. Peng, Z. Wu, X. Qi, and X. Chen, Y.and Li. Dendrimers as Potential Therapeutic Tools in HIV Inhibition. *Molecules*, 18(7):7912–7929, 2013.

[6] C.e Dufés, I.F. Uchegbu, and A.G. Schotzlein. Dendrimers in gene delivery. *Adv. Drug Delivery Rev.*, 57:2177–202, 2005.

[7] J. Haensler and F.C. Szoka. Polyamidoamine cascade polymers mediate efficient transfection of cells in culture. *Bioconjugate Chem.*, 4(5):372–379, 1993.

[8] J.D. Eichman, A. Bielinska, J.F. Kukowska-Latallo, and J.R. Baker. The use of PAMAM dendrimers in the efficient transfer of genetic material into cells. *Pharm. Sci. Technol. Today*, 3:232–245, 2000.

[9] D. Shcharbin, A. Shakhbazau, and M. Bryszewska. Poly(amidoamine) dendrimer complexes as a platform for gene delivery. *Expert Opin. Drug Deliv.*, 10(12):1687–1698, 2013.

[10] R. Duncan and M.J. Vicent. Polymer therapeutics-prospects for 21st century: The end of the beginning. *Adv. Drug Delivery Rev.*, 65(1):60 − 70, 2013.

[11] D. Shcharbin, E. Pedziwiatr, and M. Bryszewska. How to study dendriplexes I: Characterization. *J. Control. Release*, 135:186–97, 2009.

[12] D. Shcharbin, E. Pedziwiatr, J. Blasiak, and M. Bryszewska. How to study dendriplexes II: Transfection and cytotoxicity. *J. Control. Release*, 141:110–27, 2010.

[13] A. Shcharbin, D.and Janaszewska, B. Klajnert-Maculewicz, B. Ziemba, V. Dzmitruk, S. Halets, I.and Loznikova, N. Shcharbina, K. Milowska, M. Ionov, A. Shakhbazau, and M. Bryszewska. How to study dendrimers and dendriplexes III. Biodistribution, pharmacokinetics and toxicity in vivo. *J. Control. Release*, 181(0):40 − 52, 2014.

[14] V. Gimenez, C. James, A. Arminan, A. Schweins, R.and Paul, and M.J. Vicent. Demonstrating the importance of polymer-conjugate conformation in solution on its therapeutic output: Diethylstilbestrol (DES)-polyacetals as prostate cancer treatment. *J. Control. Release*, 159(2):290 − 301, 2012.

[15] O.M. Merkel and T. Kissel. Quo vadis polyplex? *J. Control. Release*, 190(0):415 − 423, 2014.

[16] J.L. Santos, H. Oliveira, J. Pandita, D.and Rodrigues, A.P. Pego, P.J. Granja, and H. Tomás. Functionalization of poly(amidoamine) dendrimers with hydrophobic chains for improved gene delivery in mesenchymal stem cells. *J. Control. Release*, 144(1):55 − 64, 2010.

[17] J.S. Choi, K.S. Ko, J.S. Park, Y.-H. Kim, S.W. Kim, and M. Lee. Dexamethasone conjugated poly(amidoamine) dendrimer as a gene carrier for efficient nuclear translocation. *Int. J. Pharm.*, 320(1â€"2):171 − 178, 2006.

[18] K. Kono, H. Akiyama, T. Takahashi, T. Takagishi, and A. Harada. Transfection Activity of Polyamidoamine Dendrimers Having Hydrophobic Amino Acid Residues in the Periphery. *Bioconjugate Chem.*, 16(1):208–214, 2005.

[19] H. Yoo and R.L. Juliano. Enhanced delivery of antisense oligonucleotides with fluorophore-conjugated PAMAM dendrimers. *Nucleic Acids Res.*, 28(21):4225–4231, 2000.

[20] J. Morales-Sanfrutos, A. Megia-Fernandez, F. Hernandez-Mateo, M.D. Giron-Gonzalez, R. Salto-Gonzalez, and F. Santoyo-Gonzalez. Alkyl sulfonyl derivatized PAMAM-G2 dendrimers as nonviral gene delivery vectors with improved transfection efficiencies. *Org. Biomol. Chem.*, 9:851–64, 2011.

[21] R.S. Dias, O. Innerlohinger, J.and Glatter, M.G. Miguel, and B. Lindman. Coil-globule transition of DNA molecules induced by cationic surfactants: a dynamic light scattering study. *J. Phys. Chem. B*, 109:10458–63, 2005.

[22] K. Qamhieh, C.F. Nylander, T.and Black, G.S. Attard, R.S. Dias, and M.-L. Ainalem. Complexes formed between DNA and poly(amido amine) dendrimers of different generations - modelling DNA wrapping and penetration. *Phys. Chem. Chem. Phys.*, 16:13112–13122, 2014.

[23] M.-L. Ainalem and T. Nylander. DNA condensation using cationic dendrimers-morphology and supramolecular structure of formed aggregates. *Soft Matter*, 7:4577, 2011.

[24] A.M. Carnerup, M.-L. Ainalem, V. Alfredsson, and T. Nylander. Watching DNA Condensation Induced by Poly(amido amine) Dendrimers with Time-Resolved Cryo-TEM. *Langmuir*, 25(21):12466–12470, 2009.

[25] J. Maldonado-Valderrama, T. Torcello-Gómez, A.and del Castillo-Santaella, J.A. Holgado-Terriza, and M.A. Cabrerizo-Vílchez. Subphase exchange experiments with the pendant drop technique. *Adv. Colloid Interface Sci.*, (0):–, 2014.

[26] F.J. Pavinatto, A. Pavinatto, L. Caseli, D.S. dos Santos, T.M. Nobre, M.E.D. Zaniquelli, and O.N. Oliveira. Interaction of Chitosan with Cell Membrane Models at the Air/Water Interface. *Biomacromolecules*, 8(5):1633–1640, 2007.

[27] S. Berenyi, J Mihály, A. Wacha, O. Töke, and A. Bóta. A mechanistic view of lipid membrane disrupting effect of PAMAM dendrimers. *Colloids Surf., B*, 118(0):164 – 171, 2014.

[28] G. Luque-Caballero, A. Martín-Molina, A.Y. Sánchez-Trevino, M.A. Rodríguez-Valverde, M.A. Cabrerizo-Vílchez, and J. Maldonado-Valderrama. Using AFM to probe the complexation of DNA with anionic lipids mediated by Ca2+: the role of surface pressure. *Soft Matter*, 10:2805–2815, 2014.

[29] J. Maldonado-Valderrama, V.B. Fainerman, M.J. Gálvez-Ruiz, A. Martín-Rodriguez, M.A. Cabrerizo-Vílchez, and R. Miller. Dilatational Rheology of beta-Casein Adsorbed Layers at Liquid-Fluid Interfaces. *J. Phys. Chem. B*, 109(37):17608–17616, 2005.

[30] I. López-Montero, P. Mateos-Gil, M. Sferrazza, P.L. Navajas, G. Rivas, M. Vélez, and F. Monroy. Active Membrane Viscoelasticity by the Bacterial FtsZ-Division Protein. *Langmuir*, 28(10):4744–4753, 2012.

[31] P. Raykar, M.C. Fung, and B. Anderson. The Role of Protein and Lipid Domains in the Uptake of Solutes by Human Stratum Corneum. *Pharm. Res.*, 5(3):140–150, 1988.

[32] S.D. Conner and S.L. Schmid. Regulated portals of entry into the cell. *Nature*, 422(6927):37–44, March 2003.

[33] A.U. Bielinska, C. Chen, J. Johnson, and J.R. Baker. DNA complexing with polyamidoamine dendrimers: implications for transfection. *Bioconjugate Chem.*, 10:843–50, 1999.

[34] D. Fischer, Y. Li, B. Ahlemeyer, and T. Krieglstein, J.and Kissel. In vitro cytotoxicity testing of polycations: influence of polymer structure on cell viability and hemolysis. *Biomaterials*, 24(7):1121 – 1131, 2003.

6

LINEAR PAAS/DNA
COMPLEXES

The sixth chapter is dedicated to the investigation of the hydrophobic interactions in the condensation process. Poly(amidoamine)s with the same cationic block but different hydrophobic chains were used to condense DNA.

Contents

6.1   Background and motivation

The main drawback of polymeric materials for the systematic investigation of structure-activity relationships is the polydispersity of their molecular weights which contributes to the heterogeneity of the complexes formed with DNA[1]. In the previous chapter we used PAMAM dendrimers with a well-defined structure as a consequence of their synthesis procedure[2]. However, it was not easy to manage the number of amino groups modified with the hydrophobic chain, and the process was controlled exclusively by the stoichiometry of the reactants. The ideal condensing agent should integrate in their backbone different domains for targeting, shielding and release among others[3]. That multifunctional polymer requires not only a rational design, but also a procedure of synthesis that grants full control of the functionalities and their position.
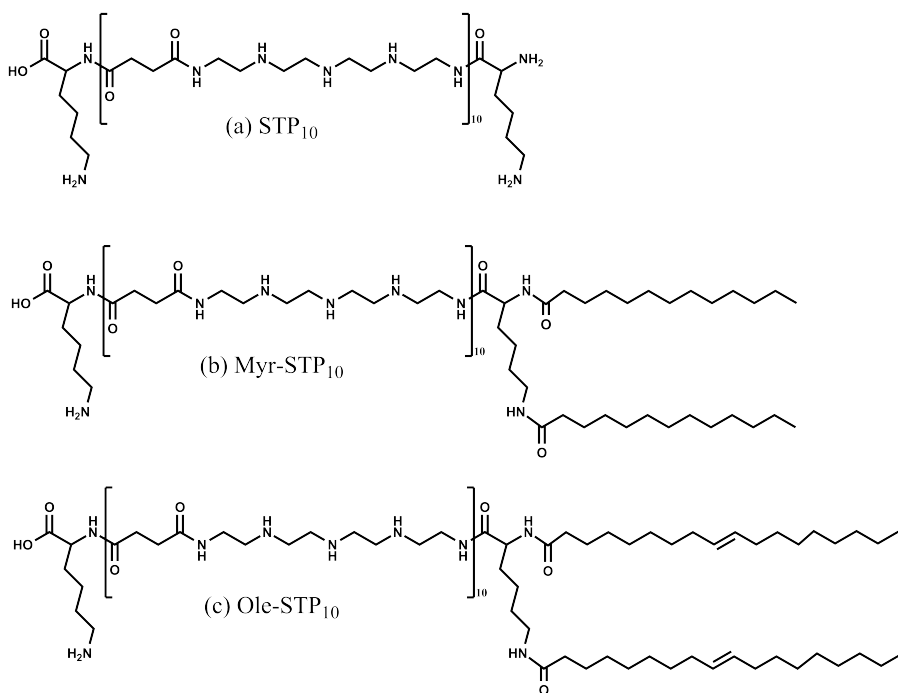
Figure 6.1: Structures of the polymers (a) STP_{10}, (b) Myr-STP_{10} and (c) Ole-STP_{10} polyplexes.

Hartman[4] et al. demonstrated the synthesis of linear poly(amidoamine)s (PAAs) using solid-phase assisted synthesis. This approach is well known and widely used for the synthesis of peptides, due to its multiple advantages. The whole process can be automated, controlled step-by-step and it is based on the use of a solid phase and reversibly protected reactive groups. Poly(amidoamine)s are versatile in structure and functionality, and their unique properties make them suitable for many biomedical applications[5].

The potential to tailor-make the domains of the polymer to modulate the interactions involved in the DNA condensation process is what has motivated the use of PAAs in this chapter. By combining a cationic building block with hydrophobic chains of different lengths[6] a family of linear sequence-defined poly(amidoamine)s can be easily synthesized.

Our main objective was to evaluate the contribution of different hydrophobic chains to the condensation of a plasmid DNA. We chose three positively charged polymers with identical cationic building blocks of 31 protonable groups, but bearing different hydrophobic tails. Figure 6.1 shows the structure of the three PAAs used. The STP_{10} polymer, which is the unmodified cationic building block, the $STP_{10} - Myr_2$, which has been modified with two tails of myristic acid (14-carbon fatty acid, saturated), and the $STP_{10} - Ole_2$ polymer, that bears two chains of oleic acid (18-carbon fatty acid, one unsaturation).

The objectives of this chapter will be:

i) To evaluate the influence of the hydrophobic moieties on the condensation process and on the morphology of the formed complexes.

ii) To analyze the interaction of the polymers with a cell membrane model.

iii) To correlate the colloidal properties of the complexes and its morphology with the transfection *in vitro*.

6.2   Results and discussion

6.2.1   DNA condensation

The ability of the STP_{10}, Myr-STP_{10} and Ole-STP_{10} linear polyaminoamides to condense DNA was studied using the gel retardation assay and the obtained results are shown in Figure 6.2. Polyplexes were formed with the pEGFP plasmid at different N/P ratios in HEPES buffer 20 mM, pH 7.4. The three investigated polymers present a similar behavior and all DNA is retained above N/P=1 regardless the polymer used, which demonstrates the strong attachment of these pAAs to DNA. Moreover, at N/P=1, DNA is partially condensed, since none of the lanes reaches the distance of the untreated DNA and the bands corresponding to Myr-STP_{10} and Ole-STP_{10} are smeared.
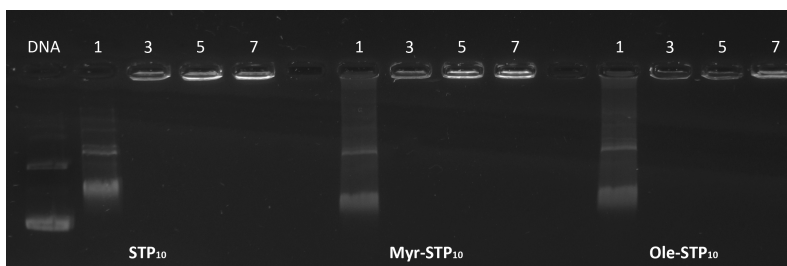
Figure 6.2: Electrophoresis mobility shift assay of STP_{10}, Myr-STP_{10} and Ole-STP_{10} polyplexes (from left to right) at different N/P ratios indicated above each lane. Lane 1, naked DNA

The average hydrodynamic diameter of the complexes at different N/P ratios was determined by dynamic light scattering (DLS) with a Malvern Nanosizer ZS. The obtained results are presented in Figure 6.3. The error bars correspond to the standard deviation of three replicate measurements. At N/P=0.5, large particles with an approximate diameter of 500-600 nm were identified. The reduction in size observed in comparison with that of free DNA indicates that the polymers are interacting with DNA and supramolecular structures are likely formed, but the amount of condensing agent is not enough to induce condensation. Further addition of polymer

dramatically decreases the size of the complexes formed, obtaining particles of 100 nm in diameter at N/P=2. According to Figure 6.2, DNA was mainly unbound at N/P=1. DNA coils and globular complexes may coexist and that would be reflected on the polydispersity index (PDI) of the samples. The table 6.1 shows the PDI of the complexes formed at N/P ratios of 0.5, 1 and 2, and the standard deviation was used as error.
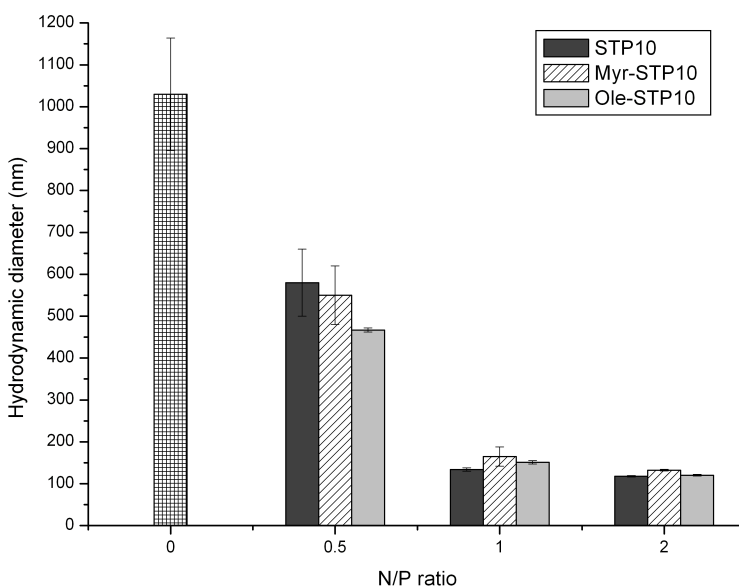
Figure 6.3: Average hydrodynamic diameter of untreated DNA (densely patterned) and STP_{10} (dark gray), Myr-STP_{10} (patterned) and Ole-STP_{10} (light gray) polyplexes at different N/P ratios.

The large structures found at N/P=0.5 have a high PDI, indicating a wide size distribution, as expected. At N/P=1, despite the small sizes found with the three polymers, high PDI values are observed. This corroborates the coexistence of different species in solution, and indicates that a higher amount of polymer would be necessary to induce full compaction. Lastly, the PDI values obtained at N/P=2 are much smaller, being ≤ 0.25, which we consider acceptable enough for interpolyelectrolyte complexes. Consequently, further studies of the polyplexes will be done at N/P=2.

	STP_{10}	Myr-STP_{10}	Ole-STP_{10}
N/P= 0.5	0.62 ± 0.07	0.59 ± 0.07	0.58 ± 0.08
N/P= 1	0.44 ± 0.07	0.65 ± 0.03	0.331 ± 0.011
N/P= 2	0.250 ± 0.024	0.194 ± 0.016	0.233 ± 0.020

Table 6.1: Polydispersity indexes of the complexes formed at different N/P ratios.

6.2.2 | Influence of the hydrophobic chains on DNA condensation

The condensing ability and hydrodynamic diameter of the complexes did not point to differences derived from the presence of the hydrophobic moieties. The driving force of DNA condensation is the electrostatic interaction between the oppositely charged polymers, and this can mask the contribution of other forces, such as the hydrophobic ones. Salt is known to enhance the hydrophobic interactions that additionally stabilize the collapsed state[7]. In order to investigate in more detail the condensation of DNA with these linear PAA we decided to progressively increase the concentration of monovalent salt, thus reducing the effective charge of the polymers. The polyplexes were formed at different initial sodium chloride (NaCl) concentration and the average hydrodynamic diameters were measured by DLS (Figure 6.4). Due to the importance of counterions and its valence in the condensation process, before performing these experiments, the plasmid DNA was extensively dialyzed against a solution of NaCl 2M, and then against HEPES buffer 20 mM, pH 7.4. This ensures that monovalent Na^+ are the only counterions in the medium[8].

The presence of a higher amount of monovalent salt during the condensation process has different effects depending on the concentration. The smaller sizes are obtained when no salt is added, indicating not only optimum condensation, but also that the formed particles present an overall surface charge high enough to keep the complexes as individual entities.

When the amount of NaCl present in solution is increased, both the polycations and the DNA will be partially neutralized. While this is expected to favor DNA condensation due to the screening of the electrostatic repulsion between like-charged chains, we observed large aggregates. This can be
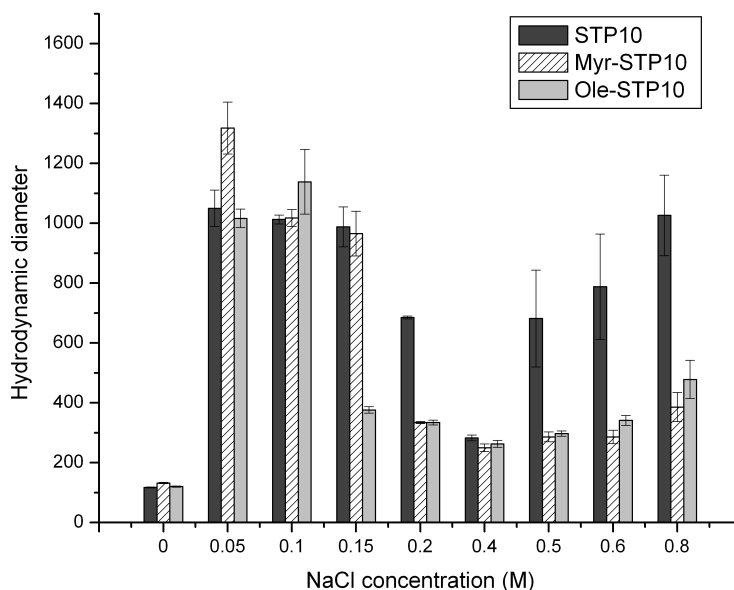
Figure 6.4: Average hydrodynamic diameter of STP_{10} (dark gray), Myr-STP_{10} (patterned) and Ole-STP_{10} (light gray) polyplexes at N/P=2 formed at the indicated NaCl concentration.

explained by considering the colloidal stability of the complexes. According to the classical DLVO theory, the increase of the ionic strength reduces the repulsive potential that comes from the electrical double layers of charged particles[9]. In the absence of other stabilizing mechanisms, the particles will aggregate. This means that the interaction of the polymers with DNA is supposed to be facilitated by the addition of a low amount of salt, but the complexes aggregate due to the screening of the repulsion among them[7,10]. This explains the DLS diameters observed at the range of 50-200 mM (depending on the polymer). However, individual entities are again found after further increase of the initial concentration of salt. And more importantly, the concentration at which this phenomenon occurs depends on the polymer used.

At 150 mM of NaCl, a decrease in size is observed exclusively with Ole-STP_{10}. At 200 mM the diminution in size is also seen with Myr-STP_{10} and it is not until 400 mM is used that STP_{10} behaves likewise. The classic DLVO theory does not predict a re-stabilization at high salt concentrations,

and aggregation would be expected in the entire range of salt concentrations evaluated. Moreover, the addition of salt might induce dissociation of interpolyelectrolyte complexes due to the screening of the electrostatic repulsions[11], which is the opposite behavior of the observed with our systems. This phenomenon can be explained by considering another stabilization mechanism: the hydration forces. This short-range repulsive force is related to the structuring of water molecules and hydrated ions surrounding hydrophilic surfaces. Detailed information can be consulted in specific references[12–14]. Since the hydration forces depend on the hydrophilicity of the particles, one would expect to find re-stabilization at lower NaCl concentrations with the more hydrophilic polymer, i.e. STP_{10}. However, the trend observed in Figure 6.4 is surprisingly inverted, being the more hydrophobic polymer (Ole-STP_{10}) the first one to show this behavior.

A similar behavior was observed by Santander-Ortega[15] et al. when using acetylated chitosan adsorbed onto lipid nanocapsules. The critical stabilization concentracion (csc) (minimum salt concentration at which the system begins to re-stabilize) decreased with the hydrophobicity of the chitosan, this is, the surface was more hydrophilic when the more hydrophobic polymer was used. They proposed that hydrophobic interactions between the chitosan and the hydrophobic patches of the lipid capsule modulated the arrangement of the polymer, which would expose only the hydrophilic parts towards the aqueous phase, resulting in a more hydrophilic surface.

Returning to our systems, a similar mechanism is proposed. The hydrophobic interactions refer to the clustering of non-polar components in aqueous environment. The lipophilic chains present in Myr-STP_{10} and Ole-STP_{10} are expected to spontaneously approximate, avoiding contact with water. This interaction is not relevant when the electrostatic attraction is dominant, i.e. at low salt concentrations. However, when the electrostatic potential is decreased as a consequence of salt screening, the hydrophobic forces might promote clustering of the polymers. The hydrophobic moieties would remain hidden, thus exposing the hydrophilic parts as in the case of chitosan. If the concentration of salt in the medium overcomes the corresponding csc of the system, a re-stabilization mechanism would explain the presence of individual particles/small clusters, instead of large aggregates. The csc values of our complexes cannot be calculated from the DLS results, but a qualitative trend of the hydrophilicity of their surfaces will be: Ole-STP_{10}

$> \mathrm{Myr\text{-}}STP_{10} > STP_{10}$.

If we focus now on the NaCl concentrations above 400 mM of Figure 6.4, the size of the STP_{10} complexes increases again. The condensation process is a balance of forces: the interactions favoring condensation must overcome those which oppose. If the electrostatic potential is further reduced by screening, the compaction of DNA cannot occur, unless other interactions compensate the collapse. In the case of Myr-STP_{10} and Ole-STP_{10}, hydrophobic interactions favor the condensed conformation, and the hydration forces stabilize the complexes. On the other hand, STP_{10} cannot condense DNA anymore and supramolecular large structures, similar to those formed at N/P=0.5, are likely formed, according to the diameters seen in Figure 6.4. Upon large excess of salt, all polymers are expected to lose their ability to condense DNA. In fact, at 800 mM of NaCl the size of the complexes seems already increased.

To sum up, the hydrophobic moieties attached to our polymers contribute not only to the condensation process of DNA, but also to the stabilization of the complexes through a combined mechanism of hydrophobic interactions and hydration forces.

6.2.3   Morphology of the polyplexes at different ionic strengths

Motivated by the striking behavior of our polyplexes in the presence of monovalent salt, we questioned whether the morphology of the complexes would be different as a consequence of a) the hydrophobicity of the polymer, and b) the ionic strength of the medium. Transmission Electron Microscopy (TEM) was used to investigate the morphology of STP_{10}, Myr-STP_{10} and Ole-STP_{10} polyplexes formed at N/P=2 in the presence of 0, 0.15, 0.4 and 0.6 M of NaCl. The software ImageJ was used to estimate the size of the complexes.

6.2.3.1   *Without NaCl*

Firstly, the morphology of the complexes without NaCl was analyzed. In Figures 6.5, 6.6 and 6.7, some representative TEM images of the polyplexes are shown.

a) The STP_{10} polymer (Fig. 6.5)produces mainly toroids of an approximate outer diameter of 60 ± 11nm. Some rods of 140 ± 12nm in length are also found.
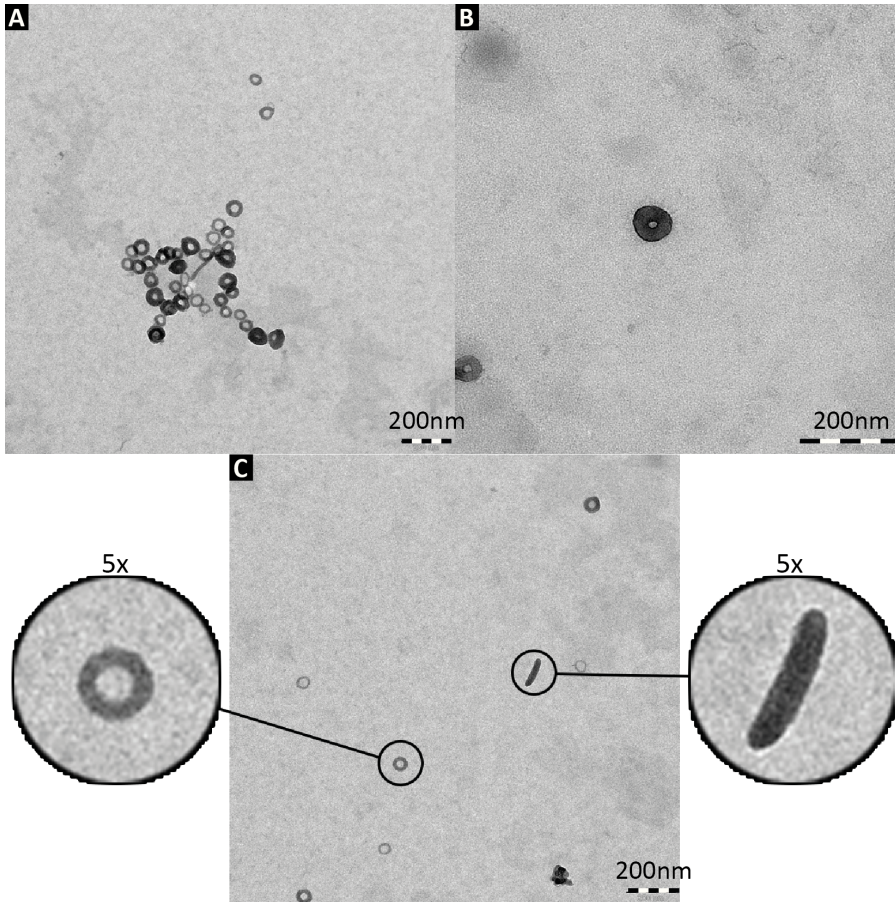
Figure 6.5: TEM micrographs of STP_{10} polyplexes at N/P=2 formed without NaCl.

b) The Myr-STP_{10} polymer (Fig. 6.6) produces predominantly amorphous globules with an average diameter of 100 ± 30nm. In addition, scarce toroids and rods can be seen.

c) The Ole-STP_{10} polymer (Fig. 6.7) produces amorphous globules of 84 ± 22nm in diameter. A few toroids are also found. Hairy particles indicate intermediate states of partially condensed DNA.
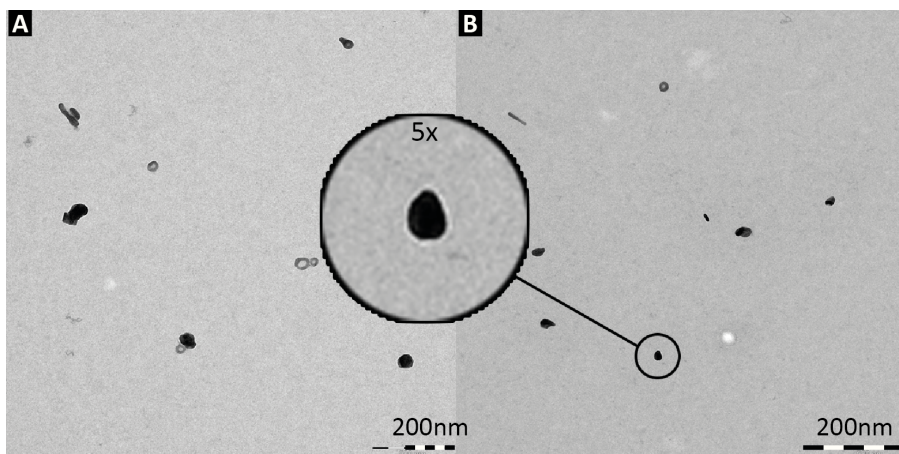
Figure 6.6: TEM micrographs of Myr-STP_{10} polyplexes at N/P=2 formed without NaCl.

All these morphologies, i.e. toroids, rods and globules, are structures commonly found when analyzing DNA condensates[16–18]. Toroids have been studied the most, and their structure is known in detail[19]. However, the mechanism of toroid formation remains unclear. Several parameters have been proved to influence the morphology of DNA condensates, such as the polarity of the solvent[20], the ionic strength[21], the length of DNA, the nature of the condensing agent[18] and even chirality[22].

It seems clear that our polymers yield different morphologies. Since the number of protonable groups is practically the same for the three of them, the hydrophobic chains must be responsible for the differences observed. The tight packaging necessary to form toroids might be sterically hindered by the alkyl chains[23], but the condensation process is favored by both, electrostatic and hydrophobic interactions. Accordingly, compact amorphous globules are found.

The size of the complexes correlates well with that obtained by DLS (Fig.6.4). The presence of agglomerates might be a consequence of the protocol followed for electron microscopy, which includes drying of the samples. This would explain why those aggregates are not detected by DLS.
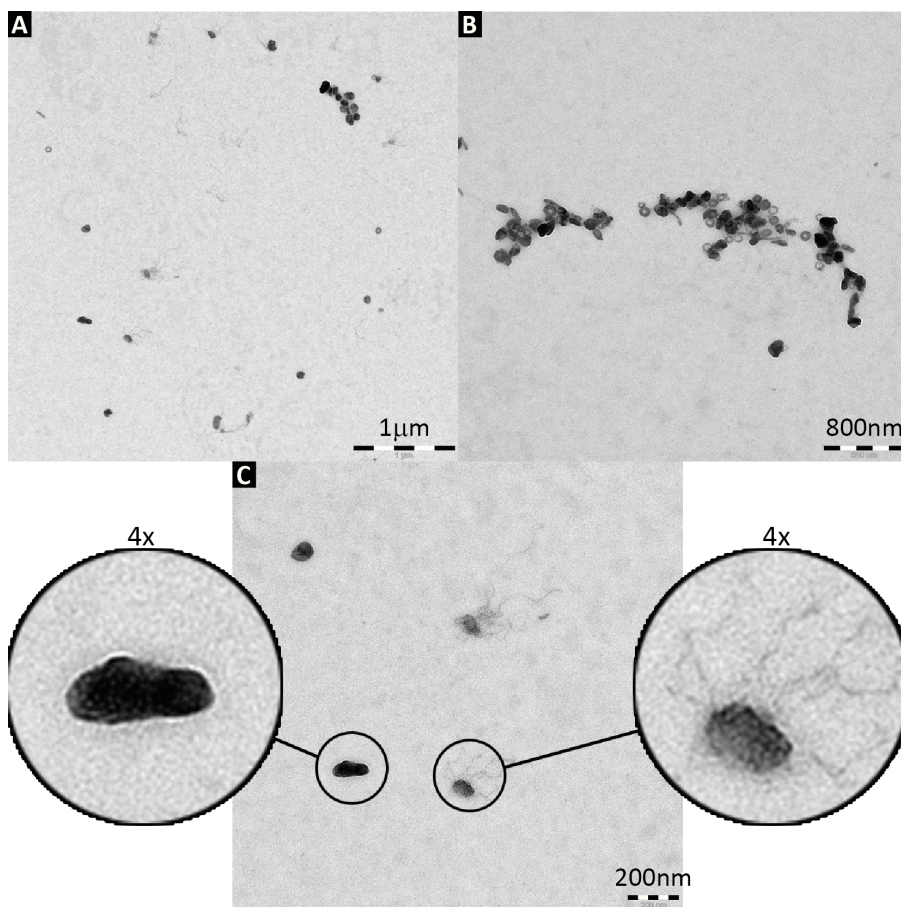
Figure 6.7: TEM micrographs of Ole-STP_{10} polyplexes at N/P=2 formed without NaCl.

6.2.3.2   *NaCl, 0.15 M*

The PAAs were now used to condense DNA in the presence of 0.15 M of NaCl, and some of the micrographs can be seen in Figures 6.8, 6.9 and 6.10.

a) The prevalent morphology when using the STP_{10} polymer (Fig. 6.8) is still toroidal (119 ± 16nm), but there are clusters interlinked with partially condensed DNA forming networks.

b) With the Myr-STP_{10} polymer (Fig. 6.9), DNA is partially condensed forming compact amorphous structures (140 ± 40 nm) interlinked with thick
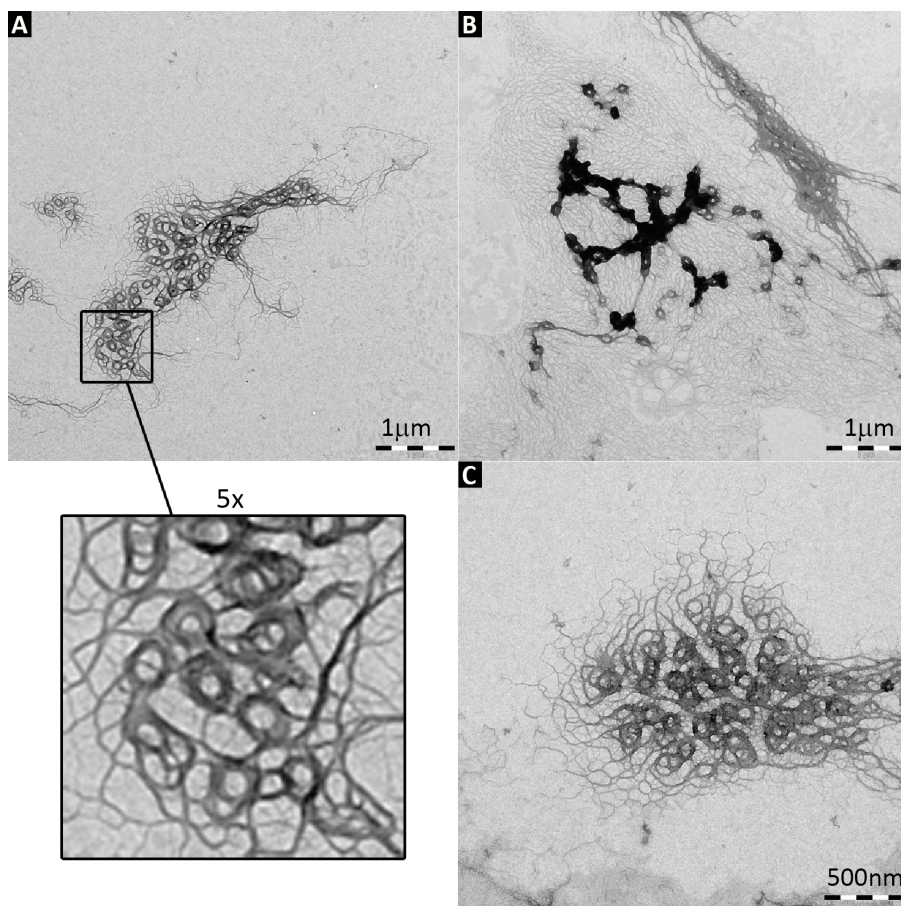
Figure 6.8: TEM micrographs of STP_{10} polyplexes at N/P=2 formed with 0.15M of NaCl.

strands.

c) The Ole-STP_{10} polymer (Fig. 6.10) produces bigger condensates than in the absence of salt but the morphology is kept. Spheroid complexes, toroids and rods are found, with an average diameter/length of 170 ± 50 nm. Hairy particles indicating intermediate states of partially condensed DNA are still found.

At this ionic strength, the interaction of the STP_{10} and the Myr-STP_{10} polymers with DNA promotes the formation of thick cord-like structures[23] of partially condensed DNA. These networks are found between fully compacted DNA with a toroidal (STP_{10}) or globular (Myr-STP_{10}) morphology.
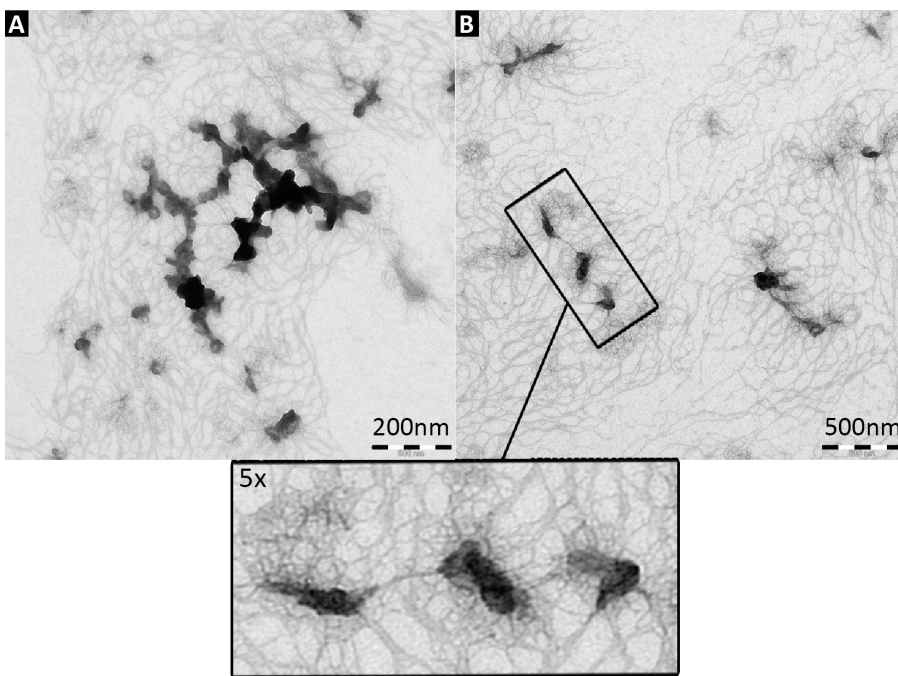
Figure 6.9: TEM micrographs of Myr-STP_{10} polyplexes at N/P=2 formed with 0.15M of NaCl.

Therefore, the large particle diameters obtained by DLS are not the consequence of aggregation, but of a completely different morphology of condensed DNA caused by the presence of a higher concentration of monovalent salt.

On the other hand, individual entities are found by DLS and TEM with Ole-STP_{10} polymer, due to the stronger hydrophobic interaction along with the moderate concentration of salt present during condensation. The hydration forces stabilize the complexes, although some networks and aggregates can also be seen.

6.2.3.3   *NaCl, 0.4 M*

The micrographs of the polyplexes formed at 0.4 M of NaCl are shown in Figures 6.11, 6.12 and 6.13.

a) The STP_{10} polymer (Fig.6.11) yield now amorphous and undefined complexes surrounded by a diffuse halo. Small white spots which might
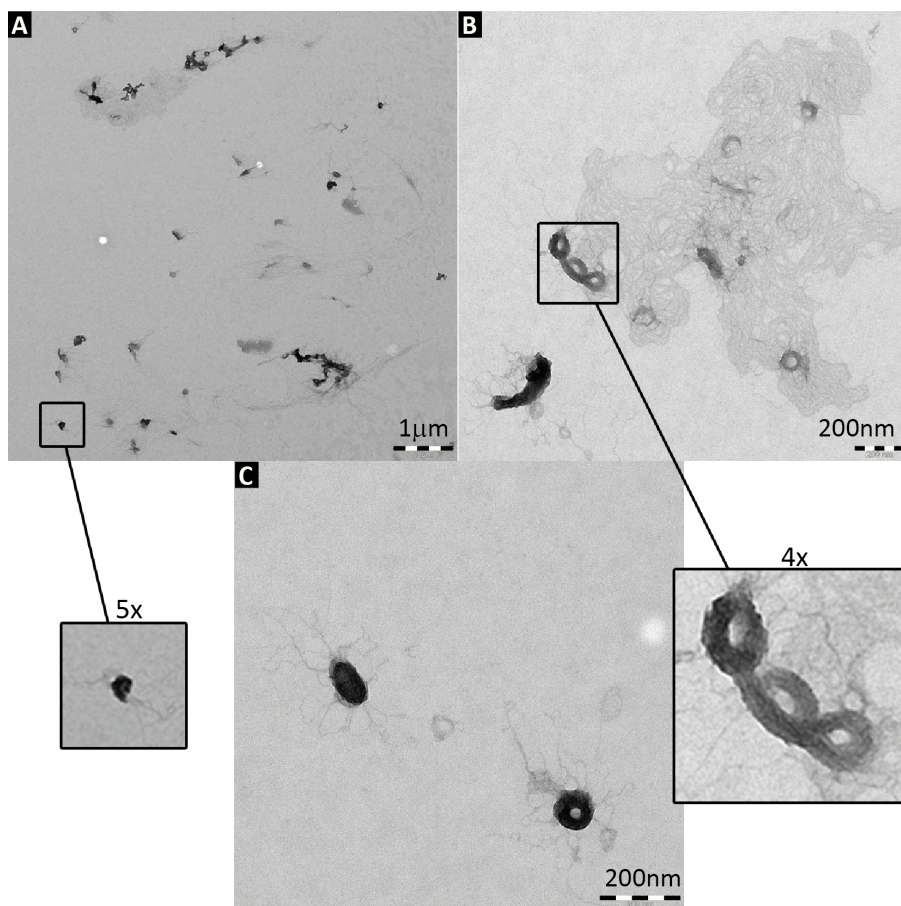
Figure 6.10: TEM micrographs of Ole-STP_{10} polyplexes at N/P=2 formed with 0.15M of NaCl.

correspond to crystals of salt after evaporation, are also found in the vicinity of the particles. The mean diameter of the complexes determined from the micrographs is 240 ± 80nm.

b) With the Myr-STP_{10} polymer (Fig. 6.12), a change in morphology is observed. Thin rods $(350 \pm 100$nm$)$, scarce toroids $(94 \pm 6$nm$)$ and intermediate hairy structures replace the amorphous globules seen at low salt conditions.

c) The Ole-STP_{10} polymer (Fig. 6.13) induces the formation of condensates with various morphologies, but predominantly rods $(250 \pm 30$nm$)$. Networks of partially condensed DNA are seen interlinking fully compacted globules
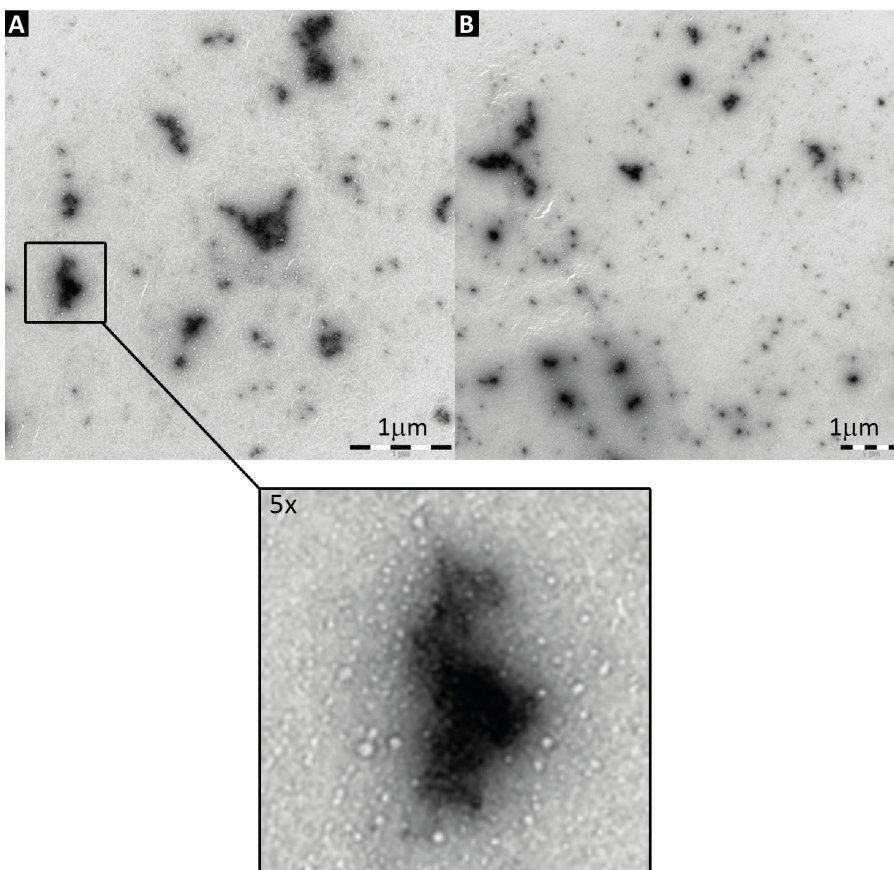
Figure 6.11: TEM micrographs of STP_{10} polyplexes at N/P=2 formed with 0.4M of NaCl.

and/or toroids.

At this ionic strength, DLS predicted individual entities regardless the polymer used (Fig. 6.4). This is confirmed with TEM, but the morphologies of the complexes depend on the nature of the polymer. The polymers bearing hydrophobic tails, Myr-STP_{10} and Ole-STP_{10}, form defined rod-like complexes. This morphology was barely seen at low salt conditions, which indicates that the screening of the charges allows tighter packaging of DNA, while the driving force is mainly hydrophobic, since it is not observed with STP_{10}. Moreover, the diminution of the electrostatic potential as a consequence of salt screening, hampers the interaction between the STP_{10}
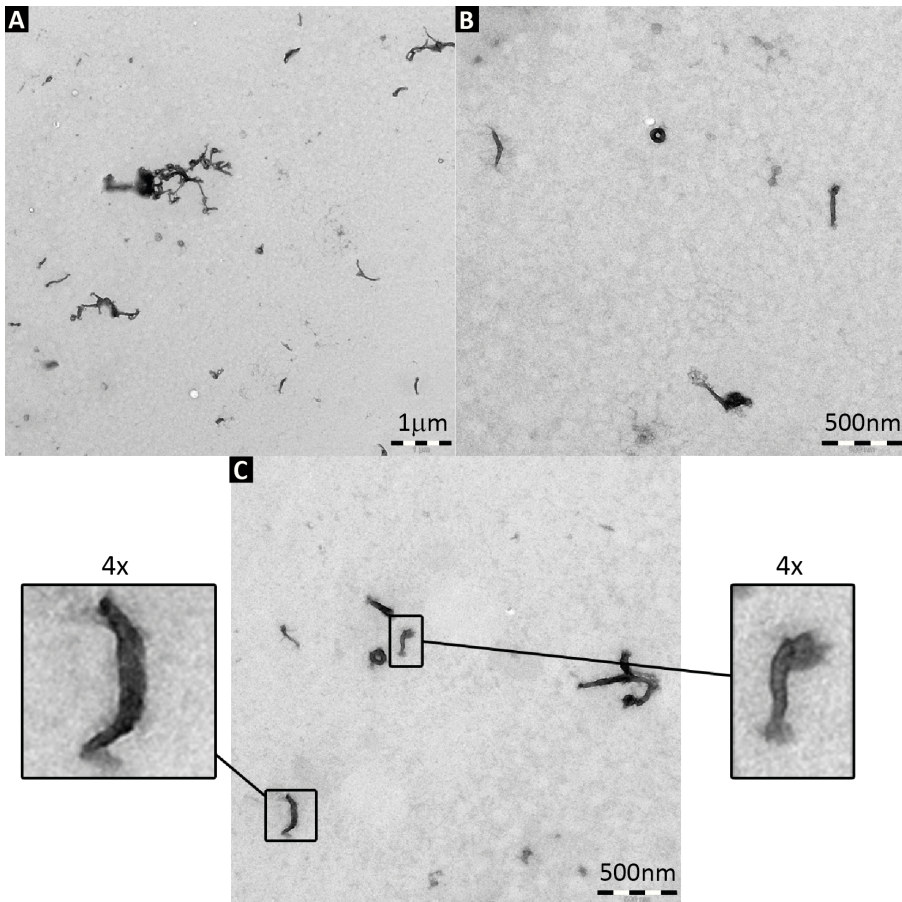
Figure 6.12: TEM micrographs of Myr-STP_{10} polyplexes at N/P=2 formed with 0.4M of NaCl.

polymer and DNA, and due to the lack of hydrophobic interactions, the complexes are loose and undefined. However, once the complex is formed, it can be stabilized by hydration forces, owing to the presence of salt. In fact, the crystals of salt formed as a consequence of water evaporation are predominantly found surrounding the complexes, which might indicate that a higher concentration of ions close to the surface in solution.

6.2.3.4 *NaCl, 0.6 M*

Finally, the complexes formed at a higher concentration of salt, 0.6 M of NaCl, were investigated and the micrographs are shown in Figures 6.14,
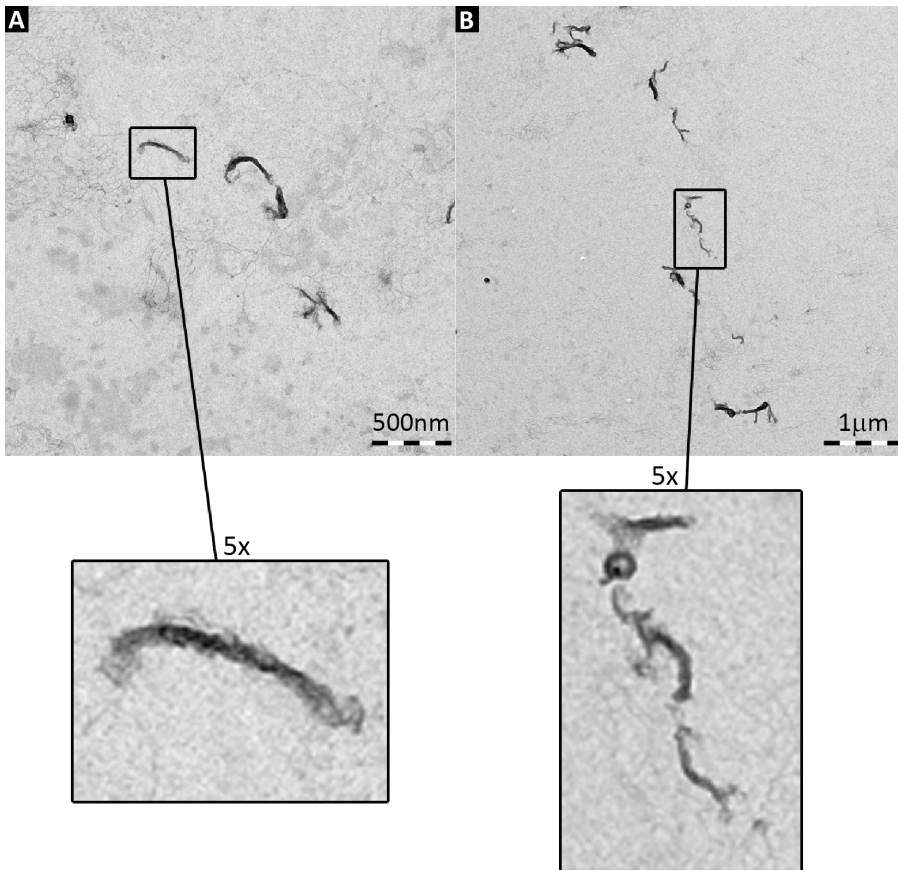
Figure 6.13: TEM micrographs of Ole-STP_{10} polyplexes at N/P=2 formed with 0.4M of NaCl.

6.15 and 6.16.

a) It was difficult to find any stained structure when using STP_{10} polymer at this ionic strength. The micrograph selected (Fig. 6.14) shows one cluster of amorphous complexes, but it was the exception and not the rule.

b) With the Myr-STP_{10} polymer (Fig. 6.15) we found again amorphous globules with a mean diameter of 100 ± 30 nm. The small white spots surrounding the complexes can also be seen.

c) The morphologies found with Ole-STP_{10} polymer (Fig. 6.16) are similar
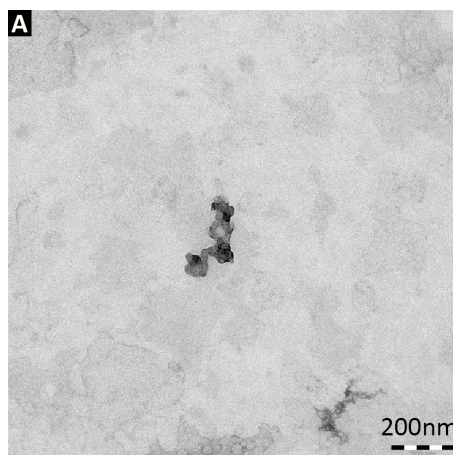
Figure 6.14: TEM micrographs of STP_{10} polyplexes at N/P=2 formed with 0.6M of NaCl.
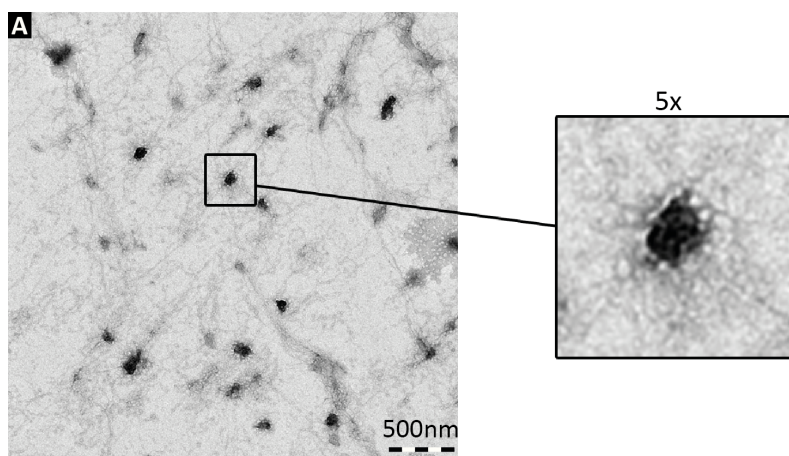
Figure 6.15: TEM micrographs of Myr-STP_{10} polyplexes at N/P=2 formed with 0.6M of NaCl.

to those obtained at 0.4 M of NaCl, predominantly rods (200 ± 100nm) and networks of partially condensed DNA interlinking fully compacted rods and/or toroids.

This amount of salt does not allow the collapse of DNA with these polymers, unless the hydrophobic interaction favors the process. The STP_{10} is not capable of condense DNA, but complexes are found with the hydrophobically modified polymers. The Myr-STP_{10} cannot maintain the ordered rod-like
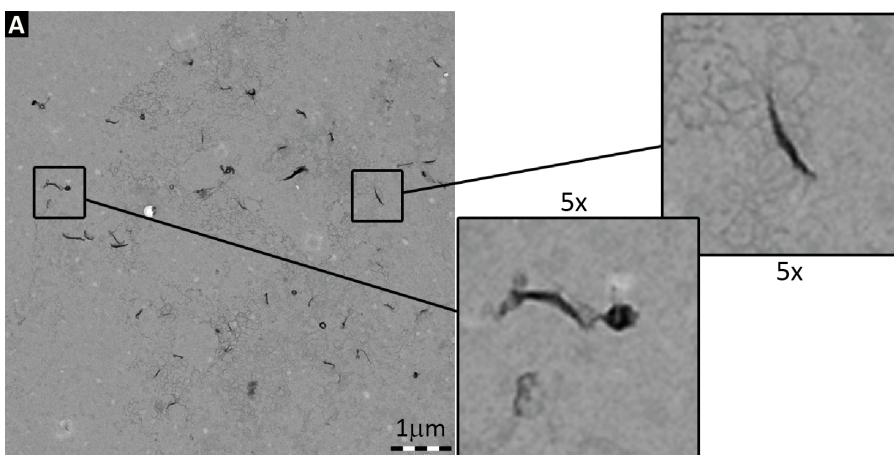
Figure 6.16: TEM micrographs of Ole-STP_{10} polyplexes at N/P=2 formed with 0.6M of NaCl.

structures seen before, but it forms globular complexes with DNA. The crystallized salt in the vicinity of the particles might be an indication of the proposed stabilization mechanism. Lastly, the Ole-STP_{10} compact DNA into individual small rods and/or thick strands that remain interlinked in a network structure. Even toroids are formed, indicating that better packaging is possible due to screening of charges and hydrophobic interaction.

The TEM results correlate well with those obtained by DLS and it was demonstrated that both, the hydrophobic modification and the ionic strength, influence the condensation process, which is reflected in a different morphology and hydrodynamic diameter.

6.2.4   Interaction of the polymers with a cell membrane model

6.2.4.1   *Adsorption kinetics*

One of the objectives of this chapter was to evaluate the possible interaction of these polymers with a cell membrane model. With that purpose, we have evaluated both, the adsorption kinetics of our polymers onto a monolayer of the zwitterionic lipid DPPC (dipalmitoylphosphatidylcholine), and the rheological properties of the mixed DPPC/polymer system. The

pendant drop technique, implemented with subphase exchange, was used with solutions of $5\mu M$ of the corresponding polymer in HEPES buffer 20 mM, pH 7.4.
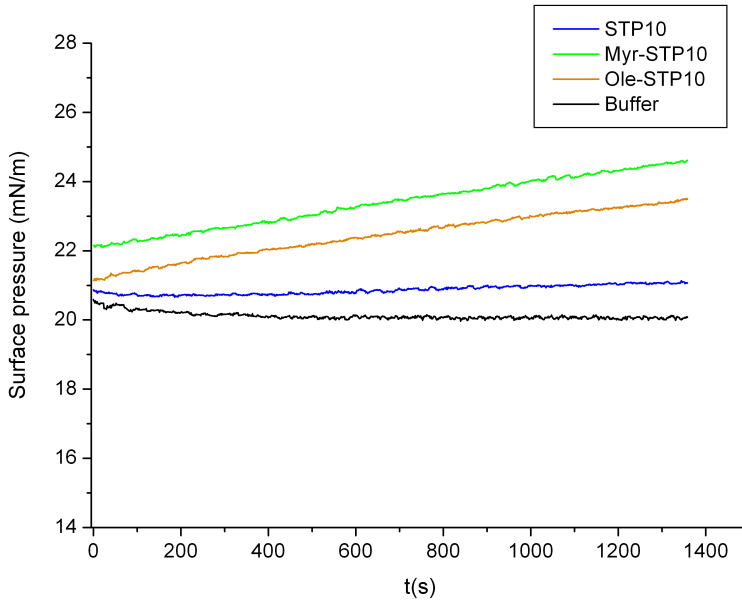
Figure 6.17: Adsorption kinetics onto a DPPC monolayer at $\pi = 20$ mN/m following subphase exchange with HEPES buffer (black) or $5\mu M$ of STP_{10} (blue), Myr-STP_{10} (green) and Ole-STP_{10} (orange)

In Figure 6.17, the time evolution of the surface pressure of a DPPC monolayer spread onto HEPES 20 mM, pH 7.4 is shown. The initial surface pressure was always fixed at 20 mN/m, although the data represented in Fig.6.17 start after the complete exchange of the subphase, which means that the surface pressure might have already changed.

The exchange with the buffer solution was done as a reference, and the surface pressure remains constant at 20 mN/m during the whole experiment. On the other hand, the introduction of the PAAs into the subphase modifies the interfacial tension, and consequently, the surface pressure.

The STP_{10} polymer increases slightly the surface pressure, but the adsorption occurs right after the exchange, and it does not continue during the experiment, as deduced by the low slope of the curve. At pH 7.4, DPPC exposes a positive charge from the choline group and a negative charge from

the phosphate. Since the polar heads of the phospholipid are oriented into the bulk, the positively charged polymers can interact electrostatically with the phosphate group[24]. Some of the STP_{10} polymer chains are therefore attached to the polar heads via Coulombic interaction, and due to the low surface density at 20 mN/m, the polymer might slightly penetrate into the interface.

The Myr-STP_{10} polymer, on the other hand, is the one with a higher interfacial activity in the presence of DPPC. The sudden increase of the surface pressure after the exchange indicates that no induction time is required, due to the electrostatic interaction with the polar heads of DPPC, which facilitates adsorption. Progressive penetration of the polymer in the interface continues during the whole adsorption assay.

The Ole-STP_{10} polymer present a similar behavior to that of Myr-STP_{10} polymer, but the change in the surface pressure of the monolayer is smaller.

Although a higher adsorption would be expected from the longer hydrophobic tails (C18) of Ole-STP_{10} polymer, the unsaturation of the oleic chains does not allow close packing at the interface. On the other hand, the myristic chains (C14) of Myr-STP_{10} have a similar length to that of the palmitic tails (C16) of DPPC, and both are saturated, which allows close packaging and a higher adsorption of the polymer at the air/water interface.

6.2.4.2 *Surface dilatational rheology*

The adsorption of the polymers at the DPPC monolayer might alter the lateral packing of the phospholipids[25]. The response behavior of the interface to small elongational perturbations allows a further understanding of the interaction of our polymers with a model membrane. Therefore, we estimated the interfacial dilatational modulus (E) of the different DPPC-polymer systems by imposing small oscillating perturbations at different frequencies to the pendant drop. In all cases the viscous component of the dilatational modulus was very small and the systems appear predominantly elastic. The interfacial elasticity moduli (E') are shown in Table 6.2. The oscillations were done at the end of each dynamic curve shown in Figure 6.17.

	E' (mN/m)		
	$\omega = 0.01s^{-1}$	$\omega = 0.1s^{-1}$	$\omega = 1s^{-1}$
HEPES	58.40 ± 0.18	64.7 ± 1.2	70 ± 2
STP_{10}	60.1 ± 0.5	68.1 ± 0.3	74.5 ± 0.6
Myr-STP_{10}	67.6 ± 1.5	74.0 ± 2.1	80 ± 3
Ole-STP_{10}	62.8 ± 2.1	71 ± 3	76 ± 3

Table 6.2: Dilatational surface elasticity moduli of the DPPC/polymer systems investigated at different frequencies.

The elasticity modulus quantifies the stiffness of the interface. At low frequencies, the molecules have time to rearrange during the perturbation, and the interface is more elastic (lower E'). On the other hand, if the oscillations are too fast (high frequency), the ability to restore the surface pressure when subjected to deformation decreases, and the interface is more rigid (higher E'). Therefore, in the linear regime the elasticity modulus increases with the oscillation frequency[26]. This trend was observed for all the systems studied.

The three polymers investigated increase the elasticity modulus of the interface. During the expansion/compression process of the droplet, the polymers are rapidly adsorbed at the DPPC monolayer, which leads to a larger change in the surface pressure, yielding a higher E'. Therefore, the polymers with a higher degree of penetration into the DPPC monolayer (Fig. 6.17) will further increase the stiffness of the interface.

It can be concluded that the Myr-STP_{10} polymer is the one with higher degree of penetration, thanks to the myristic chains, which allows a better lateral packing at the interface. The STP_{10} polymer interacts electrostatically with the polar heads of the phospholipids slightly modifying the interfacial properties of the monolayer. The Ole-STP_{10} presents an intermediate behavior with the long oleic chains penetrating into the DPPC monolayer, but the presence of an unsaturation reduces the amount of adsorbed polymer. However, in a real membrane with higher phospholipid surface coverage, the disruption of the lateral packing produced by the unsaturated chains might lead to the destabilization of the membrane.

| 6.2.5 | Transfection efficiency and toxicity |

The polyplexes at N/P = 2 formed with the three polymers investigated in this chapter were used to transfect *in vitro* HeLa cells with the pEGFP plasmid DNA, which encodes the Green Fluorescent Protein (GFP). In order to compare between the different morphologies observed with electron microscopy, the polyplexes were formed at various NaCl concentrations. The percentages of transfected HeLa cells and their relative viability are shown in Figure 6.18.
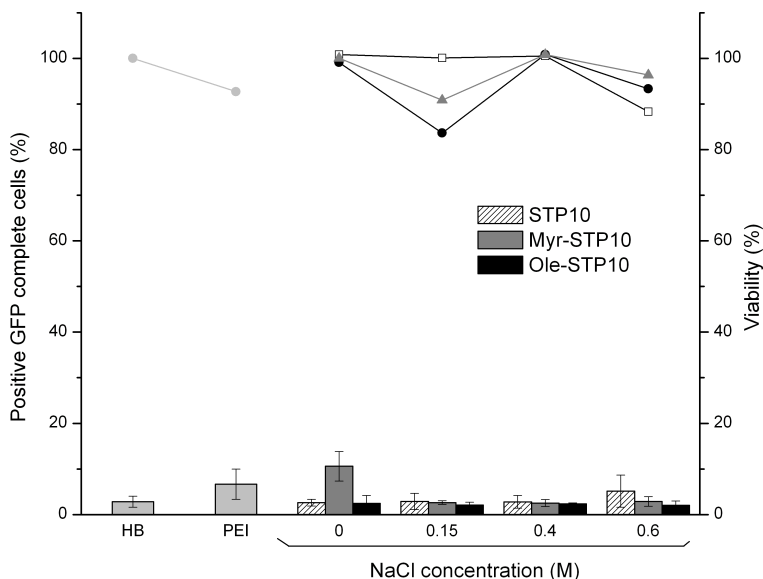
Figure 6.18: Transfection efficiency (bars) and relative viability (symbols). HeLa cells were transfected with the polyplexes at N/P=2 formed at different NaCl concentrations. HEPES buffer was used as negative control and PEI polyplexes at N/P=6 were considered positive control (light gray). STP_{10} (Patterned bars, squares) , Myr-STP_{10} (gray bars, triangles) and Ole-STP_{10} (black bars, circles).

The values of tranfection are extremely low, even with the PEI positive control, which indicates that higher concentration of the polyplexes per well, or longer incubation time, was required for efficient transfection. For this reason, no comparison is possible among the different polyplexes. The only system that expressed a little amount of GFP was the Myr-

STP_{10} without salt. Those complexes were mainly amorphous globules of approximately 100 nm in diameter, similar in size and structure to those of Ole-STP_{10}. However, the interaction of the myristic chains with a phospholipid membrane might be higher, according to the interfacial behavior (Fig. 6.17), which likely enhances the uptake of the complexes.

The relative viability of the cells was also studied with the MTT assay. The higher toxicity (20 %) was seen with the Ole-STP_{10} at 0.15 M of NaCl. This might be ascribed to the membrane disruption that the oleic chains can induce, although it is not clear why this is only seen at this ionic strength. On the other hand, at 0.6 M of NaCl, the lowest viability is found with STP_{10}. At this ionic strength this polymer could not condense DNA, and free polymer can cause more cellular death.

Notwithstanding, further *in vitro* studies are required to correlate the morphologies of the polyplexes with the transfection activity.

6.3   Conclusions

Three poly(amidoamine)s, STP_{10}, Myr-STP_{10} and Ole-STP_{10}, with the same cationic block but different hydrophobicity were used to condense plasmid DNA. Their condensation ability was demonstrated by gel retardation and dynamic light scattering at different N/P ratios, obtaining complexes of approximately 100 nm in diameter above N/P=1 regardless of the polymer.

The hydrophobic contribution to the condensation of DNA was investigated by screening the electrostatic interaction with sodium chloride. The size, polydispersity index and morphologies of the complexes at N/P=2 were analyzed and we concluded that:

- At low salt conditions the sizes of the complexes were similar independently of the polymer used, but different morphologies were found. Tight toroidal packaging was predominant with the polymer without hydrophobic chains, and amorphous globules were formed with the other two.

- The increase of the ionic strength produced screening of the charges. The hydrophobic interaction favored the collapse, and the hindrance of the lipophilic residues yielded hydrophilic surfaces. Stabilization by hydration forces was proposed, explaining the compact structures found at moderate-high ionic strengths.

- The concentration of monovalent salt modulated the morphology of the complexes, which in turn depended on the polymer used.

The interaction with a cell membrane model was also evaluated, and the myristic chains of the Myr-STP_{10} allowed a better lateral packing at the DPPC interface, achieving a higher penetration degree. Lower adsorption was found with the oleic chains in spite of being longer, due to the unsaturation that might disrupt the lateral packing.

The transfection studies were not conclusive and no correlation with the colloidal properties was possible, although a better performance was achieved with the Myr-STP_{10}, which presented a higher adsorption at the cell membrane model.

The hydrophobic interactions play an important role in the DNA condensation process, modulating the compaction ability, the stabilization mechanisms and the morphology of the complexes formed. Besides, the long hydrophobic moieties can improve the interaction with the cell membranes, which can promote the uptake.

6.4   Bibliography

[1] R. Duncan. The dawning era of polymer therapeutics. *Nat. Rev. Drug Discov.*, 2(5):347–360, May 2003.

[2] J.D. Eichman, A. Bielinska, J.F. Kukowska-Latallo, and J.R. Baker. The use of PAMAM dendrimers in the efficient transfer of genetic material into cells. *Pharm. Sci. Technol. Today*, 3:232–245, 2000.

[3] D.B. Rozema, D.L. Lewis, D.H. Wakefield, S.C. Wong, J.J. Klein, P.L. Roesch, S.L. Bertin, T.W. Reppen, Q. Chu, A.V. Blokhin, J. E. Hagstrom, and J.A. Wolff. Dynamic polyconjugates for targeted

in vivo delivery of siRNA to hepatocytes. *Proc. Natl. Acad. Sci.*, 104(32):12982–12987, 2007.

[4] L. Hartmann, E. Krause, M. Antonietti, and H.G. Börner. Solid-phase supported polymer synthesis of sequence-defined, multifunctional poly(amidoamines). *Biomacromolecules*, 7(4):1239–1244, 2006. PMID: 16602744.

[5] P. Ferruti, M.A. Marchisio, and R. Duncan. Poly(amido-amine)s: Biomedical Applications. *Macromol. Rapid Commun.*, 23(5-6):332–355, 2002.

[6] D. Schaffert, C. Troiber, and E. Wagner. New sequence-defined polyaminoamides with tailored endosomolytic properties for plasmid DNA delivery. *Bioconjugate Chem.*, 2012.

[7] O.E. Philippova, T. Akitaya, I.R. Mullagaliev, A.R. Khokhlov, and K. Yoshikawa. Salt-Controlled Intrachain/Interchain Segregation in DNA Complexed with Polycation of Natural Origin. *Macromolecules*, 38:9359–9365, 2005.

[8] E. Raspaud, D. Durand, and F. Livolant. Interhelical spacing in liquid crystalline spermine and spermidine-DNA precipitates. *Biophys. J.*, 88(1):392 – 403, 2005.

[9] M.J. Santander-Ortega, A.B. Jódar-Reyes, N. Csaba, D. Bastos-González, and J.L. Ortega-Vinuesa. Colloidal stability of Pluronic F68-coated PLGA nanoparticles: A variety of stabilisation mechanisms. *J. Colloid Interface Sci.*, 302(2):522 – 529, 2006.

[10] T. López-León, E.L.S. Carvalho, B. Seijo, J.L. Ortega-Vinuesa, and D. Bastos-González. Physicochemical characterization of chitosan nanoparticles: electrokinetic and stability behavior. *J. Colloid Interface Sci.*, 283(2):344 – 351, 2005.

[11] V. A. Kabanov and A. B. Zezin. Soluble interpolymeric complexes as a new class of synthetic polyelectrolytes. *Pure Appl. Chem.*, 56:343–354, 1984.

[12] R. M. Pashley. Hydration forces between mica surfaces in aqueous electrolyte solutions. *J. Colloid Interface Sci.*, 80(1):153–162, 1981.

[13] N.V. Churaev and B.V. Derjaguin. Inclusion of structural forces in the theory of stability of colloids and films. *J. Colloid Interface Sci.*, 103(2):542–553, 1985.

[14] J.A. Molina-Bolívar and J. L. Ortega-Vinuesa. How proteins stabilize colloidal particles by means of hydration forces. *Langmuir*, 15(8):2644–2653, 1999.

[15] M.J. Santander-Ortega, J.M. Peula-García, F. M. Goycoolea, and J.L. Ortega-Vinuesa. Chitosan nanocapsules: Effect of chitosan molecular weight and acetylation degree on electrokinetic behaviour and colloidal stability. *Colloids Surf., B*, 82(2):571 – 580, 2011.

[16] V.A. Bloomfield. DNA condensation by multivalent cations. *Biopolymers*, 44:269–82, 1997.

[17] I.D. Vilfan, C.C. Conwell, T. Sarkar, and N.V. Hud. Time study of DNA condensate morphology: Implications regarding the nucleation, growth, and equilibrium populations of toroids and rods. *Biochemistry*, 45(26):8174–8183, 2006. PMID: 16800642.

[18] M.X. Tang and F.C. Szoka. The influence of polymer structure on the interactions of cationic polymers with dna and morphology of the resulting complexes. *Gene Ther.*, 4(8):823–832, 1997.

[19] N.V. Hud and I.D. Vilfan. Toroidal dna condensates: Unraveling the fine structure and the role of nucleation in determining size. *Annu. Rev. Biophys. Biomol. Struct.*, 34(1):295–318, 2005. PMID: 15869392.

[20] P.G. Arscott, C. Ma, J.R. Wenner, and V.A. Bloomfield. DNA condensation by cobalt hexaammine(iii) in alcohol–water mixtures: Dielectric constant and other solvent effects. *Biopolymers*, 36(3):345–364, 1995.

[21] C.C. Conwell, I.D. Vilfan, and N.V. Hud. Controlling the size of nanoscale toroidal DNA condensates with static curvature and ionic strength. *Proc. Natl. Acad. Sci.*, 100(16):9296–9301, 2003.

[22] A.A. Zinchenko, N. Chen, S. Murata, and K. Yoshikawa. How does DNA compaction favor chiral selectivity with cationic species? higher selectivity with lower cationic charge. *ChemBioChem*, 6(8):1419–1422, 2005.

[23] M.M Patel and T. J. Anchordoquy. Contribution of hydrophobicity to thermodynamics of ligand-dna binding and DNA collapse-. *Biophys. J.*, 88(3):2089 – 2103, 2005.

[24] S. Berenyi, J Mihály, A. Wacha, O. Töke, and A. Bóta. A mechanistic view of lipid membrane disrupting effect of PAMAM dendrimers. *Colloids Surf., B*, 118(0):164 – 171, 2014.

[25] G. Luque-Caballero, A. Martín-Molina, A.Y. Sánchez-Trevino, M.A. Rodríguez-Valverde, M.A. Cabrerizo-Vílchez, and J. Maldonado-Valderrama. Using AFM to probe the complexation of DNA with anionic lipids mediated by Ca2+: the role of surface pressure. *Soft Matter*, 10:2805–2815, 2014.

[26] I. López-Montero, P. Mateos-Gil, M. Sferrazza, P.L. Navajas, G. Rivas, M. Vélez, and F. Monroy. Active Membrane Viscoelasticity by the Bacterial FtsZ-Division Protein. *Langmuir*, 28(10):4744–4753, 2012.

7

Conclusions/Conclusiones

The seventh chapter exposes the main conclusions of this thesis and future work ideas.

The main conclusions of this dissertation can be summarized as follows:

- Various families of cationic polymers, with subtle selected variations in their backbones, were successfully used to condense plasmid DNA into compact structures capable of transfecting HeLa cells *in vitro*. The experimental techniques used to characterize the complexes have been proved efficient to establish differences based on the condensation mechanism, and indirectly, on the structure of the polymer.

- The presence of small hydrophobic ethyl groups in the backbone was seen to induce a cooperative binding mechanism of free polymer to pre-formed complexes, yielding particles with a core-shell structure with a higher positive charge and hydrophobic character. The protective shell provided better protection of the DNA against enzymatic digestion and extended temporal stability of the particles in solution. However, the short hydrophobic moieties did not influence directly the transfection efficiency of the polyplexes. Depending on the cationic segment and on the solution conditions, the long hydrophobic residues can determine whether the DNA is condensed or not. Differences in the temporal stability and morphology of the polyplexes highlighted the key role of the hydrophobic interactions in the conformational change of DNA.

- By using the pendant drop technique, we demonstrated that the long acyl chains increased the adsorption kinetics onto a phospholipid monolayer at the air-water interface. The saturated alkyl tails allow a better lateral packing of the phospholipids, which is translated into a higher interaction with the model membrane. The polymers with higher adsorption yielded better transfection results, which reveals the potentiality of this technique to establish structure-activity relationships.

- The *in vitro* activity of the complexes was not dependent on the condensation pH, demonstrating that, for the pH-dependent degradable polymer studied, an acidic pH improved the storage of the complexes, increased the temporal stability and it did not reduce the transfection efficiency.

- The concentration of monovalent salt modulated the morphology of the complexes, which in turn depended on the structure of the polymer used. The screening of the charges at moderate concentrations of salt

revealed the importance of the hydrophobic interactions. A mechanism of re-stabilization by hydration forces was proposed to explain the presence of compact structures at moderate-high ionic strengths.

Las principales conclusiones de este trabajo se resumen a continuación:

- Varias familias de polímeros catiónicos, con ligeras diferencias seleccionadas en sus esqueletos, se han utilizado con éxito para condensar ADN plasmídico, obteniendo estructuras compactas capaces de transfectar células HeLa *in vitro*. Las técnicas experimentales utilizadas para caracterizar los complejos son válidas para establecer diferencias basadas en el mecanismo de condensación, e indirectamente, en la estructura del polímero.

- Se ha observado que la presencia de pequeños grupos etilo en la estructura del polímero induce un mecanismo de unión cooperativa de polímero libre a complejos pre-formados, resultando en partículas con una estructura de núcleo-coraza de elevada carga positiva y cierto carácter hidrófobo. La coraza protectora proporciona una mejor protección frente a la digestión enzimática y prolonga la estabilidad temporal de las partículas en disolución. Sin embargo, estas cadenas hidrofóbicas de pequeña longitud no parecen influir directamente en la eficiencia de transfección de los poliplejos. Dependiendo del segmento de carga positiva del polímero, y de las condiciones del medio, las cadenas hidrofóbicas de más longitud pueden llegar a determinar si el ADN es condensado o no. Las diferencias que se encontraron en estabilidad temporal y morfología de los complejos revelan el papel fundamental de las interacciones hidrofóbicas en los cambios conformacionales del ADN.

- Utilizando la técnica de la gota pendiente se ha demostrado que las largas cadenas hidrocarbonadas incrementan las cinéticas de adsorción a una monocapa de fosfolípidos en la interfase aire/agua. Si las cadenas lipídicas son saturadas, se alcanza un mayor grado de empaquetamiento lateral de las colas, lo que se traduce en una mayor interacción con la membrana modelo utilizada. Los polímeros que presentaron una mayor adsorción fueron los que lograron mejores resultados de transfección, lo que destaca la potencialidad de esta técnica para establecer relaciones de estructura-transfección.

- La actividad *in vitro* de los complejos formados con un polímero con degradación pH-dependiente no se vio influida por el valor del pH durante la condensación, demostrando que para ese polímero, un pH más ácido

mejoraba el almacenamiento de los complejos puesto que incrementaba su estabilidad temporal, sin disminución de la eficacia de transfección.

- La concentración de sal monovalente modula la morfología de los complejos, que a su vez depende de la estructura del polímero utilizado. El apantallamiento de las cargas a concentraciones moderadas de sal revela la actuación e importancia de las interacciones hidrofóbicas. Se ha propuesto un mecanismo de re-estabilización por fuerzas de hidratación para explicar la presencia de estructuras compactas a una fuerza iónica moderada-alta.